



UNIVERSITY *of the*
WESTERN CAPE

The effect of glycine supplementation on the skeletal muscle properties of captive cheetahs (*Acinonyx jubatus*)

Luqmaan Adamson

4073342

October 2022

Submitted in fulfilment of the requirements of the degree
Magister Scientiae in Medical Bioscience in the
Faculty of Natural Sciences
University of the Western Cape (UWC)
Bellville

Supervisor : Professor Tertius Abraham Kohn

Co-supervisor : Professor Adrian Stephen Wolferstan Tordiffe

Dedication

I dedicate this thesis to my family, close friends and colleagues for their unconditional support and unwavering confidence in me throughout my academic career.

To my mom, whose simple words will continue to resonate with me.

“Net ‘n bietjie Sabr. Alles wat tyd. Gaan net aan...”



Keywords

Captive cheetah

Diet and nutrition

Glycine supplement

Skeletal muscle

Fibre type

Cross-sectional area

Enzyme activity

Anaerobic metabolism

Aerobic metabolism

Glycogen



Abstract

The effect of glycine supplementation on the skeletal muscle properties of captive cheetahs (*Acinonyx jubatus*)

L. Adamson

M.Sc thesis, Department of Medical Bioscience, University of the Western Cape (UWC)

The fastest known land mammal – the cheetah, possesses many anatomical adaptations that enables high-speed running. Current literature regarding the physiological aspects that facilitate their incredible sprinting ability, however, remains limited. Although ensuring the survival of the species, captive cheetahs experience several complications including reduced fecundity and an increased incidence of degenerative disorders rarely observed in free-ranging cheetahs. A key difference in captive and free-ranging cheetahs is that their diets differ substantially with regards to nutrient composition and availability, and previous studies have highlighted the potential link between the diet of cheetahs and their overall poor performance in captivity. Glycine is considered to be a crucial amino acid lacking in adequate amounts in the diets of captive cheetahs. In addition, the skeletal muscle and physiology of the cheetah implies a significant metabolic demand for glycine as creatine (a glycine derivative) is a crucial metabolite for cheetahs to enable muscle activity. Large quantities of glycine are additionally lost in the form of glycine conjugates *via* their urine. It was therefore speculated that they may be at risk of a glycine deficiency. The aim of this study was to determine the fibre type composition, maximum enzyme activities and glycogen content in the VL muscle of 10 captive cheetahs to develop a better understanding of their skeletal muscle properties, and to determine whether a glycine-supplemented diet elicits any significant changes to the muscle profile. After an initial habituation period, 2 groups of cheetahs received a control (meat only) and a supplemented diet (meat + glycine powder) for 4 weeks per diet trial in a cross-over study design. Analyses were performed on muscle samples collected on 3 occasions following each trial. Muscle fibre type composition and cross-sectional area were determined to evaluate the skeletal muscle morphology, whereas total muscle glycogen and maximum 3-hydroxacyl CoA dehydrogenase (3HAD), citrate synthase (CS), lactate dehydrogenase (LDH), creatine kinase (CK), phosphofructokinase (PFK), and phosphorylase (PHOS) enzyme activities were determined to evaluate the skeletal muscle metabolism of captive cheetahs. Glycine elicited no significant changes in skeletal muscle structure and metabolism after 4 weeks of supplementation. Type IIX fibres comprised the majority of fibres in the muscle of captive cheetah ($61 \pm 5\%$), followed by type IIA ($20 \pm 5\%$) and type I ($19 \pm 6\%$). Similarly, the cross-sectional area of fibres decreased

from type IIX ($5127 \pm 1131 \mu\text{m}^2$) to type I fibres ($3009 \pm 769 \mu\text{m}^2$). High CK ($10872 \pm 1824 \mu\text{mol}\cdot\text{min}^{-1}\cdot\text{g}^{-1}$) and LDH ($2144 \pm 348 \mu\text{mol}\cdot\text{min}^{-1}\cdot\text{g}^{-1}$) activities, and low 3HAD ($25 \pm 5 \mu\text{mol}\cdot\text{min}^{-1}\cdot\text{g}^{-1}$) and CS ($18 \pm 5 \mu\text{mol}\cdot\text{min}^{-1}\cdot\text{g}^{-1}$) activities are reported, suggesting that cheetahs are efficient at utilising anaerobic metabolism for energy supply. Glycine has important roles in muscle function and maintenance *via* protein regulation and may have important implications in fat metabolism. This is the first study to evaluate the muscular effects of glycine supplementation in captive cheetahs, and the results obtained here show that 4 weeks of supplementation does not affect muscle structure or metabolism.

October 2022



Declaration

I declare that this thesis is an original report of my research, has been composed by me and has not been submitted for any previous degree. The experimental work is almost entirely my own work; the collaborative contributions have been indicated clearly and acknowledged. Due references have been provided on all supporting literatures and resources.



Luqmaan Adamson

October 2022



Acknowledgments

First and foremost, I would like to thank the Almighty God for granting me all the faculties to achieve the undertaking and completion of this research project, and for granting me the strength and patience during one of the most challenging periods of my life.

To my supervisor, mentor and friend Prof. Tertius. A Kohn for his continual support and patience throughout my postgraduate career. For teaching me all the necessary skills and techniques required by a researcher, providing me with priceless experience and offering beneficial academic and personal advice, I am sincerely grateful.

Special thank you to Prof. Adrian S.W. Tordiffe, my co-supervisor. He has played a fundamental role in this study. Thank you for your tireless efforts during sample collection and assistance during the final preparation of my thesis. Your enduring dedication to your field is evident in the quality of your research.

Kathryn, utmost thanks for your endless assistance and constant support during lab experiments and the preparation of this thesis, respectively. Your persevering consistency and unwavering work ethic are qualities I hope to achieve. Without the collective efforts of Tertius, Adrian and Kathryn, the conception and execution of this project would not have been possible. There is nothing that can quantify the amount of gratitude I harbour.

Thank you to the staff of Congo Wildlife Ranch and Conservation Centre for providing the cohort of cheetahs for the study. Without their hard work, guidance and assistance during the intervention and sampling periods, the success of this project would have been drastically impacted. Your time and efforts are duly appreciated.

My immediate family, for serving as an immovable anchor during my brief time on this planet, I am grateful. Eternal thanks for the on-going assistance (in which ever form) and prayers during this journey.

I am indebted to the National Research Foundation of South Africa (NRF) and the South African Veterinary Foundation (SAVF) whose funding facilitated the actualization of this project. To the South African National Zakah Fund (SANZAF), I express my deepest appreciation for the continuous funding throughout my academic career.

Lastly, to my wife and daughter, the greatest source of my motivation and contentment.

Table of contents

The effect of glycine supplementation on the skeletal muscle properties of captive cheetahs (<i>Acinonyx jubatus</i>)	1
Dedication	2
Keywords	3
Abstract	4
Declaration	6
Acknowledgments	7
Table of contents	8
List of abbreviations	11
List of figures	14
Chapter 1: Preface	17
1.1. Background	17
1.2. Motivation for the study	18
1.3. Aims and objectives	18
1.4. Thesis layout	18
Chapter 2: Literature review	20
2.1. Ecology and conservation	20
2.2. Skeletal muscle structure	21
2.2.1. Fibre types	22
2.3. Skeletal muscle metabolism	24
2.3.1. Aerobic enzymes	24
I. 3-hydroxyacyl-Coenzyme-A dehydrogenase (3HAD)	24
II. Citrate synthase (CS)	25
2.3.2. Anaerobic enzymes	25
I. Creatine kinase (CK)	25
II. Phosphofructokinase (PFK)	26
III. Lactate dehydrogenase (LDH)	27
IV. Phosphorylase (PHOS)	27
2.4. The skeletal muscle of cheetahs	27
2.5. Glycine	29
2.5.1. Physiological effects of glycine	29
2.5.2. Glycine metabolism	30

2.6. Benefits of dietary glycine supplementation.....	32
2.7. Glycine and skeletal muscle.....	33
2.8. Glycine deficiency in captive cheetahs.....	34
2.9. Anticipated gain in knowledge.....	35
2.10. Research aims.....	36
Chapter 3: Methodology and materials	37
3.1. Ethics and permits.....	37
3.2. Research design and layout.....	37
3.3. Research setting.....	37
3.4. Study population.....	38
3.4.1. Animals.....	38
3.4.2. Animal diet prior to study initiation.....	38
3.5. Diet intervention.....	39
3.5.1. Habituation.....	39
3.5.2. Intervention diets.....	40
3.6. Sample collection.....	41
3.6.1. Anaesthesia.....	41
3.6.2. Muscle biopsy.....	42
3.6.3. Muscle processing, storage and transport.....	42
3.7. Immunohistochemistry.....	43
3.7.1. Sample preparation and sectioning.....	43
3.7.2. Staining procedure.....	43
3.7.3. Image visualisation and processing.....	44
3.8. Enzyme assays.....	45
3.8.1. Homogenate preparation.....	45
3.8.2. Protein content.....	45
3.8.3. Enzyme assays.....	46
3.9. Glycogen assay.....	47
3.9.1. Glycogen extraction.....	47
3.9.2. Glucose analysis and glycogen determination.....	48
3.10. Statistical analysis.....	48
Chapter 4: Skeletal muscle morphology	49
4.1. Results.....	49



4.1.1. Fibre type composition	49
4.1.2. Fibre cross-sectional areas (CSA).....	49
4.2. Discussion.....	52
4.2.1. Skeletal muscle morphology of captive cheetahs	52
4.2.2 Glycine and skeletal muscle structure	56
Chapter 5: Skeletal muscle metabolism	61
5.1. Results.....	61
5.1.1. Enzyme activities	61
5.1.2. Glycogen concentration.....	64
5.2. Discussion.....	64
5.2.1. Skeletal muscle metabolism of captive cheetah	64
5.2.2. Glycine and skeletal muscle metabolism	68
Chapter 6: Conclusion and future directions.....	72
Limitations of the study	75
Bibliography	77
Appendices	92
Appendix A: Immunohistochemistry protocol.....	92
Appendix B: Fluorometric enzyme analysis.....	95
Appendix C: Glycogen assay	107
Appendix D: Cheetah pre-study diets.....	111
Appendix E: Permit certificates	112

List of abbreviations

3HAD	3-Hydroxyacyl-Coenzyme A dehydrogenase
AA	Amino acid
AGT	Alanine: glyoxylate aminotransferase
Akt	Protein kinase B
ANOVA	Analysis of variance
ATP	Adenosine triphosphate
ATPase	Adenosine triphosphatase
BCAA	Branched-chain amino acids
BSA	Bovine serum albumin
BW	Body weight
CK	Creatine kinase
cSHMT	Cytosolic serine hydroxymethyltransferase
CoA	Coenzyme-A
CP	Crude protein
Cr	Creatine
CRT	Creatine transporter
CS	Citrate synthase
CSA	Cross-sectional area
DNA	Deoxyribonucleic acid
d.w.	dry weight
EAA	Nutritionally essential amino acid
ECM	Extracellular matrix
ETC	Electron transport chain
FFA	Free fatty acid
g	gram



GAA	Guanidinoacetic acid
GCS	Glycine cleavage system
g·l ⁻¹	grams per litre
GLYAT	Glycine N-acetyltransferase
IGF-1	Insulin-like growth factor 1
IHC	Immunohistochemistry
IUCN	International Union for the Conservation of Nature
km ²	square kilometre
LDH	Lactate dehydrogenase
M	Molar
mg	milligram
MHC	Myosin heavy chain
min	minute
ml	millilitre
mSHMT	Mitochondrial serine hydroxymethyltransferase
mTOR	Mammalian target of rapamycin
NADH	Nicotinamide adenine dinucleotide
NADPH	Nicotinamide adenine dinucleotide phosphate
NEAA	Nutritionally nonessential amino acid
PBS	Phosphate buffered saline
PCr	Phosphocreatine
PFK	Phosphofructokinase
PHOS	Phosphorylase
P _i	Inorganic phosphate
PI(3)K	Phosphoinositide 3 kinase
prot.	protein



RNA	Ribonucleic acid
SD	Serine dehydrogenase
S.D.	Standard deviation
SDH	Succinate dehydrogenase
SHMT	Serine hydroxymethyltransferase
TCA	Tricarboxylic acid cycle
µl	microlitre
µm ²	square micrometre
µmol	micromole
VL	<i>Vastus lateralis</i>
w.w.	wet weight



List of figures

Figure 1: The known distribution of cheetahs in the past vs. present in A, Africa and B, Asia, adapted from Durant et al., (2017). Grey areas denote historical ranges and red areas denote current ranges that wild cheetahs are known to inhabit. 20

Figure 2: Macro- and ultrastructure of skeletal muscle and the motor unit, adapted from www.Kenhub.com. Illustration by Paul Kim. (https://www.kenhub.com/en/library/anatomy/the-neuromuscular-junction-structure-and-function)..... 22

Figure 3: Energy-producing metabolic pathways in skeletal muscle. 3HAD, 3-Hydroxyacyl-Coenzyme A dehydrogenase; ADP, adenosine diphosphate; ATP, adenosine triphosphate; ATPase, adenosinetriphosphatase; CPT1/2, carnitine palmitoyltransferase 1/2; CRT, creatine transporter; CS, citrate synthase; CK_c, creatine kinase cytosolic isoform; CK_m, creatine kinase mitochondrial isoform; ETC, electron transport chain; F-1,6-BP, fructose-1,6-bisphosphate; F-6-P, fructose-6-phosphate; FADH₂, dihydroflavine-adenine dinucleotide; FAT/ CD36, fatty acid translocase/ cluster of differentiation 36; G-1-P, glucose-1-phosphate; G-6-P, glucose-6-phosphate; GLUT1/4, glucose transporter 1/4; GS, glycogen synthase; HK, hexokinase; LDH, lactate dehydrogenase; MCT4, monocarboxylate transporter 4; NAD⁺, nicotinamide adenine dinucleotide (oxidised form); NADH, nicotinamide adenine dinucleotide (reduced form); P-Creatine, phosphorylated creatine; PCM, phosphoglucomutase; PDH, pyruvate dehydrogenase; PFK, phosphofructokinase; PHOS, phosphorylase; Pi, inorganic phosphate; TCA, tricarboxylic acid cycle, based on Akram, (2013; 2014), Houten et al., (2015) and Negro et al., (2019). 26

Figure 4: *In vivo* synthesis of glycine and its main metabolic products. AGT, alanine:glyoxylate aminotransferase; BAD, betaine alanine dehydrogenase; BTM, betaine transmethylase; CO, choline oxidase; DGO, dimethylglycine oxidase; SaDH, sarcosine dehydrogenase; SD, serine dehydrogenase; SHMT, serine hydroxymethyl transferase; TDH, threonine dehydrogenase, based on Razak et al., (2017) and Wang et al., (2013). ... 31

Figure 5: Schematic diagram of the layout for the 2-period crossover glycine diet intervention. Group A (shaded box) initially received the glycine-supplemented diet while group B (white box) initially received the control diet for 3 weeks. The groups then crossed over following a 2-week washout period. The asterisks (*) indicates the sampling occasions. Muscle biopsies were taken from the VL muscle and was staggered over a period of 2 days. 40

Figure 6: Fluorescent IHC of a cross-section from the VL muscle of a captive cheetah (*Acinonyx jubatus*). A, type I fibres expressing MHC I strongly positive for BA-D5 (blue); B, type IIA fibres and basal lamina expressing MHC IIA and laminin, respectively. MHC IIA and laminin were stained using 2F7 and C4 (both indicated by green); C, type IIX fibres expressing MHC IIX stained using 6H1 (red); and D, composite image displaying all 3 fibre types and the basal lamina. Type IIA/X fibres are indicated (D). These fibres stained lightly for both 2F7 and 6H1 but represented less than 3% of the fibre population and were divided between type IIA and type IIX fibres. The scale bar is presented at the bottom right and applies to all panels, 100 μm . All images were captured at 10x magnification..... 50

Figure 7: Fibre type composition (%) of the VL muscle of 10 captive cheetahs (*Acinonyx jubatus*) for different dietary interventions. Muscle biopsies were sampled on alternating legs on 3 occasions. Fibre type composition (%) (determined by IHC analyses) is displayed on the y-axis and fibre type are displayed on the x-axis. Baseline values are depicted by white bars, control diet is depicted by light grey bars and the glycine diet is depicted by dark grey bars. Bars represent the means \pm S.D. for each fibre type, and individual values for each cheetah are depicted by white circles (n=10). Due to the cross-over nature of the study, the control and glycine groups from each sampling period were pooled together..... 51

Figure 8: Cross-sectional area (μm^2) of the VL muscle of 10 captive cheetahs (*Acinonyx jubatus*) for different dietary interventions. CSA is displayed on the y-axis and different treatment groups are displayed on the x-axis. Data are displayed as means \pm S.D. with each bar representing a different fibre type. Type I, type IIA and type IIX fibres are depicted by white, light grey and dark grey bars, respectively. Each white circle represents the data for individual cheetahs (n=10) in each treatment group. Control and glycine groups display pooled data from each sampling period. *Significantly different from type I fibres in each group.* 52

Figure 9: Maximum activity of aerobic enzymes in the VL muscle of 10 captive cheetahs (*Acinonyx jubatus*). Data from different intervention periods were pooled for each group. A, average 3HAD enzyme activity; B, average CS enzyme activity. All enzyme activities are presented as the of amount substrate turnover per minute per gram of protein ($\text{g}\cdot\text{l}^{-1}$) present in the homogenate ($\mu\text{mol}\cdot\text{min}^{-1}\cdot\text{g}^{-1}$ prot.). Light grey bars represent the maximum enzyme activity in each group and displayed as means \pm S.D. for each group. White circles indicate the individual values for each cheetah in the study. *Significantly different from the baseline group ($P < 0.05$)..... 62

Figure 10: Maximum activities of anaerobic enzymes in VL muscle of 10 captive cheetahs (*Acinonyx jubatus*) on different diets. The light grey bars represent pooled data from different intervention periods of each treatment group. A, average maximum LDH; B, creatine kinase (CK); C, phosphofructokinase (PFK) and D, phosphorylase (PHOS) enzyme activity ($\mu\text{mol}\cdot\text{min}^{-1}\cdot\text{g}^{-1}$ prot.). Data are displayed as means \pm S.D. White circles represent individual values for each cheetah in the study..... 63

Figure 11: Total glycogen concentration ($\text{mmol}\cdot\text{kg}^{-1}$ d.w.) present in the VL muscle of 10 captive cheetahs (*Acinonyx jubatus*). Light grey bars represent pooled data from different intervention periods and are displayed as means \pm S.D. for each group. White circles depict the values from individual cheetahs..... 64



Chapter 1: Preface

1.1. Background

The cheetah is known as the fastest living terrestrial mammal, capable of reaching speeds of up to 114 kilometres per hour (Sharp, 1997; Hayward *et al.*, 2006). Anatomically, the cheetah is well-suited for high-speed running. It has a slender body and thin long legs with ridged foot pads to provide traction. Their locomotor muscles are largely composed of fast-twitch fibres and a highly flexible spine allows for greater stride length and frequency (Williams *et al.*, 1997; Hudson *et al.*, 2012). They possess sharp claws which they utilise as running spikes that provide increased traction during pursuits, and allows them to apply large propulsive forces while supporting minimal body weight (Williams *et al.*, 1997; Krausman & Morales, 2005; Hudson *et al.*, 2012). The anatomical adaptations for the high performance of the cheetah are well-documented (Hudson *et al.*, 2011b, a; Hudson *et al.*, 2012). However, there is limited research that highlights the physiological profile of cheetah and how this may enable their sprinting ability.

Currently, the cheetah is divided into 4 subspecies categorised by the Cat Classification Task Force of the IUCN Cat specialist group: *A. jubatus hecki* (Northwest African cheetah, also known as the Saharan cheetah), *A. j. soemeringii* (Northeast African cheetah), *A. j. jubatus* (Southern and East African cheetah) and *A. j. venaticus* (Western and Southern Asiatic cheetah) (Charruau *et al.*, 2011). Historically, cheetahs were widespread across Africa and southwestern Asia, but today, there are approximately 7100 adult and adolescent cheetahs remaining globally. Of those, more than half (61%) survive in southern African countries and exists as a single population (Durant *et al.*, 2017). To date, this is the largest known population of free-ranging cheetahs as most populations (about 91%) consists of 200 individuals or fewer (Weise *et al.*, 2017). The subspecies *A. j. hecki* and *A. j. venaticus* are currently listed as critically endangered on the IUCN Red List (Sillero-Zubiri *et al.*, 2015; Farhadinia *et al.*, 2017). The latter subspecies, a remnant population of Asiatic cheetah survives in protected areas in the eastern-central region of Iran only and is estimated to comprise of less than 50 individuals (Durant *et al.*, 2017).

Due to an increased metabolic demand and a divergent diet from the free-ranging population, captive cheetahs may be at risk of receiving inadequate amounts of certain essential nutrients (Bond & Lindburg, 1990; Marnewick *et al.*, 2007). Recent studies highlighted the possible link between the diet of captive cheetahs and the progression of disorders only seen in this population (such as gastrointestinal diseases), making diet an

important factor to consider for the overall well-being of captive cheetahs (Lane *et al.*, 2012; Whitehouse-Tedd *et al.*, 2015). Yet, the research pertaining to cheetah nutrition is still limited with most studies confined to either rodents or domesticated farm species such as pigs and chicken, while the nutritional requirements of captive cheetahs are largely based on the metabolic demands of domestic cats (Dierenfeld *et al.*, 2015).

1.2. Motivation for the study

Captive cheetah may be at risk of a deficiency of the simplest amino acid glycine due to their metabolic demand and reduced dietary intake. The current study is an aspect of ongoing research investigating the effects of glycine supplementation on the entire metabolome of captive cheetahs. The physiological properties of cheetah skeletal muscle and how that relates to their sprinting ability are also rarely documented in the literature. Furthermore, it is unknown whether supplementing the diets of captive cheetahs with glycine will affect their skeletal muscle structure and metabolism.

1.3. Aims and objectives

The aims of this research study were to investigate the structure and physiological properties of skeletal muscle of 10 captive cheetahs, and to determine the effect of a glycine-supplemented meat-based diet on the aforementioned parameters. The objectives were thus sampling and analysing the VL muscle of captive cheetah for fibre type and CSA using IHC analyses. Total muscle glycogen content, and maximum activity of oxidative and glycolytic enzymes were determined using enzymatic assays.

1.4. Thesis layout

The current thesis comprises of 2 aspects; 1) the skeletal muscle profile of captive cheetahs and 2) whether cheetah skeletal muscle structure and metabolism is affected by glycine supplementation. The preface provides a brief background on the cheetah and its global status, summarises the study motivations and primary aims of the study. Chapter 2 contains a review of the literature pertaining to the most important aspects of the current study. This chapter highlights the problems experienced by captive cheetahs, draws attention to their skeletal muscle profile and metabolic properties, as well as the potential role of diet on cheetah well-being. A justification for the use of supplementary glycine is also presented in this chapter. Chapter 3 provides insight into the experimental design, layout and research methodology employed during the progression of the study. Chapter 4 focuses on the skeletal muscle morphology, and chapter 5 addresses skeletal muscle metabolism and

glycogen content of cheetah muscle. These chapters also discuss the potential effects in response to glycine supplementation. Finally, chapter 6 summarises the findings presented in chapters 4 and 5, and provides an overall conclusion based on the aims of the study highlighted in chapter 1. Potential avenues for future research are suggested, and the limitations of the present study are discussed.



Chapter 2: Literature review

2.1. Ecology and conservation

Globally, the cheetah is listed as a vulnerable species on the IUCN Red List primarily due to declining populations and contracted habitat ranges (Durant *et al.*, 2015). Documented as one of the most wide-ranging carnivores, the home range and movements of free-ranging cheetah can span areas of up to 3000 km² (Marker *et al.*, 2008; Weise *et al.*, 2015). Comparatively, the home range of other species of the felid family such as the lion (*Panthera leo*) and leopard (*Panthera pardus*) cover areas of up to 630 km² (Bauer & De longh, 2005; Loveridge *et al.*, 2009) and 388km², respectively (Norton, 1985; Stein *et al.*, 2011). Cheetah past distribution comprised of most non-rainforest regions of Africa and extended across Western and Southern Asia, from the Arabian Peninsula up to southern Kazakhstan and across India (Caro, 1994; Prost *et al.*, 2020). Currently, they are confined to less than 9% of their past distribution (2% in Asia and 13% in Africa), which is the greatest range reduction observed among the large felid species (IUCN/SSC, 2015; Jacobson *et al.*, 2016; Wolf & Ripple, 2017).

To illustrate, in 2007, the cheetah distribution in Zimbabwe consisted of a contiguous population extending over 132 931 km². By 2015, this was reduced to a fragmented population occupying only 49 124 km², denoting a 63% range contraction over the brief

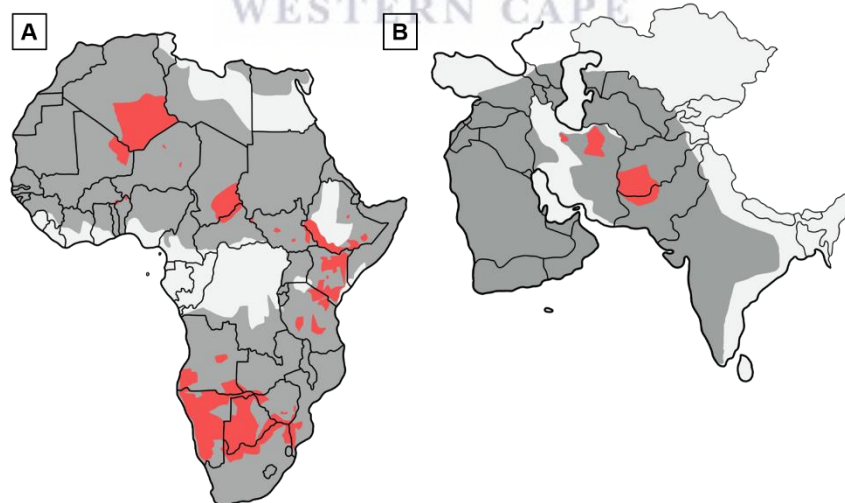


Figure 1: The known distribution of cheetahs in the past vs. present in A, Africa and B, Asia, adapted from Durant *et al.*, (2017). Grey areas denote historical ranges and red areas denote current ranges that wild cheetahs are known to inhabit.

period (IUCN/SSC, 2007, 2015). It is also estimated that this population of cheetah experienced a decline of at least 85% in number between 1999 and 2015 (van der Meer, 2016). The population of remaining cheetahs is likely an overestimation of the true population, as accurate census data are only obtained from protected areas. In regions where they are most threatened, cheetah status is usually unpredictable as those areas lack sufficient data (Martin *et al.*, 2012). In a recent article, the population estimate was reported to be 11% lower than the IUCN's assessment for cheetah presence in southern Africa (Weise *et al.*, 2017). For these reasons, there has been a recent call for the cheetah to be reclassified from vulnerable to endangered status (Durant *et al.*, 2017).

The captivity of wild animals has many advantages rooted in wildlife conservation, education and the progression of wildlife research. For many wild animal species, captivity is associated with enhanced longevity, improved health and enhanced fecundity (Mason, 2010). However, there are many animal species such as the cheetah where captivity may be detrimental. Cheetahs succumb to high mortality and morbidity rates in captivity. They also suffer from various diseases rarely reported in their free-ranging counterparts which may affect many of their vital organs (Munson *et al.*, 2005; Tordiffe *et al.*, 2016; Gillis-Germitsch *et al.*, 2017). For instance, gastritis (which causes inflammation and subsequent dysfunction of the stomach mucosa) affects over 95% of the global captive cheetah population. Low genetic diversity, lack of exercise, captivity-related stress and more recently, diet and nutrition have been suggested as a potential causal factors (Terio *et al.*, 2004; Whitehouse-Tedd *et al.*, 2015).

2.2. Skeletal muscle structure

Skeletal muscle is one of the largest and most dynamic tissues in the body. The main function of skeletal muscle is converting chemical energy to mechanical energy, thereby producing force to generate movement (enabling locomotion) and maintain posture (Marieb & Hoehn, 2007; Frontera & Ochala, 2015). Metabolically, skeletal muscle serves as a multi-functional organ involved in respiration, thermoregulation, blood circulation and immune function, and maintains body homeostasis by contributing to energy metabolism (Wolfe, 2006). In humans, skeletal muscle comprises approximately 40% of gross BW, making it one of the largest reservoirs of glucose and many major metabolites (Shaffer & Neblett, 2010; Frontera & Ochala, 2015).

A motor unit consists of a single motor neuron and all the muscle fibres it innervates (MacIntosh *et al.*, 2006). Muscle fibres innervated by a motor neuron share metabolic and structural properties. Within a muscle, there are numerous motor units with different

metabolic properties that, as a collective, enables a wide variety of movement to meet functional demands (Schiaffino & Reggiani, 2011). Single muscle fibres are composed of functional units called sarcomeres with each sarcomere containing many proteins that work together in order to enable contraction and generate movement (Scott *et al.*, 2001; MacIntosh *et al.*, 2006). Actin and myosin are the major myofibrillar proteins enabling muscle contraction by generating ATP. The composition of these proteins are important determinants of the metabolic and structural properties of muscle fibres (Saltin, 1983; Pette, 1985).

2.2.1. Fibre types

There are 3 main fibre types within the limb and axial skeletal muscles of large mammals: 1) slow oxidative, (slow-twitch) type I fibres, 2) fast oxidative (fast-twitch) type IIA fibres, and 3) fast glycolytic, (very fast-twitch) type IIX fibres (Sandow, 1970; Kohn *et al.*, 2011a). A fourth fibre type (type IIB) exists that is only found in the limbs of small animals such as rats and mice, and confined to certain muscles in human beings (Talmadge & Roy, 1993); (Andersen *et al.*, 2002; Kohn & Myburgh, 2007). Each muscle fibre has distinguishable structural and metabolic properties and is classified based on the MHC protein it expresses (Bottinelli, 2001).

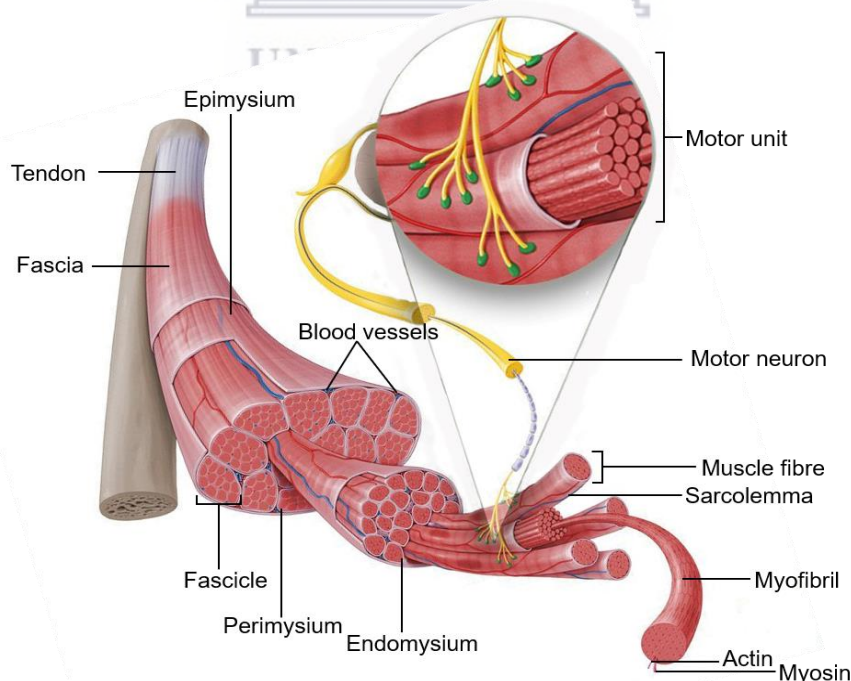


Figure 2: Macro- and ultrastructure of skeletal muscle and the motor unit, adapted from www.kenhub.com. Illustration by Paul Kim. (<https://www.kenhub.com/en/library/anatomy/the-neuromuscular-junction-structure-and-function>).

Type I fibres are distinguishable by their red colour due to their high myoglobin content (Essén-Gustavsson & Henriksson, 1984). These fibres are highly oxidative as they contain a large number of mitochondria and a dense capillary supply. They primarily utilise carbohydrates (from blood glucose and muscle glycogen) and fats *via* aerobic metabolism to generate ATP. Thus, type I fibres are highly resistant to fatigue. They have the smallest CSA of the 3 fibre types and express the MHC I isoform, which has the slowest ATP hydrolysis rate (Saltin, 1983; Kohn *et al.*, 2005; Kohn, 2014). Therefore, type I fibres have the slowest contraction speed compared to type IIA and IIX fibres (Saltin, 1983).

Type IIX fibres are pale in colour and contain less myoglobin than type I fibres (Jansson & Sylvén, 1983). They have a low capillary supply and contain very few mitochondria. Accordingly, anaerobic metabolism is the primary pathway for ATP production *via* glycolysis (from glucose and muscle glycogen) and high energy phosphates (such as PCr) (Pette, 1985). Thus, due to the limited fuel supply, type IIX fibres fatigue easily. In contrast to type I fibres, they have a large CSA, express the MHC IIX isoform and is capable of very fast contraction speeds (Saltin, 1983; Kohn *et al.*, 2011a).

Type IIA fibres express the MHC IIA isoform and share characteristics of both type I and type IIX fibres. They contain a sufficient number of mitochondria that allows for the efficient utilisation of both aerobic and anaerobic metabolism for ATP production. As a result, they are able to resist fatigue and have fast contraction speeds (Kohn & Noakes, 2013). Generally, the CSA of type IIA fibres are larger than type I fibres, but smaller than type IIX fibres (Kohn *et al.*, 2005; Kohn *et al.*, 2011a).

Skeletal muscle plays significant roles with regards to general lifestyle and athletic performance. In humans, endurance training is associated with a high proportion of type I fibres compared to type IIX fibres in the primary working muscle (Gollnick *et al.*, 1972; Jansson & Kaijser, 1977). In contrast, resistance-trained individuals contain more type IIX fibres compared to type I fibres as seen in sprinters and powerlifters (Gollnick *et al.*, 1972; Tesch & Karlsson, 1985). Similarly, animals with enhanced endurance (such as the dog and horse) possess a higher proportion of oxidative (type I and IIA) fibres compared to animals that primarily utilise fast, rapid movements such as the caracal and cheetah (Toniolo *et al.*, 2007; Rivero & Hill, 2016). Accordingly, the latter species possess a higher proportion of fast-twitch type IIX fibres to accommodate their movements (Williams *et al.*, 1997; Kohn *et al.*, 2011a).

2.3. Skeletal muscle metabolism

Skeletal muscle fibres generate force *via* the hydrolysis of ATP to ADP and *P_i*. Intramuscular ATP and PCr stores, glycolysis and oxidative phosphorylation are the main sources of ATP resynthesis. Additionally, ATP can be produced from other metabolic pathways such as the metabolism of AAs, but only contributes a small percentage of total ATP production (Schiaffino & Reggiani, 2011; Frontera & Ochala, 2015).

The different muscle fibre types possess large metabolic diversity primarily due to the type of substrate being utilised and its capacity for aerobic and anaerobic metabolism, which is determined by the predominant enzymes present and their respective catalytic activities (Essen *et al.*, 1975; Pette, 1985; Spamer & Pette, 2019). Muscle fibres efficient at utilising aerobic metabolism for ATP production are high in oxidative enzyme activity and content. In contrast, fibres efficient at anaerobic metabolism exhibits high glycolytic enzyme activity and content, with low oxidative capacity (Essén-Gustavsson & Henriksson, 1984; Pette, 1985). Consequently, key enzymes participating in aerobic and anaerobic metabolic pathways are used as markers to represent the oxidative and glycolytic capacity of muscle fibres, respectively.

2.3.1. Aerobic enzymes

The dominant source of skeletal muscle ATP generation in mammals is *via* aerobic metabolism. This energy pathway is able to use FFA and the end-products of glycolysis to generate ATP *via* the TCA cycle and oxidative phosphorylation (Mukund & Subramaniam, 2020). Generally, type I and type IIA fibres of certain animal species display high activities of 3HAD, CS and SDH. These enzymes are important regulatory enzymes in aerobic substrate oxidation and can be used to evaluate the aerobic capacity of muscle. (Pette, 1985; Simoneau & Bouchard, 1989; Kohn, 2014).

I. 3-hydroxyacyl-Coenzyme A dehydrogenase (3HAD)

In mitochondria, 3HAD is responsible for the β -oxidation of fatty acids. Once within the muscle fibre, FFA mobilised from intramuscular triglyceride stores and *via* blood uptake are activated by the addition of a CoA group by fatty acyl-CoA synthase (Mukund & Subramaniam, 2020). Transport of activated fatty acids (in the form of acyl-CoA) across the mitochondrial membrane is facilitated by the transport protein carnitine. The oxidation of acyl-CoA to acetyl-CoA is catalysed by 3HAD and thiolase. Finally, acetyl-CoA is utilised in the TCA cycle where its by-products feed into the mitochondrial ETC (Schulz, 1991; Berg *et al.*, 2002; Yang *et al.*, 2005).

II. Citrate synthase (CS)

The TCA cycle comprises a series of mitochondrial reactions. Its main function is oxidising metabolites (from glucose, FFA and proteins) to generate NADH and FADH₂. These molecules are shuttled to the ETC where they are coupled to ATP production (Hänninen & Atalay, 1998; Akram, 2014). CS is a key regulating and rate-limiting enzyme in the TCA as it catalyses the condensation of acetyl-CoA to oxaloacetate, forming citrate. Moreover, CS is responsible for the integration of all carbon units into the TCA cycle as it is the only enzyme in the cycle capable of facilitating the catalysation of bonds between carbon units (Wiegand & Remington, 1986). Two thirds of total ATP production is accounted for by the TCA cycle, making it the primary metabolic pathway for aerobic metabolism (Baldwin & Krebs, 1981; Akram, 2014).

2.3.2. Anaerobic enzymes

During high intensity activities, anaerobic metabolism is the immediate source of ATP regeneration in skeletal muscle primarily from intramuscular ATP and PCr stores (Mukund & Subramaniam, 2020). Due to the limited amount of stored ATP and PCr, these activities can only be maintained for short durations (Schiaffino & Reggiani, 2011; Negro *et al.*, 2019). Glycolytic ATP replenishment (from blood glucose and muscle glycogen) is mainly due to anaerobic glycolysis and the Cr/ PCr system (Wyss & Kaddurah-Daouk, 2000). Generally, type IIX fibres are suited for anaerobic metabolism, reflected by elevated LDH, CK, and in some cases PFK and PHOS activities (Essén-Gustavsson & Henriksson, 1984; Pette, 1985).

I. Creatine kinase (CK)

Skeletal muscle has fluctuating energy requirements. ATP is immediately regenerated from ADP *via* the transfer of high-energy phosphate groups from pools of intramuscular PCr, and this reaction is catalysed by CK. There are different CK isoforms distributed across different subcellular compartments of muscle fibres that comprises the PCr energy shuttle system. (Wyss & Kaddurah-Daouk, 2000; Negro *et al.*, 2019). CK isoforms occur in the cytoplasm in areas with high ATP demand (such as myofibrils and the sarcoplasmic reticulum) and in mitochondria. In the cytoplasm, CK catalyses the phosphorylation of Cr to PCr and regenerates ATP from PCr *via* the transfer of its phosphoryl group to ADP. The mitochondrial isoform ensures the conversion to PCr from Cr and ATP supplied by the ETC, thus stimulating oxidative phosphorylation by restoring ADP levels. (Bessman & Carpenter, 1985; Wallimann & Hemmer, 1994; Negro *et al.*, 2019).

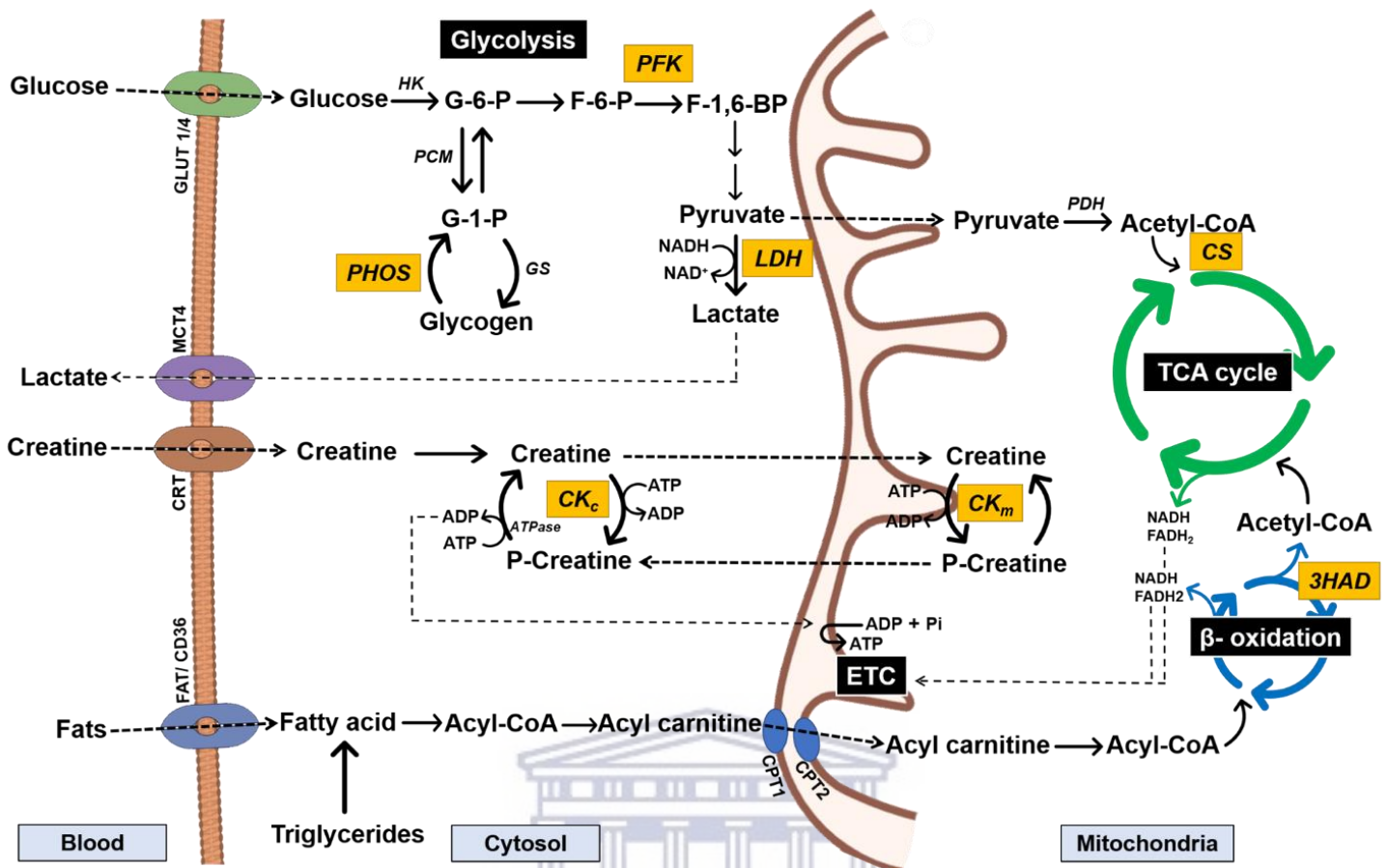


Figure 3: Energy-producing metabolic pathways in skeletal muscle. 3HAD, 3-Hydroxyacyl-Coenzyme A dehydrogenase; ADP, adenosine diphosphate; ATP, adenosine triphosphate; ATPase, adenosinetriphosphatase; CPT1/2, carnitine palmitoyltransferase 1/2; CRT, creatine transporter; CS, citrate synthase; CK_c, creatine kinase cytosolic isoform; CK_m, creatine kinase mitochondrial isoform; ETC, electron transport chain; F-1,6-BP, fructose-1,6-bisphosphate; F-6-P, fructose-6-phosphate; FADH₂, dihydroflavine-adenine dinucleotide; FAT/ CD36, fatty acid translocase/ cluster of differentiation 36; G-1-P, glucose-1-phosphate; G-6-P, glucose-6-phosphate; GLUT1/4, glucose transporter 1/4; GS, glycogen synthase; HK, hexokinase; LDH, lactate dehydrogenase; MCT4, monocarboxylate transporter 4; NAD⁺, nicotinamide adenine dinucleotide (oxidised form); NADH, nicotinamide adenine dinucleotide (reduced form); P-Creatine, phosphorylated creatine; PCM, phosphoglucomutase; PDH, pyruvate dehydrogenase; PFK, phosphofructokinase; PHOS, phosphorylase; Pi, inorganic phosphate; TCA, tricarboxylic acid cycle, based on Akram, (2013; 2014), Houten et al., (2015) and Negro et al., (2019).

II. Phosphofructokinase (PFK)

The fate of glucose and muscle glycogen during glycolysis is highly dependent on oxygen availability. In the absence of oxygen, glucose undergoes anaerobic glycolysis *via* a series of catalytic reactions to yield pyruvate (Akram, 2013; Mukund & Subramaniam, 2020). The phosphorylation of fructose-6-phosphate to fructose-1,6-bisphosphate is catalysed by the enzyme PFK and is the rate-limiting enzyme in glycolysis. In addition to hexokinase and pyruvate kinase, PFK is also an important regulator of glycolysis (Mansour, 1972; Schiaffino & Reggiani, 2011).

III. Lactate dehydrogenase (LDH)

Pyruvate, the end product of glycolysis has 2 fates dependant on oxygen availability and the metabolic demand for ATP. Under anaerobic conditions, the reversible conversion of pyruvate to lactate is catalysed by LDH (Markert, 1984). Additionally, lactate released into the blood can be transported to the liver, where LDH converts lactate to pyruvate *via* the Cori cycle (Holbrook *et al.*, 1975; Farhana & Lappin, 2020).

IV. Phosphorylase (PHOS)

In skeletal muscle, glucose is stored as glycogen. Glycogen is a highly branched molecule, and requires cleaving in order to yield glucose that can be utilised for ATP production (Krebs & Fischer, 1964). PHOS catalyses the initial step of glycogen degradation by cleaving the glycosidic bonds between terminal glucose units in glycogen chains. Hence, the primary function of PHOS is to supply the glycolytic pathway with phosphorylated glucose in response to the energy requirements of the muscle (Rocha Leão, 2003; Donnier-Maréchal & Vidal, 2016).

Like fibre type, the metabolic profile of an organism is generally aligned with the lifestyle and main activity employed by that organism. The skeletal muscle of animals with enhanced endurance abilities (horses, endurance athletes) are highly oxidative due to increased activities of aerobic enzymes in their muscle fibres (Gollnick *et al.*, 1972; Holloszy & Booth, 1976; Rivero & Hill, 2016). Endurance training is also associated with increased 3HAD and TCA cycle enzyme activities whereas resistance and sprint training has shown to increase the activities of certain anaerobic enzymes including LDH and PHOS (Holloszy & Booth, 1976; Roberts *et al.*, 1982). Animals that rely on rapid ATP mobilisation for quick bursts of energy such as the caracal and cheetah has also been shown to possess high anaerobic enzyme activities (Williams *et al.*, 1997; Kohn *et al.*, 2011b).

2.4. The skeletal muscle of cheetahs

To date, there are only 4 studies that investigated the distribution of muscle fibres in the cheetah. Of those, only 1 study briefly describes the skeletal muscle metabolic capacity.

The paper by Williams *et al.* (1997) is one of the earliest studies to investigate the histology and biochemistry of free-ranging (n=3) and captive cheetahs (n=3). Fibre type was determined by histochemical analysis using the ATPase stain to visualise type I and type II fibres. Subsequently, a NADH stain was performed to distinguish between type IIA and IIX fibres (Williams *et al.*, 1997). Slow oxidative (type I), fast oxidative glycolytic (type IIA) and

fast glycolytic (type IIX) fibres were visualised at pH 9.6. In the VL, approximately 72% of the total fibre population was type IIX fibres, 11% type IIA and 17% type I. In addition, the *Gastrocnemius* was comprised of approximately 60% type IIX fibres, 3% type IIA and 37% type I fibres. Similar observations for the *Gastrocnemius* muscle in a captive cheetah are reported by Hyatt et al. (2010) using gel electrophoresis and Western blotting. The latter study additionally reported the presence of type IIB fibres but this was only detected in 1 muscle group (Hyatt et al., 2010). There was no significant difference in fibre type proportion between free-ranging and captive cheetahs. Additionally, the capacities of key oxidative enzymes such as 3HAD and CS were lower in cheetahs compared to humans and other mammals (Essen et al., 1975; Kohn et al., 2011a; Kohn, 2014). In contrast, LDH and pyruvate kinase displayed high activities, suggesting a strong capability to utilise anaerobic metabolism for ATP production (Williams et al., 1997). This metabolic profile supports its apparent hunting behaviour, which consists of a quick high-speed pursuit followed by a slowing period for capturing prey (Wilson et al., 2013). Since most of the type II fibres reacted similarly with NADH, one of the limitations of the study was that very few type IIA fibres were detected (10% in the VL and in only 1 of the *Gastrocnemius* samples) and thus may not be an accurate depiction of the overall fibre population.

A comprehensive study by Goto et al. (2013) examined the skeletal muscle fibre population in the whole body of 2 captive cheetahs using immunohistochemical staining. In the hindlimb muscle, 50% of the fibre population was represented by type IIX fibres, followed by type IIA (29%) and type I (21%) fibres. In the neck and trunk muscles, the total fibre population consisted of 40% type IIX fibres, 32% type IIA and 28% type I fibres. Similarly, the muscle fibre population in the forelimb muscle comprised of 36% type IIX, 30% type IIA and 34% type I fibres. Moreover, the VL muscle of captive cheetah contains more type IIX fibres, followed by type I fibres, and the least number of types IIA fibres which conforms with the results presented by Williams et al. (1997) (Williams et al., 1997; Goto et al., 2013).

Evidently, a large proportion of muscles in the cheetah is characterised by a high percentage of type IIX fibres and low percentage of type I fibres as observed in many of the muscles. This is consistent with observations in other members of the Felidae family such as the tiger, lion, caracal and domestic cat (Hyatt et al., 2010; Kohn et al., 2011a; Goto et al., 2013). Although, in cheetahs the distribution of muscle fibres was not uniform across different muscle groups and muscle depths (Hyatt et al., 2010; Goto et al., 2013). Cheetah skeletal muscle display high glycolytic capacity and a low oxidative capacity, as indicated by elevated glycolytic enzyme activities and decreased oxidative enzyme activities, respectively. They are also capable generating a relatively large amount of force from their type II fibres,

compared to type I (West *et al.*, 2013) – an observation reported in lions, baboons, and trained athletes (Altringham & Johnston, 1990; Kohn & Noakes, 2013; Dada *et al.*, 2018). However, when comparing the results, it is evident that there are clear disparities in the literature. These may arise from limitations including the number as well as the status of the cheetah prior to analyses, the depth at which the muscle sample was obtained and the technique utilised to identify the fibre types. The high proportion of type IIX fibres in cheetah may suggest a high requirement for its main fuel type which is Cr/ PCr. Glycine, an important and potentially limiting AA in the diet of captive cheetahs, can be used to synthesise Cr (Razak *et al.*, 2017).

2.5. Glycine

Glycine is the simplest AA found in nature, representing 11.5% of total AAs in the human body. It has crucial structural, functional and protective roles in the metabolism of many mammals (Wu, 2010; Alves *et al.*, 2019).

AAs are classified as either nutritionally essential (EAA) or nutritionally nonessential (NEAA). EAAs are those whose carbon skeleton cannot be endogenously synthesised in mammals and must be included in diets, whereas the carbon skeleton of NEAAs can be endogenously synthesised in amounts sufficient to meet the basic metabolic requirements, and may be omitted in diets (Wu *et al.*, 2013). Glycine is classically categorised as a NEAA for mammals such as humans, pigs and rodents as it is synthesised *in vivo*, and thus its incorporation into the diet as a supplement was not previously considered (Gibson *et al.*, 2002). However, there are numerous studies suggesting that endogenous glycine synthesis may not be sufficient to meet the metabolic requirements in these species (Meléndez-Hevia *et al.*, 2009; Hou *et al.*, 2016; Liu *et al.*, 2017). In birds, for example, glycine is a vital requirement for growth and development, as foetuses and neonates are unable to synthesise sufficient quantities to maintain metabolic demands (Corzo *et al.*, 2004; Siegert & Rodehutschord, 2019). Hence, *de novo* glycine synthesis and its metabolism may be species-dependant and therefore, glycine is now considered as a conditionally essential AA in humans and some mammals (Wang *et al.*, 2013; Hou *et al.*, 2016).

2.5.1. Physiological effects of glycine

Of whole-body glycine, 80% is utilised for protein synthesis in mammals. Collagen and elastin are ubiquitous structural proteins and the primary components of the ECM in humans. Not only is glycine located at every third position in the collagen triple helix, it also stabilises the triple helical structure (Shoulders & Raines, 2009; Gillies & Lieber, 2011).

Glycine is responsible for the flexibility of enzyme active sites (Yan & Sun, 1997), and can serve as a precursor for a wide variety of substrates for energy producing pathways (Akinde, 2014). In the central nervous system, it serves as an important inhibitory neurotransmitter (Razak *et al.*, 2017). It participates in pivotal biosynthetic pathways including the production of purines (DNA and RNA synthesis), porphyrins and haem (necessary for oxygen transport), glutathione, serine, and Cr – an important metabolite in nerve and muscle metabolism and energy production (Hall, 1998). It indirectly regulates immunity, and is the major contributor to bile acid conjugation in mammals, thus having a role in the digestion and absorption of lipids (Hafkenscheid & Hectors, 1975). Holistically, glycine is an essential AA with important roles in metabolism, immunity, growth and overall survival in humans and animals (Razak *et al.*, 2017). Notably, glycine also has many therapeutic implications in gastrointestinal health, gastric ulcer treatment, serves as a protective agent for kidney and liver cells and improves cardiovascular health, all of which affects captive cheetahs globally (Razak *et al.*, 2017).

2.5.2. Glycine metabolism

The primary organs involved in glycine metabolism includes the liver, kidneys and pancreas (Hu *et al.*, 2017). In some animal species, dietary glycine intake satisfies at most approximately 50% of glycine requirements for optimum growth and metabolic maintenance. The remaining 50% must be synthesised endogenously to ensure optimal health (Li & Wu, 2018). Glycine is endogenously synthesised from choline, threonine, serine, and recently, hydroxyproline and glyoxylate (Wu *et al.*, 2011; Razak *et al.*, 2017).

Glycine can be synthesised from choline *via* its degradation by betaine aldehyde dehydrogenase (Zhang *et al.*, 1992). Methyl groups liberated from this reaction are utilised in downstream reactions in the formation of glycine from sarcosine in the presence of sarcosine dehydrogenase (Razak *et al.*, 2017). Choline dietary intake is usually low, ranging between 400 – 500 mg/day. Therefore, the contribution of choline to glycine synthesis is low (Wang *et al.*, 2013).

Glycine is produced as a by-product following the degradation of threonine *via* SHMT and threonine dehydrogenase (Razak *et al.*, 2017). In adult humans, only 11% of threonine is degraded by threonine dehydrogenase and essentially no threonine is converted to glycine in infants (Parimi *et al.*, 2005; Wang *et al.*, 2013). Previous studies have shown that choline and threonine contribute to less than 6% of glycine needs in young pigs (Li & Wu, 2018).

Serine obtained from dietary sources is converted to glycine in the cytoplasm and mitochondrial matrix of mammalian cells *via* cytosolic and mitochondrial SHMT, respectively (Razak *et al.*, 2017). The majority of glycine synthesis is facilitated by mSHMT whereas cSHMT converts serine to glycine to a much lower extent and is only expressed in the liver and kidneys (Wang *et al.*, 2013). Briefly, SHMT catalyses the reversible transfer of activated carbon units from serine to tetrahydrofolate (an important SHMT cofactor), yielding glycine. Pyruvate, a critical metabolite in skeletal muscle to fuel muscle contraction and relaxation, can also be synthesised from glycine *via* this metabolic pathway (Hall, 1998; Koopman *et al.*, 2017).

Finally, the synthesis of glycine from hydroxyproline and glyoxylate involves a transamination reaction catalysed by the enzyme AGT, yielding glycine and pyruvate (Wang *et al.*, 2013). Glyoxylate-derived glycine synthesis is very sparse as dietary intake of glycolate (a glyoxylate precursor) is limited in humans and other mammals. Therefore, metabolism of hydroxyproline in mitochondria is the primary source of glyoxylate in mammals (Wu *et al.*, 2011; Wang *et al.*, 2013). It is important to note that with each of the mentioned pathways, there are species, tissue, and development-specific differences amongst animals.

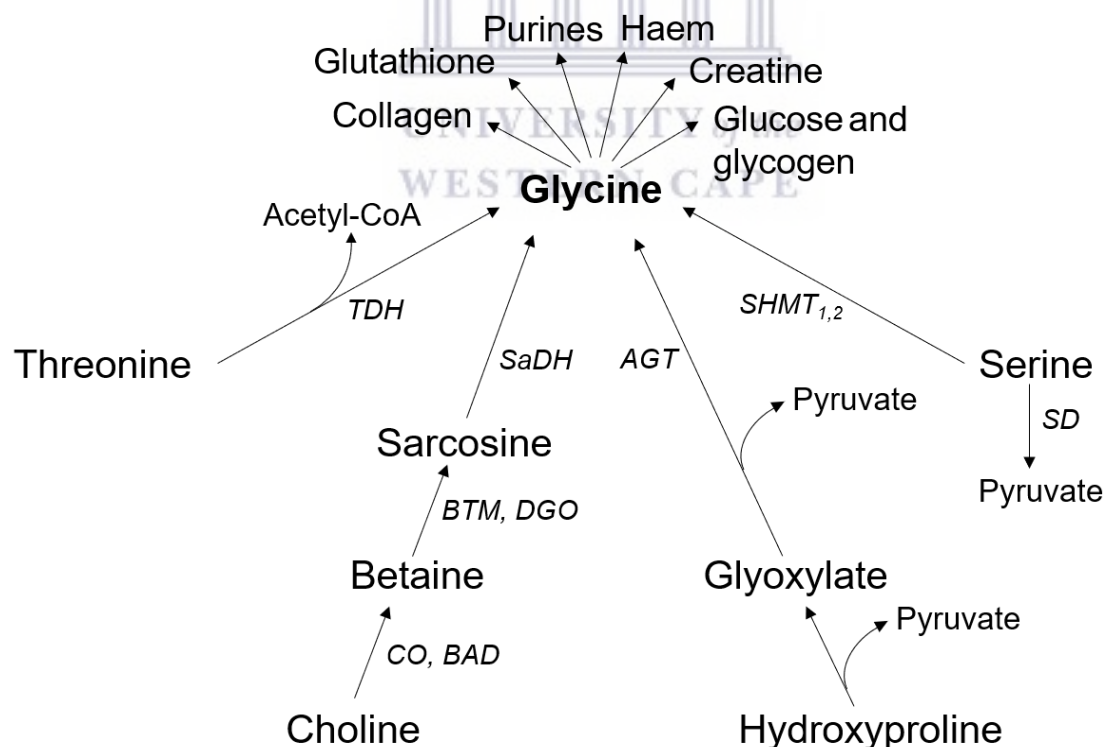


Figure 4: *In vivo* synthesis of glycine and its main metabolic products. AGT, alanine:glyoxylate aminotransferase; BAD, betaine alanine dehydrogenase; BTM, betaine transmethylase; CO, choline oxidase; DGO, dimethylglycine oxidase; SaDH, sarcosine dehydrogenase; SD, serine dehydrogenase; SHMT, serine hydroxymethyl transferase; TDH, threonine dehydrogenase, based on Razak *et al.*, (2017) and Wang *et al.*, (2013).

Glycine degradation in mammalian cells occur *via* 3 primary pathways and is essentially the reverse reaction of its synthesis: 1) conversion of glycine to serine by SHMT, 2) conversion into glyoxylate by d-amino acid oxidase and 3) deamination and decarboxylation of glycine by the GCS. The GCS found in most animals is responsible for the majority of glycine catabolism in the body (Wang *et al.*, 2013; Alves *et al.*, 2019).

Importantly, Cr synthesis requires the presence of glycine and arginine. In the kidneys, *L*-arginine: glycine amidinotransferase catalyses the transfer of an amidino residue from arginine to glycine to form GAA and *L*-ornithine. Subsequently, a methyl group is transferred to GAA *via* *N*-GAA methyltransferase, producing creatine. This step primarily occurs in the liver (Curt *et al.*, 2015).

2.6. Benefits of dietary glycine supplementation

As previously mentioned, glycine serves as a precursor for a variety of biologically important compounds. However, glycine cannot be recycled after its incorporation into many of these compounds (Gibson *et al.*, 2002). In birds, a glycine-dependant pathway rapidly produces uric acid as a waste product and in pigs, it has been shown that the glycine content in sows' milk is low (Liu *et al.*, 2017). In addition, endogenous glycine synthesis in these animals is not enough to support optimal growth, thereby emphasising the importance of a glycine-supplemented diet (Hou *et al.*, 2016).

Lowering the CP content is an effective way to reduce the expense of animal feed. Plant-based feeds have been shown to already contain a low glycine and serine content (Li *et al.*, 2011). Hence, lowering the total CP may severely affect the availability and utilisation of these AAs. For this reason, the majority of the glycine supplementation studies to date have been performed on bird species and domesticated farm animals.

Corzo *et al.* (2004) evaluated the dietary glycine needs of 0 to 21-day-old broiler chicks by enriching their diets with glycine in increasing increments. The addition of ~1% glycine significantly improved BW, feed conversion and increased plasma free glycine (Corzo *et al.*, 2004). Comparable results were reported by Ngo *et al.* (1977) and Waldroup *et al.* (2005) where glycine supplementation improved growth performance, BW, liver weight, daily weight gain, feed conversion and increased Cr content in the pectoral muscle of male broilers. In contrast, broilers on a glycine-deficient diet had decreased body and liver weight, reduced daily weight gain and significantly lower protein content (Ngo *et al.*, 1977; Waldroup *et al.*, 2005). Similar observations were reported by Dean *et al.*, (2006). Glycine supplementation has also been shown to increase intestinal villus height in poultry, thereby potentiating nutrient absorption and AA efficiency (Akinde, 2014).

In 14-day old piglets, glycine supplementation improved plasma glycine concentrations, daily weight gain and BW as well as enhanced glycine transport (Wang *et al.*, 2014). Glycine supplementation promoted cardiovascular function in rats by upregulating genes associated with oxidative capacity and fatty acid oxidation, thereby improving mitochondrial function (Cieslik *et al.*, 2018). Similarly, in skeletal muscle, the expression of genes associated with fatty acid biosynthesis, oxidation and transport in growing pigs on a glycine diet were increased. Interestingly, the pigs on a supplemented diet also had more oxidative fibres and less glycolytic fibres as determined by their gene expression (Zhou *et al.*, 2021). Glycine serves an intracellular modulator of calcium, which is vital for muscle contraction and also enhances the phosphorylation of enzymes involved in skeletal muscle protein synthesis (Wang *et al.*, 2013; Zhou *et al.*, 2021). In fish species, improved oxidative capacity, collagen deposition, growth rate and weight gain have been reported (Xie *et al.*, 2014; Koopman, 2017 #140; Xie *et al.*, 2016).

2.7. Glycine and skeletal muscle

Glycine has various important biological functions pertaining to skeletal muscle. The ECM is an important component of skeletal muscle and consists primarily of collagen, which is the largest and most abundant protein occurring in the body (Gillies & Lieber, 2011; Razak *et al.*, 2017). Glycine is a major constituent of collagen, and comprises a third of its triple helical structure (Wang *et al.*, 2013). Glycine can also be metabolised *via* numerous metabolic pathways to be incorporated in skeletal muscle metabolism by serving as a substrate or a precursor to a substrate that can be used for energy production. Cr, a crucial metabolite stored in skeletal muscle and essential for muscle contraction, can directly be synthesised from glycine (Wu, 2009). Additionally, other metabolites utilised by skeletal muscle such as pyruvate, acetyl-CoA and NADPH are produced *via* glycine metabolism (Wang *et al.*, 2013; Razak *et al.*, 2017).

Enhanced skeletal muscle growth and whole body collagen production were reported in 5 to 21-day old broilers following a diet supplemented with 0.2% glycine (Corzo *et al.*, 2005). Conversely, a long-term glycine deficiency results in a loss of muscle mass (Kohlmeier, 2015). Oral supplementation of glycine improved skeletal muscle function and longevity in 14-day old chicks by suppressing myofibrillar proteolysis (Nakashima *et al.*, 2008). In dogs and rodents, glycine supplementation has pivotal roles in muscle function, preventing muscle necrosis, and protecting skeletal muscle from ischemia and reperfusion injury (Ascher *et al.*, 2001; Ham *et al.*, 2014). Collectively, glycine serves as a vital AA actively involved in maintaining skeletal muscle mass and protein synthesis, while preventing muscle wasting (Riddle *et al.*, 2016; Koopman *et al.*, 2017).

2.8. Glycine deficiency in captive cheetahs

Poor nutrition and inappropriate feeding methods contribute to poor health, and it is speculated that 7% of the mortality in captive cheetahs are due to nutritional deficiencies (Bechert *et al.*, 2002). Particularly, glycine deficiency may be a prevalent health concern observed in captive cheetahs. Although short-term deficits may not be apparently detrimental, chronic glycine shortages may lead to compromised growth and immune function, abnormal nutrient metabolism, loss of muscle mass and compromised health (Razak *et al.*, 2017); (Alves *et al.*, 2019). Moreover, reproductive success, dental pathologies, gut health and psychological welfare have also been associated with dietary factors (Bond & Lindburg, 1990).

The diet of free-ranging cheetahs consists of a wider variety of animals compared to their captive counterparts. They have been reported to prey on birds (*Aves sp.*), hares (*Lepus sp.*), warthogs (*Phacochoerus africanus*), juvenile zebras (*Equus quagga*), giraffes (*Giraffa camelopardalis*), wildebeest (*Connochaete sp.*) and other antelope (*Bovidae*) species (Eaton, 1970; Hayward *et al.*, 2006; van der Meer, 2016). The soft flesh, skeletal muscle and most of the organs are consumed. Importantly, they also consume the carcass components such as bones, cartilage, tendons, skin, hair and feathers – all of which contain glycine-rich collagen (Krausman & Morales, 2005; Nickols, 2016). Studies have shown that feeding cheetahs carcass components significantly reduces the production of toxic phenolic compounds and markers of acute intestinal inflammation, improves stool consistency and increases the production of beneficial fatty acids (Depauw *et al.*, 2013; Depauw *et al.*, 2014; Whitehouse-Tedd *et al.*, 2015; Tordiffe *et al.*, 2016).

In contrast, captive cheetahs are generally fed commercially-prepared feed and diets consisting of muscle meat only, largely from horse, donkey, bovine or chicken origins (Bechert *et al.*, 2002). Glycine content of these diets are relatively low as the glycine-rich carcass components are usually omitted (Tordiffe, 2017). The exact nutritional dietary needs for cheetahs are still largely unknown and nutritional requirements are based on data from domestic felid species, although commercial canine formulations are routinely employed in feeding programmes for captive cheetahs (Bechert *et al.*, 2002; Ziegler-Meeks, 2009). Chemical analysis revealed that commercial diets and several supplemented meat diets contain disproportionate amounts of specific vitamins and minerals necessary to maintain felid requirements and lack an apparent source of glycine (Bechert *et al.*, 2002). Whole carcass feeding is considered the best method to mimic a naturalistic feeding regime (Bond & Lindburg, 1990; Whitehouse-Tedd *et al.*, 2015). However, this practice is rarely

implemented as the cost trumps that of commercial feed. Thus, a relatively cheaper and more practical alternative is to supplement the diet with glycine.

The physiology of the cheetah may suggest a high demand for glycine as type IIX fibres contain higher concentrations of Cr and PCr compared to other fibre types (Karatzaferi *et al.*, 2001; Gray *et al.*, 2008). The skeletal muscle of cheetah is dominated by type IIX fibres and display elevated glycolytic capacity, suggesting a strong dependence on anaerobic-based metabolism and a high demand for Cr - a metabolic product of glycine (Goto *et al.*, 2013; Razak *et al.*, 2017). Cheetahs have been reported to excrete up to 12 g of creatinine per day, approximately 6x more than human beings despite only weighing half as much as the average human (Feher, 2017; Tordiffe *et al.*, 2017). A typical meat diet (~1.5 kg of beef) contains approximately 3 g of creatine, suggesting that 9 g of creatine would have to be supplied by endogenous synthesis, thus requiring large quantities of glycine. Cheetahs produce high concentrations of potentially toxic phenolic compounds that are excreted *via* the urine and/ or faeces (Depauw *et al.*, 2014; Tordiffe *et al.*, 2017). Detoxification of these compounds is achieved *via* a chemical process called glycine conjugation, and consequently, also require large quantities of glycine (Tordiffe *et al.*, 2017). Hence, a high metabolic demand for glycine coupled with a low dietary glycine supply puts captive cheetahs at risk of suffering from a severe deficiency. Glycine supplementation and its benefits have been extensively researched, primarily in domesticated animals. However, there are no studies to date investigating the effects of glycine on skeletal muscle morphology and metabolism in captive cheetah.

2.9. Anticipated gain in knowledge

The current study would add to the existing body of literature by assisting in the characterisation of skeletal muscle fibre composition and metabolism of captive cheetah, as there is not much research done on their muscle physiology. In addition, the effects of a dietary glycine supplement on the health status of captive cheetahs are largely unknown, and there are no studies evaluating the potential implications in skeletal muscle. There is evidence to suggest that the diet plays a significant role in the incidence and progression of the diseases suffered by cheetahs in captivity (Depauw *et al.*, 2014; Whitehouse-Tedd *et al.*, 2015). The results obtained may potentially elucidate the interactions between glycine and muscle which would advance our understanding of skeletal muscle metabolism in a dietary context.

Glycine supplementation may be more practical and cheaper to maintain as opposed to whole carcass feeding. Thus, there would be benefit to manufacturers of wild and captive

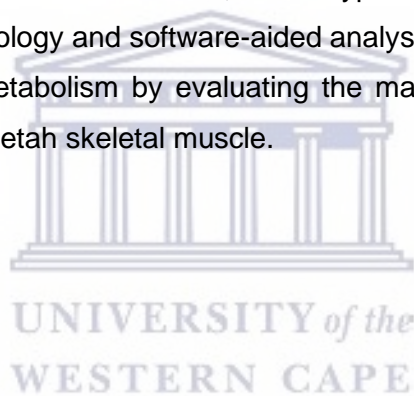
animal feed, zookeepers, conservationists and sanctuaries with regards to optimum nutrient composition and the incorporation of additional essential supplements to the diets of captive cheetahs and other wild animals.

Finally, the current research falls part of a bigger study investing the metabolomic effects of glycine supplementation in captive cheetahs and may serve as a foundation for wildlife researchers and veterinarians to gain further insight into the disparity between the health status of free-ranging and captive cheetahs as well as its potential causes.

2.10. Research aims

The aims of the present study were to investigate the skeletal muscle morphology and physiology, and to determine the effects of a 4-week glycine-supplemented diet on the skeletal muscle properties of captive cheetah. This was achieved by:

- 1) Determining skeletal muscle structure, fibre type distribution and CSA using immunofluorescent histology and software-aided analyses.
- 2) Determining muscle metabolism by evaluating the maximum enzyme capacity and glycogen content in cheetah skeletal muscle.



Chapter 3: Methodology and materials

3.1. Ethics and permits

Ethical approval for the study was obtained from the Animal Research Committee of the University of the Western Cape (reference: AR20/3/4). A Department of Agriculture, Forestry and Fisheries (DAFF) permit was also obtained under Section 20 of the Animal Diseases Act 1984 (reference: 12/11/1/7 (387)). Cape Nature permits were granted for the transport of animal samples (reference: CN44-31-5381). The current study also obtained a standing TOPS permit in collaboration with the University of Pretoria (UP) for the usage of endangered or protected species sample tissue (reference: N78/7707135156084). All relevant certificates are disclosed in Appendix E.

3.2. Research design and layout

The current study was a controlled experiment, based on a randomised longitudinal cross-over/ repeated measures research design. In such a design, each individual in the experiment receives all the treatments, and the results are measured over a period of time. Each participant serves as their own control, such that any differences measured can be compared to data collected from the same participant over time.

An advantage of each participant serving as their own control is that the factors contributing to between-subjects variability is reduced, resulting in a greater statistical power. Thus, a repeated measures experiment can be achieved with a small number of participants and increased efficiency. Individuals are still, however, susceptible to order and carryover effects. To control for such factors, the assignment of individuals to treatment groups were randomised, and a "washout" period was employed between treatments. The experimental layout is provided in Figure 5.

3.3. Research setting

The cheetahs were all housed and maintained at Cango Wildlife Ranch and Conservation Centre (Oudtshoorn, South Africa) (-33°33'34.79" S, 22°12'29.40" E) which is an internationally recognised and credible facility focusing on the conservation of cheetahs and other species through captive breeding and research. All staff are highly trained in the monitoring and maintenance of cheetahs. Each enclosure is of appropriate size equipped

with shaded and secluded areas to ensure the comfort of the cheetahs. The enclosures are also furnished with rocks, tree stumps and a variety of other natural artifacts that serve as vantage points, marking areas or scratching posts.

Diet intervention and sample collection took place at Cango Wildlife Ranch and Conservation Centre. The 3 sampling collection periods were during the months of spring (August – November 2020). Average minimum and maximum temperatures for the sampling months were 8°C and 18°C for August, 9°C and 20°C for September, and 13°C and 22°C for November 2022. Feed preparation and animal feeding were done on site. All sample collections were performed on site in the available surgical suite. Experimental analysis was performed in the Myology laboratory at the University of the Western Cape (UWC), (South Africa).

3.4. Study population

3.4.1. Animals

The study sample included 10 cheetahs (6 males and 4 females) selected from the captive population housed at the Cango Wildlife Ranch and Conservation Centre. Cheetahs are not easily accessible, as they are exotic and endangered species and COVID-19 restrictions made it near impossible to access cheetah sanctuaries. The sample size of 10, therefore, was the maximum number of cheetahs that the project and budget allowed for. All cheetahs were born in captivity and thus habituated to the environment and staff prior to study commencement. At the start of the study, the average age of the cheetahs was 3 ± 2 years. Average weight and BMI of the cheetahs at the start of the study were 40 ± 5 kg and 52 ± 4 kg·m⁻², respectively, where “m” represents a size index calculated by the product of length (m) and height (m). Cheetahs selected for the study were considered healthy with no prior signs of severe illness or disease, albeit 2 of the 10 cheetahs presented with mild to moderate gastritis, confirmed by a qualified veterinarian *via* gastric endoscopy. All animals remained on-site throughout the progression of the study and their transport was no more than 1 km. All animals successfully completed the diet intervention and none were euthanised during or upon termination of the study.

3.4.2. Animal diet prior to study initiation

All cheetahs included in the study were fed according to specific standardised feeding protocols employed by Cango Wildlife Ranch and Conservation Centre. Before the initiation

of the diet intervention, cheetahs were fed a daily diet consisting of ground horse muscle mince (1.3 – 2 kg) with 1 starve day (Sunday). This was based on the BW of the cheetah with adjustments for each animal's feeding history, appetite and response to food. Cheetahs also received additional organ (100 g) and skin mince (100 g) daily. All cheetahs were fed within their respective enclosures. These diets were supplemented with Carnivore Calcium Mixture (Kyron laboratories Pty LTD, Johannesburg, South Africa), Predator Supplement (V-tech Pty LTD, Healthtech laboratories, Johannesburg, South Africa) and iodised salt that was administered with the meat diets on alternate days (Appendix D). The total amount of food given and total food/ glycine ingested were monitored and recorded daily.

3.5. Diet intervention

Cheetahs were randomly selected and allocated into 2 groups: group A (n=4) and group B (n=6) matched for BW and BMI. Each group was then randomly chosen to start the intervention as either the treatment group or control group. After completion of the respective treatments, both groups were subjected to a cross-over, so that each group received both treatments. Feeding time, food type and food quantity were kept constant throughout the progression of the study.

3.5.1. Habituation

A habituation period of 3 weeks was implemented before commencement of the diet intervention, during which all cheetahs were fed a uniform diet consisting of horse meat supplemented with 10 g/kg of meat and Panthera Supplement only (WildCat Nutrition Pty LTD, Pretoria, South Africa). Habituation periods are routinely employed to allow animals to acclimatise to their temporary surroundings or experimental conditions. Dietary habituation serves to determine any apparent effects of the experimental diet on the study subjects. As all cheetahs were not receiving the same dietary treatments prior to the initiation of the study, it was also included to normalise the dietary intake of the cheetahs and mitigate any residual effect from their previous diet and/ or supplements. Habituation periods of 3 days to 2 months are generally practiced (Barnard *et al.*, 1970; Serrano *et al.*, 2000; Xie *et al.*, 2014; Xie *et al.*, 2016). A period of 3 weeks was decided, as the metabolic and dietary needs of cheetahs are largely unknown.

3.5.2. Intervention diets

The study comprised of 2 intervention periods, each lasting 4 weeks. A 2-week washout period was included between diet interventions to mitigate any carryover effects. The meat diets were standardised for all cheetahs and the feeding schedules and method of feeding implemented by Congo Wildlife Ranch and Conservation Centre were followed. The overall timeline and layout of the study are presented in Figure 5. The 2 diet interventions were as follows:

1. Control – diet consisted of 1.3 – 2.0 kg horse meat supplemented with 10 g/kg of meat Panthera Supplement (WildCat Nutrition Pty LTD, Pretoria, South Africa) sprinkled into deep cuts made within the meat.
2. Intervention – This diet consisted of 1.3 – 2.0 kg horse meat supplemented with 10 g/kg of meat Panthera Supplement (WildCat Nutrition Pty LTD, Pretoria, South Africa) and an additional 30 g/kg meat Glycine Supplement (WildCat Nutrition Pty LTD, Pretoria, South Africa) sprinkled into deep cuts made in the meat.

Horse meat supplemented with 10 g/kg of meat Panthera Supplement (WildCat Nutrition Pty LTD, Pretoria, South Africa) was fed to the cheetahs during the 2-week washout period.

Both control and intervention diets were fed to all cheetahs once per day, 6 times per week with a starve day on every Sunday. Monitoring sheets and observation were utilised to

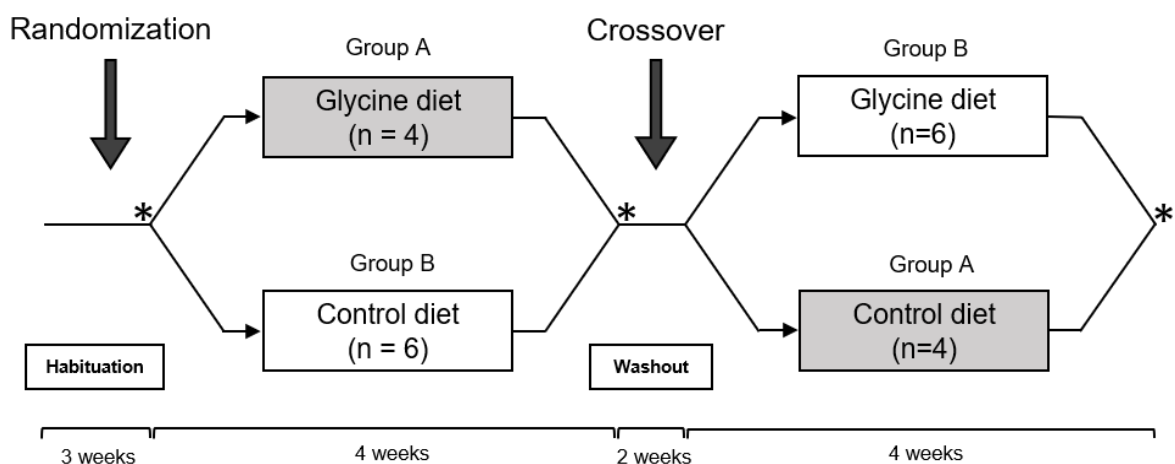
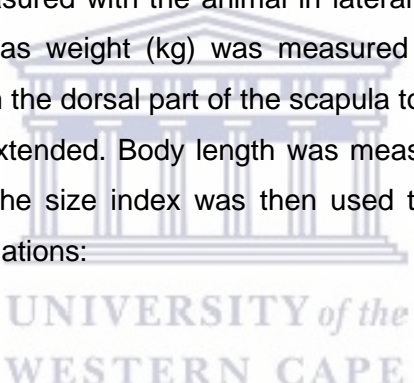


Figure 5: Schematic diagram of the layout for the 2-period crossover glycine diet intervention. Group A (shaded box) initially received the glycine-supplemented diet while group B (white box) initially received the control diet for 3 weeks. The groups then crossed over following a 2-week washout period. The asterisks (*) indicates the sampling occasions. Muscle biopsies were taken from the VL muscle and was staggered over a period of 2 days.

record the total amount of food given, food ingested and food left over for each cheetah throughout the progression of the intervention. No animal loss due to attrition was observed as all cheetahs successfully completed both diet interventions.

3.6. Sample collection

Muscle sample collection occurred on 3 occasions following the termination of the habituation and diet interventions. Collection of muscle samples was accomplished over a period of 2 days, and sampling sequence and time were kept constant for all sampling periods. Cheetahs were immobilised *via* hand-injections to the hindlimb by their respective caregivers in their enclosures. This ensured minimal stress, pain and discomfort experienced by the animals. Cheetahs were carried by means of a scoop stretcher and transported from their enclosures to the designated on-site surgical suite *via* a pickup truck ("bakkie"). Physical parameters were measured for every cheetah at each sampling cycle. Height (m) and body length (m) were measured with the animal in lateral recumbency using a flexible plastic measuring tape, whereas weight (kg) was measured on a walk-on scale. Height measurements were taken from the dorsal part of the scapula to the middle of the metatarsal pad with the entire limb fully extended. Body length was measured from the occiput of the skull to the base of the tail. The size index was then used to calculate the BMI of each cheetah using the following equations:



Size index (SI) = Height (m) × Body length (m), and

$$\text{Body Mass Index (BMI)} = \frac{\text{Weight (kg)}}{\text{Size index (SI)}}$$

Vital signs (heart rate, respiratory rate, oxygen saturation, and rectal temperature) were closely monitored during the surgery. The depth of immobilisation, mucus membrane colour, muscle tone, and body condition score were recorded every 5 minutes (data not shown).

3.6.1. Anaesthesia

The injection contained 30 µg/kg Medetomidine hydrochloride (Kyron Laboratories Pty LTD, Johannesburg, South Africa) and 1 mg/ml Zolazepam/tiletamine (Zoletil®, Virbac, South Africa). Reversal of the anaesthetic was achieved by injection of Atipamezole (Antisedan,

Wildlife Pharmaceuticals, South Africa). All anaesthesia data were recorded *via* a monitoring sheet.

3.6.2. Muscle biopsy

Samples were obtained from the VL (midway between the hip and knee) *via* an open muscle biopsy technique using a sterile scalpel and medical forceps. The VL muscle is one of the largest muscle groups in mammals, making it more accessible and relatively easier to sample compared to other muscles. Due to its size, it is also the safest option to perform multiple biopsies with the least risk of injury. As the most common muscle sampled and studied in both animal and human models, it also ensures data comparison (Nowak & Reyes, 2008). The sampling area was first shaved of fur using hair clippers and disinfected using Bioscrub™ (B. Braun Medical Pty LTD, Randburg, South Africa) and F10® SC veterinary disinfectant (Health and Hygiene Pty LTD, Roodepoort, South Africa). An incision was made approximately 2 cm in length and 2 cm deep. A portion of the mid VL muscle (400 - 500 mg wet mass) still attached to the connective tissue was harvested and immediately deposited into a tube containing saline-wetted gauze and temporarily placed on ice (4 °C). Muscle biopsies were performed on alternating legs for each sampling period and took no longer than 10 minutes. As skeletal muscle possesses no pain receptors, stress and pain were kept to a minimum. Excessive movements and loud noises were kept to the minimum during sampling.

Dermal looping sutures stabilised *via* stapling or intradermal sutures were used to close the incised wound after each muscle biopsy.

3.6.3. Muscle processing, storage and transport

Muscle samples were divided into appropriately-sized portions on a cork cutting board kept damp with saline using a medical scalpel and forceps. Orientation of the muscle fibres were determined using a magnifying glass with the length of the muscle indicating the direction of fibres. Muscle pieces were rapidly frozen in liquid nitrogen and transferred to pre-frozen cryovials. These were subsequently stored in a Styrofoam container on dry ice (-60 °C) lined with newspaper and kept in an on-site chest freezer at -20 °C.

Samples were transported from the venue in a Styrofoam container on dry ice lined with newspaper and stored at -80 °C until analyses.

3.7. Immunohistochemistry

Immunofluorescent histological analysis was performed on VL muscle sections *via* incubation with antibodies specific for MHC isoforms as described by Dada et al., (2018) with modifications. Muscle fibre types were visualised following immunofluorescent staining. Skeletal muscle fibre distribution and the CSA of each fibre type were subsequently determined. A more detailed protocol is described in Appendix A.

3.7.1. Sample preparation and sectioning

A portion of VL muscle was mounted on a small piece of cork, submerged in Tissue-Tek® O.C.T Compound (Sakura Finetek, California, USA) and rapidly frozen in liquid nitrogen during tissue collection. The frozen muscle samples were sectioned using a cryostat (Leica CM1100, Leica Biosystems, Wetzlar, Germany) set to and maintained at a temperature of -25 °C. Serial cross sections of 10 µm were obtained and each section was transferred onto frosted glass microscope slides (Lasec® SA Pty LTD, Cape Town, South Africa). The orientation of each section was ascertained under a microscope and stored at -20 °C until further processing.

3.7.2. Staining procedure

Microscope slides were retrieved from the freezer (-20 °C) and equilibrated to room temperature. The sections were fixed in pre-chilled acetone at -20 °C for 2 min. Excess acetone was tapped off, the slides allowed to reach room temperature, and the sections hydrated in PBS, pH 7.4 for 2 min. Donkey serum solution (5%) prepared in PBS was used to block non-specific binding sites. The sections were incubated in a humidifying chamber for 1 hour at room temperature. Thereafter, the sections were incubated at 4 °C overnight with monoclonal primary antibodies specific to the MHC isoform type I (BA-D5), type IIA (2F7) or type IIX (6H1). An additional monoclonal primary antibody specific to the glycoprotein laminin (C4) was utilised to visualise the basal lamina of the muscle fibres. All primary antibodies were purchased from Developmental Studies Hybridoma Bank (DSHB, University of Iowa, USA). The sections were then hydrated with PBS and incubated with fluorescently-tagged secondary antibodies for 2 hours at room temperature in a humidifying chamber. Secondary antibodies utilised were AMCA AffiniPure goat anti-mouse IgG2b (code number: 115-115-207), AlexaFlour® 488 goat anti-mouse IgG1 (code number: 115-545-205), and Cy™3 AffiniPure donkey anti-mouse IgM (code number: 715-165-140). All secondary antibodies were purchased from Jackson laboratories (Jackson ImmunoResearch Inc.,

Pennsylvania, USA). Primary and secondary antibodies were diluted at a ratio of 1:50 and 1:500, respectively except for laminin (C4), which was diluted at a ratio of 1:100 and 1:500, respectively. The sections were hydrated once more in PBS. Mowiol mounting media (Mowiol®, Sigma-Aldrich, USA) containing Antifade Solution (Chemicon®, Merck, Germany) was prepared to mount cover slips covering all sections and stored at 4 °C until image processing.

3.7.3. Image visualisation and processing

Sections were visualised using a fluorescence microscope (Nikon Eclipse 80i, New York, USA) fitted with a digital camera (Canon EOS 650D, Pretoria, South Africa) at 10x magnification. Images at the specific excitation/ emission wavelengths for each fluorophore were acquired and merged to show all fibre types on a single image for subsequent fibre counting and calculation of CSAs.

3.7.3.1. Fibre counting and distribution

All fibres within the view-field were included in the fibre counting. Muscle fibres were classified as either type I, type IIA, type IIX or hybrid type IIA/X fibres based on their fluorescence. An average of 539 ± 190 fibres were counted and typed. Muscle fibre distribution (%) was determined using the following calculation:

$$\text{Fibre type (\%)} = \frac{\text{number of fibres counted per type}}{\text{total number of fibres counted per section}} \times 100$$

3.7.3.2. Cross-sectional area (CSA)

The Java image processing computer program ImageJ Version 1.8.0 (National Institute of Health, Bethesda, Maryland, USA) was used to determine the CSAs of the fibres based on pixel measurement set to a pre-calibrated scale. CSA was measured for a maximum of 30 fibres per fibre type and reported as mean (μm^2) \pm S.D. Three sections of the image were selected and the CSA of 10 fibres per fibre type was measured in each section. Only whole and in-tact muscle fibres were included for CSA measurement such that muscle fibres partially out of the field of view were excluded. Swollen or longitudinal fibres were also excluded from the analyses.

3.8. Enzyme assays

Fluorometric enzyme activity analyses were performed on the VL muscle to evaluate the maximum enzyme capacities within the muscle fibres. Total protein content was determined and the maximum oxidative and glycolytic capacities of each cheetah subsequently evaluated.

Briefly, the principle of the enzyme analyses relies on the conversion of NAD/ NADP⁺ to its reduced forms NADH/ NADPH + H⁺ or vice versa. The direct or coupled reaction can either cause an increase or a decrease in these molecules, dependant on the metabolic pathway of the enzyme. A more detailed protocol can be found in Appendix B.

3.8.1. Homogenate preparation

Muscle samples were prepared for enzyme analysis as outlined by the protocol described by Curry et al. (2012) with minor modifications. An average w.w. of 62 ± 14 mg frozen muscle tissue was used. The tissue was diluted with 0.1 M potassium phosphate buffer, pH 7.3 to a ratio of 1:19 (19 µl homogenising buffer added for every 1 mg frozen tissue). The tissue was homogenised on ice using a glass homogeniser. The tissue was sonicated thrice for 10 seconds at 3 W (Virsonic 100, Virtis, Gardiner NY, USA). Further dilutions were prepared from the sample homogenate for subsequent protein content determination and enzyme analyses. Sample homogenates and dilutions were stored at -80 °C until analysis.

3.8.2. Protein content

The protein content of each tissue sample was determined using the Bradford method based on the principle of protein-dye binding (Bradford, 1976). A 5x dilution was prepared in 0.1 M potassium phosphate buffer, pH 7.30, from the sample homogenate. A sample volume of 5 µl was pipetted in duplicate into a clear-bottom 96-well microplate and 270 µl Bradford reagent added. The microplate was covered with aluminium foil and allowed to incubate for 10 minutes at room temperature. An end-point absorbance reading was made at 595 nm using a SpectraMax® iD3 multi-mode microplate reader (Molecular Devices, LLC, California, USA) and the unknown protein concentration was calculated from a BSA standard curve (0 – 3 g·l⁻¹) using the formula:

$$x_1 = \frac{-b \pm \sqrt{(-b)^2 - 4(a)(c)}}{2(a)} \times Df,$$

Where: X_1 , root of the quadratic function, protein concentration ($\text{g}\cdot\text{l}^{-1}$); a, b and c, coefficients of the function; and Df, dilution factor.

The Bradford assay is a widely accepted protocol and one of the most common methods of protein quantification used in research, and the primary method employed by our lab thus ensuring comparability. Compared to other methods of protein quantification techniques (e.g., Biuret, Lowry, and bicinchoninic acid method), the Bradford assay offers the best cost-effective approach as it is a rapid, sensitive, inexpensive assay with no prior evidence of interfering substances significantly affecting results. It is also stable for up to 1 hour at room temperature (Vuori *et al.*, 1979; Bellof *et al.*, 2007; Olson & Markwell, 2007). A previous study confirmed that the Bradford assay provided greater reagent stability, protein-reagent stability and range of linearity compared to the Lowry assay in the determination of protein content from skeletal muscle (Seevaratnam *et al.*, 2009).

3.8.3. Enzyme assays

Enzymes representing the respective metabolic pathways were evaluated for maximum enzyme activities. CS and 3HAD activities representing the flux through the TCA cycle and β -oxidation, respectively, were determined to evaluate the oxidative potential of muscle fibres. LDH (representing lactate production), PFK (flux capacity of glycolysis) and PHOS (glycogen breakdown and utilisation) activities were determined to evaluate the glycolytic potential of fibres, whereas CK was measured for rapid ATP replenishment. The protocol described by Kohn *et al.* (2011a) and Kohn *et al.* (2007) were followed with some adjustments.

Respective dilutions were prepared from the sample homogenate as specified by the protocol (Appendix B). The working reagents for each assay were made up prior to analysis and kept at room temperature. A small sample volume was pipetted in duplicate into a black-bottom 96-well microplate followed by 250 μl of the respective working reagent which initiated the reaction. Maximum enzyme activities were determined by measuring the change in NADH and NADPH at set time intervals. All enzymes were measured fluorometrically at 25 °C using a SpectraMax® iD3 multi-mode microplate reader (Molecular Devices, LLC, California, USA) with excitation and emission wavelengths set at 340 nm and 460 nm, respectively. The slope (change in fluorescence over time) was calculated for each sample. An NADH or NADPH standard curved was generated to determine the maximum enzyme activity of each sample ($\mu\text{mol}\cdot\text{min}^{-1}\cdot\text{g}^{-1}$ protein) using the following formula:

$$\text{Enzyme activity } (\mu\text{mol} \cdot \text{min}^{-1} \cdot \text{g}^{-1} \text{ prot.}) = \frac{\left(\frac{(Dt) \times (\Delta Fl)}{(m) \times (Dm)} \times Ds \right) \times (Dm)}{Cp}$$

Dt, total dilution factor; Dm, muscle dilution; Ds, sample dilution; ΔFl , change in fluorescence over time; m, slope of the standard curve; and Cp, protein concentration ($\text{g} \cdot \text{l}^{-1}$).

Details pertaining to working reagent and assay specifications are outlined in Appendix B.

3.9. Glycogen assay

The total muscle glycogen concentration in the VL was determined *via* the measurement of glucose equivalents. After glycogen digestion, total glucose concentration was determined spectrophotometrically using an enzymatic method of glucose measurement.

The determination of glucose was based on the production of the reduced forms of NADP⁺ in an enzymatic reaction coupled to glucose utilisation. The total glucose content was then determined using a standard curve and glycogen subsequently calculated. A detailed protocol can be found in Appendix C.

The current method of glycogen quantification has been utilised in previous and on-going research performed in our lab. It is a widely accepted protocol and is based on previously published methods (Passonneau & Lowry, 1993; Webster *et al.*, 2016).

3.9.1. Glycogen extraction

Approximately 51 ± 15 mg of frozen muscle was weighed and transferred to pre-labelled and weighed microtubes. The final weight for each microtube was recorded for final glycogen concentration calculation. Glycogen extraction was achieved using a previously defined protocol with modifications (Passonneau *et al.*, 1993). Following alkaline digestion with 40% potassium hydroxide (KOH), the tissue was placed in a heating bath set to 100 °C for 30 min with occasional mixing. After cooling to room temperature, the glycogen was precipitated with a volume of absolute ethanol. The microtubes were centrifuged and incubated at 4 °C overnight. The next day, the samples were centrifuged and the supernatant decanted. After air-drying, the glycogen pellet was washed with absolute ethanol. The glycogen pellet was then hydrolysed to glucose by the addition of 2 M hydrochloric acid (HCl) and incubation in a

heating block at 100 °C for 3 hours with regular mixing. After cooling, 0.2 M Tris buffer, pH 7.5 and 2 M sodium hydroxide (NaOH) was added to each microtube. Universal indicator was added to each sample and the pH adjusted with 1 M HCl or 1 M NaOH. The microtubes were weighed to determine the final volume before glucose analysis.

3.9.2. Glucose analysis and glycogen determination

Glucose concentration was analysed using the enzymatic method of determination described by Passonneau *et al.* (1993). A volume of sample was pipetted in duplicate into a clear-bottom 96-well microplate followed by 250 µl glucose reagent to initiate the reaction. After a 15 min incubation, absorbance was measured using a SpectraMax® iD3 multi-mode microplate reader (Molecular Devices, LLC, California, USA) set to a wavelength of 340 nm at 25 °C. A glucose standard curve was generated and used to calculate the unknown glucose concentrations (mmol·l⁻¹) of each sample. The glycogen concentration (mmol·kg⁻¹ dry weight) was calculated using the following formula:

$$[\text{Glycogen}] (\text{mmol} \cdot \text{kg}^{-1} \text{ d.w}) = \frac{[\text{glucose}] (\text{mmol} \cdot \text{l}^{-1}) \left(\frac{W_f(g) - W_t(g)}{W_s(g)} \right) \times 4}{0.23}$$

Wf, final weight; Wt microtube weight; Ws, muscle sample weight

3.10. Statistical analysis

Data are reported as mean ± S.D. Normality of all data was determined and confirmed using a Shapiro-Wilk test. A one-way ANOVA with repeated measures was subsequently performed to compare the means between treatment groups and a Tukey post-hoc test to determine significance between groups and pairs. Statistical procedures and figure construction were performed using GraphPad Prism for Windows 10, version 5.03 (GraphPad Software Inc., La Jolla California, USA). Significance was set to $P < 0.05$.

The current study only had access to 10 cheetahs, and took samples on 3 occasions. Although no power analysis was performed, the sample size of 10 is nevertheless the highest number of cheetahs reported on in a study of this nature and sufficient for statistical analyses.

Chapter 4: Skeletal muscle morphology

4.1. Results

4.1.1. Fibre type composition

IHC analyses were performed to determine the fibre type in VL muscle of 10 captive cheetahs (Figure 6D). Primary antibodies BA-D5, 2F7 and 6H1 were used to visualise type I, type IIA and type IIX fibres, respectively (Figure 6A - C). All primary antibodies bound strongly to MHCI, MHCIIA, MHCIIIX or laminin (Figure 6B). A small proportion of fibres reacted with both 2F7 and 6H1 primary antibodies and these were labelled as hybrid type IIA/X fibres. However, these fibres represented a small percentage (<3%) of the total fibre population and were equally added to type IIA and IIX fibres.

Figure 7 displays the fibre type composition (%) of type I, IIA and IIX fibres in the VL muscle across the various treatment groups. The proportion of fibre types remained unchanged in response to the glycine-supplemented diet. At baseline, type I fibres amounted to $18 \pm 4\%$ (range; 9 - 23%), type IIA fibres to $19 \pm 6\%$ (12 - 30%) and type IIX fibres were the highest proportion, comprising $63 \pm 5\%$ (55 - 72%) of the total fibre population. After the 4 weeks of consuming the control diet (control group), the proportion of fibre types were similar compared to baseline, i.e., type I fibres, followed by type IIA and type IIX, comprising of $19 \pm 7\%$ (9 - 29%), $21 \pm 6\%$ (12 - 31%), and $61\% \pm 5$ (56 - 73%), respectively. Likewise, cheetahs after consuming the glycine-supplemented diet had a type I, type IIA and type IIX distribution of $21 \pm 5\%$ (14 - 30%), $19 \pm 4\%$ (12 - 26%), and $60 \pm 4\%$ (52 - 66%). Overall, type IIX fibres were the predominant fibre type observed in cheetahs across all treatment groups ($61 \pm 5\%$), followed by type IIA fibres ($20 \pm 5\%$), with type I fibres representing the lowest proportion of all fibre types ($19 \pm 6\%$). A Shapiro-Wilks test confirmed normality in all groups and a repeated measures one-way ANOVA with a Tukey's post-hoc test detected no significance between the baseline, control and glycine groups ($P < 0.05$).

4.1.2. Fibre cross-sectional areas (CSA)

The average CSA of all cheetah fibre types for the treatment groups in VL muscle is displayed in Figure 8. CSA was determined by measuring the circumference of individual fibres using image-analysis software. There were no significant changes to CSA following a glycine-supplemented diet. The average CSA of type I, type IIA and type IIX fibres at baseline were $3268 \pm 533 \mu\text{m}^2$, $4810 \pm 805 \mu\text{m}^2$, and $5427 \pm 957 \mu\text{m}^2$, respectively. The range of type I, type IIA and type IIX fibres were $2340 - 3884 \mu\text{m}^2$, $3237 - 5693 \mu\text{m}^2$, and

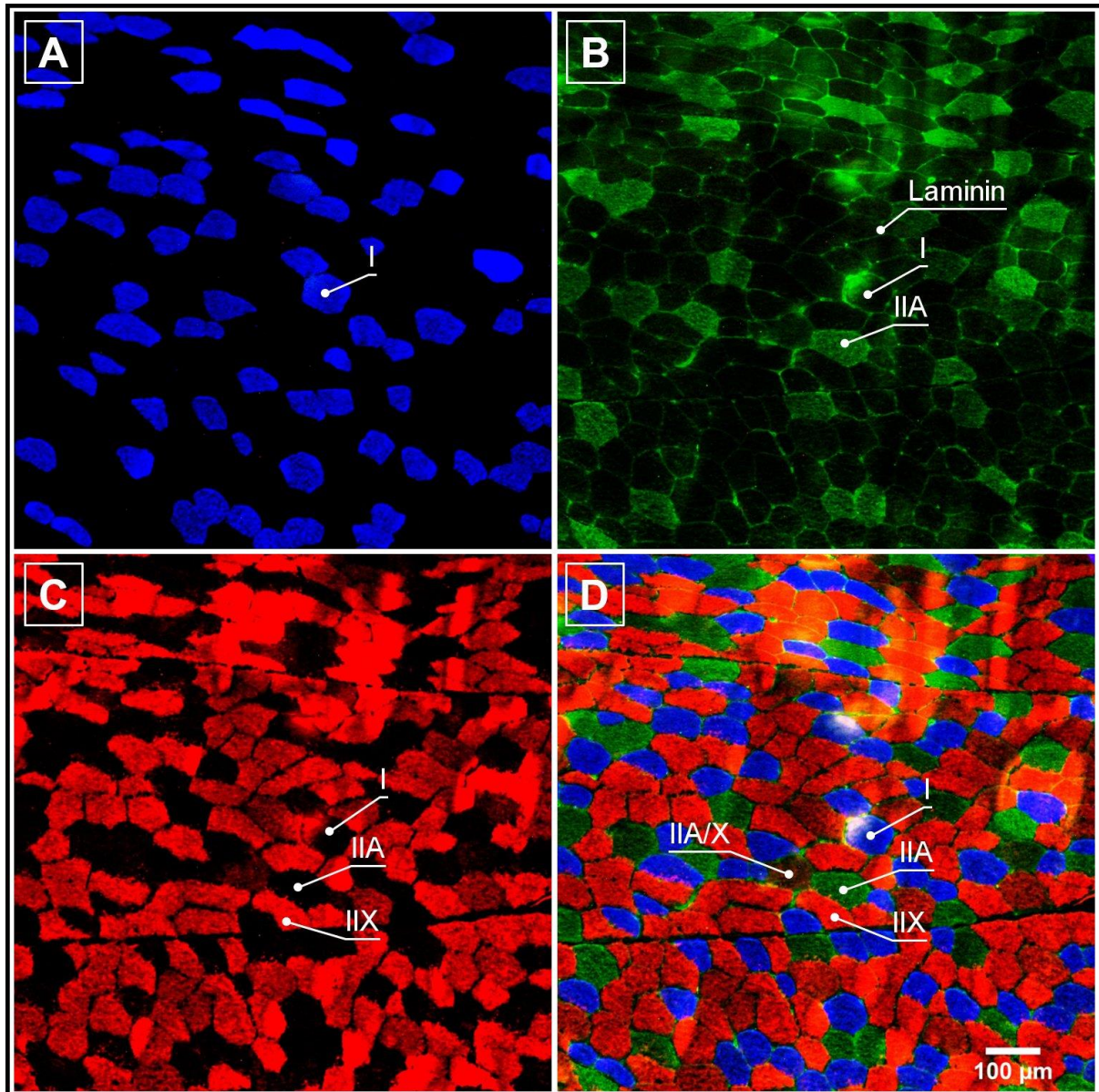


Figure 6: Fluorescent IHC of a cross-section from the VL muscle of a captive cheetah (*Acinonyx jubatus*). A, type I fibres expressing MHC I strongly positive for BA-D5 (blue); B, type IIA fibres and basal lamina expressing MHC IIA and laminin, respectively. MHC IIA and laminin were stained using 2F7 and C4 (both indicated by green); C, type IIX fibres expressing MHC IIX stained using 6H1 (red); and D, composite image displaying all 3 fibre types and the basal lamina. Type IIA/X fibres are indicated (D). These fibres stained lightly for both 2F7 and 6H1 but represented less than 3% of the fibre population and were divided between type IIA and type IIX fibres. The scale bar is presented at the bottom right and applies to all panels, 100 μm . All images were captured at 10x magnification.

4096 - 7338 μm^2 , respectively. In the control group, type I fibres had an average CSA of $2861 \pm 873 \mu\text{m}^2$ (1751 - 4346 μm^2), type IIA fibres; $4236 \pm 845 \mu\text{m}^2$ (3341 - 5971 μm^2), and the average CSA of type IIX fibres were $5010 \pm 1357 \mu\text{m}^2$ (3108 - 7249 μm^2). Similarly, the average CSA of cheetah VL in the glycine group was $2898 \pm 864 \mu\text{m}^2$ (1699 - 4775 μm^2) for type I fibres, $4448 \pm 949 \mu\text{m}^2$ for type IIA fibres (2884 - 6479 μm^2), and $4943 \pm 1102 \mu\text{m}^2$ for type IIX fibres (3080 - 6955 μm^2). Overall, the largest average CSA across all treatment

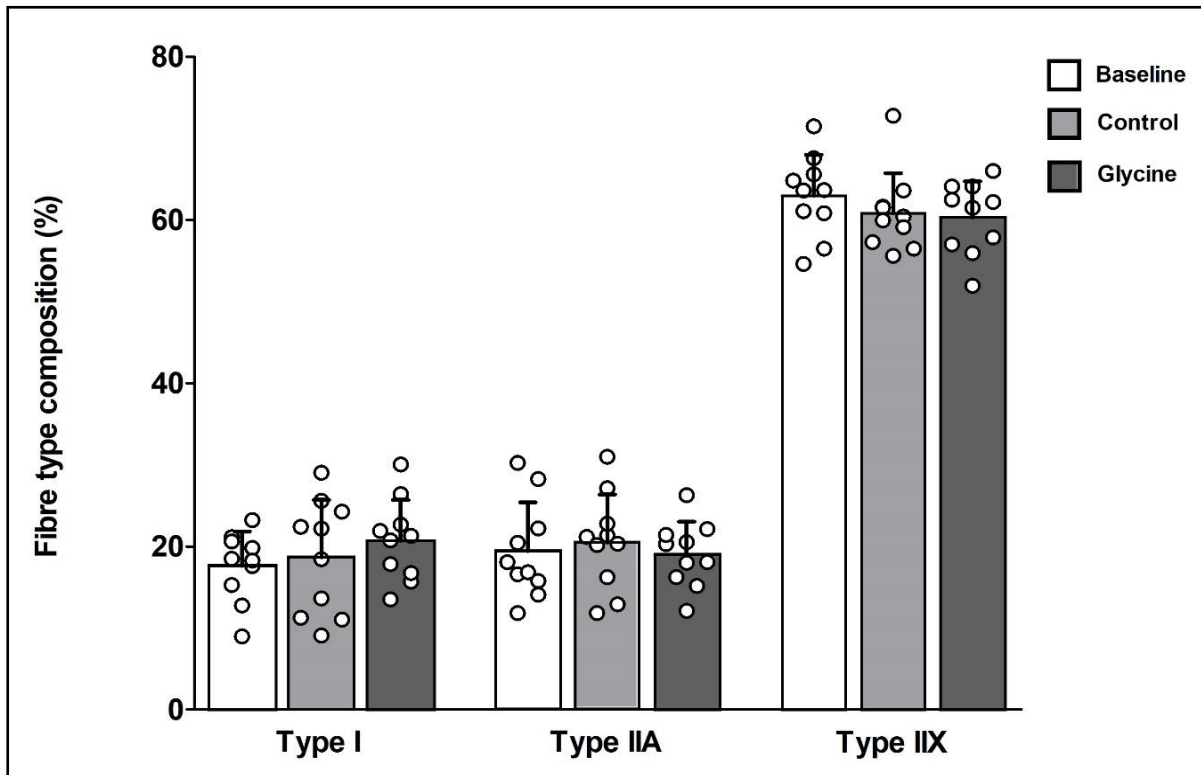


Figure 7: Fibre type composition (%) of the VL muscle of 10 captive cheetahs (*Acinonyx jubatus*) for different dietary interventions. Muscle biopsies were sampled on alternating legs on 3 occasions. Fibre type composition (%) (determined by IHC analyses) is displayed on the y-axis and fibre type are displayed on the x-axis. Baseline values are depicted by white bars, control diet is depicted by light grey bars and the glycine diet is depicted by dark grey bars. Bars represent the means \pm S.D. for each fibre type, and individual values for each cheetah are depicted by white circles (n=10). Due to the cross-over nature of the study, the control and glycine groups from each sampling period were pooled together.

groups appeared to be type IIX fibres ($5127 \pm 1131 \mu\text{m}^2$), followed by type IIA fibres ($4498 \pm 872 \mu\text{m}^2$). Type I fibres had the smallest CSA ($3009 \pm 769 \mu\text{m}^2$) amongst the fibre types. No significant differences were detected between type I fibres, type IIA fibres or type IIX fibres across treatment groups using a repeated measures one-way ANOVA. The S.D. of the CSAs of type I, type IIA and type IIX fibres were large, as observed by the wide spread of the data points (Figure 8). Tukey's multiple comparison test revealed significant differences between type I and type IIA fibres for all treatment groups, and type I and type IIX fibres, but not between type IIA and type IIX fibres of the same treatment groups across all treatments ($P < 0.05$).

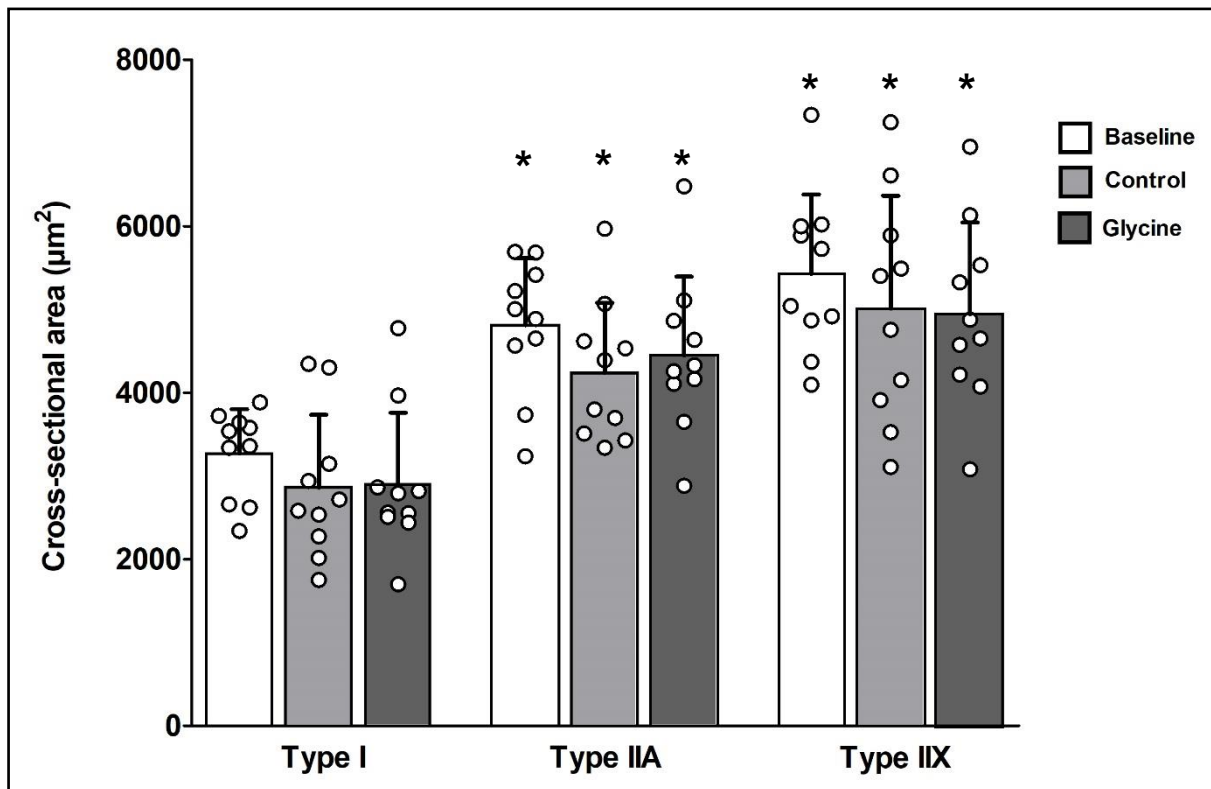


Figure 8: CSA (μm^2) of the VL muscle of 10 captive cheetahs (*Acinonyx jubatus*) for different dietary interventions. CSA is displayed on the y-axis and fibre types are displayed on the x-axis. Data are displayed as means \pm S.D. with each bar representing a different diet treatment. Baseline, control and glycine diets are depicted by white, light grey and dark grey bars, respectively. Each white circle represents the data for individual cheetahs ($n=10$) in each treatment group. Control and glycine groups display pooled data from each sampling period. *Significantly different from type I fibres.

WESTERN CAPE

4.2. Discussion

4.2.1. Skeletal muscle morphology of captive cheetahs

The present study reported a predominance of fast-twitch type IIX fibres followed by fast-twitch type IIA fibres and finally, slow-twitch type I fibres representing the lowest proportion – a finding which is supported by previous studies performed on cheetahs (Williams *et al.*, 1997; Goto *et al.*, 2013). This observation was consistent across the different treatment groups (baseline, control and glycine). Thus, the distribution of muscle fibres in the cheetah remained unchanged, indicating that the administration of a glycine supplement had no detectable effect on the fibre population of the VL muscle. This also highlights the consistency of sampling at similar depths.

4.2.1.1. Fibre type

The fibre type composition of the VL muscle in 2 deceased captive cheetahs reported by Goto et al. (2013) was found to comprise of 24% type I fibres, 23% type IIA fibres and 67% type IIX fibres which nearly parallels the findings reported here (Goto *et al.*, 2013). Importantly, the fibre type visualisation technique employed by the aforementioned study share similarities with the techniques employed in the present study. Although Goto et al. (2013) did not use an antibody that specifically detects type IIX fibres, the results are still in accord with the present study's findings, highlighting the reproducibility of the fibre typing technique. Using histochemical analysis and subsequent NADH staining, Williams et al. (1997) found that the VL muscle of free-ranging cheetah (n = 2) was represented by approximately 15% type I fibres, 9% type IIA fibres and 76% type IIX fibres. Similarly, the VL muscle of the captive population (n = 3) consisted of 19% type I fibres, 12% type IIA fibres and 69% type IIX fibres with no significant difference between the free-ranging and captive cheetah populations (Williams *et al.*, 1997). These results are in agreement to that reported in the present study for type I and type IIX fibres. The combined percentage of type IIA fibres in the VL of free-ranging and captive cheetahs reported by Williams et al. (1997) was found to be almost half of what was determined for the type IIA fibres reported in the current study (10% vs. 20%, respectively).

Comparatively, the *Gastrocnemius* muscle of free-ranging cheetah was also shown to possess a relatively low amount of type IIA fibres (3%) compared to type I (37%) and type IIX (60%) fibres (Williams *et al.*, 1997). This disparity may partially be due to the technique (NADH staining) utilised to distinguish between type IIA and type IIX fibres wherein the authors reported a relatively uniform reaction of fast-twitch type II (A and X) fibres to NADH tetrazolium reductase. Hence, type IIA fibres accounted for a very small proportion of muscle fibres in the VL (approximately 10%) and was only detected in 1 of the *Gastrocnemius* samples. Therefore, the majority of the muscle fibres were classified as fast glycolytic type IIX fibres. Goto et al. (2013) also reported a low proportion of type IIA fibres in the *Gastrocnemius* (6%) which agrees with the study by Williams et al. (1997), but also found a low proportion of type I fibres (4%) compared to type IIX fibres (90%). Interestingly, Hyatt et al. (2010) identified an additional fibre type in the cheetah using an antibody specific to MHC IIB: type IIB fibres. These highly glycolytic fibres have been identified in the limb muscles of cats, rabbits and rodents, and is present in specialised muscles of humans such as the eye and larynx (Hyatt *et al.*, 2010; Schiaffino & Reggiani, 2011; Curry *et al.*, 2012). These were solely detected in the *Gastrocnemius* muscle of the cheetah, which was found to be composed of 12% type IIB fibres. These fibres possess very fast contraction speeds and

their peak power output is greater than that of type IIX fibres (Bottinelli *et al.*, 1991; Bottinelli *et al.*, 1996). To this regard, the presence of type IIB fibres in this muscle of the cheetah would align with its high-speed performance, as the *Gastrocnemius* is crucial for enabling explosive movements and is one of the primary muscles utilised during sprinting (Pandy *et al.*, 2021). Hyatt *et al.* (2013) is the only paper to report the detection of the MHC IIB isoform in medial *Gastrocnemius* muscle of cheetah, which could suggest that this fibre type is muscle group specific (Hyatt *et al.*, 2010). The current study did not use an antibody specific to type IIB fibres, therefore none were detected. Further research may be required to confirm this observation

It is evident that all fibre types are not always represented in certain muscles, and the distribution of muscle fibres varies across different muscle depths and muscle groups in the cheetah (Hyatt *et al.*, 2010; Goto *et al.*, 2013). The superficial regions of the *Gastrocnemius* and *Plantaris* muscles, for instance had a higher proportion of type IIX fibres than type I fibres, whereas in the deep portion of the muscle, the reciprocal was observed (Hyatt *et al.*, 2010). Similar observations are observed in horses and rodents (Serrano *et al.*, 2000; Kohn & Myburgh, 2007; Rivero & Hill, 2016). Additionally, the proportion of type IIA and type IIX fibres in the hindlimb of the cheetah was greater compared to the forelimb - an observation also confirmed in other galloping animals such as the horse and dog (Acevedo & Rivero, 2006; Goto *et al.*, 2013; Rivero & Hill, 2016). Different muscle groups are required to enable a variety of movement and the proportion of fibres may therefore differ in each muscle based on the type of movement or activity the organism is involved in. This adaption may also potentially contribute to the ability of the cheetah to attain such high speeds within a short period of time, as the hindlimb in many animals is predominantly utilised for force production to enable movement, whereas the forelimb generally supports a fraction of BW during standing (Alexander, 2003; Rivero & Hill, 2016).

The muscle fibre composition of other felid species lies within close proximity of the data presented here. Similar to the cheetah, the skeletal muscle of lions, tigers and caracals are characterised by a high proportion of type IIX fibres and a low proportion of type I fibres. Type IIA fibre composition of both lion and caracal were similar to the results reported in the cheetahs (Kohn *et al.*, 2011a). Caracals hunt similarly to the cheetah, but also possess the ability to jump up to 3m high from a standing position. Lions on the other hand, require increased strength for grappling and taking down prey during hunting (Kohn *et al.*, 2011a). These abilities are largely facilitated by the muscle fibres of these animals, which are also able to produce large amounts of force – far greater than that observed in human beings (Kohn & Noakes, 2013). Nonetheless, the sprinting performance of the cheetah appears to

be largely facilitated by the increased proportion of type IIX muscle fibres, as there exists a strong relationship between MHC IIX content and maximum sprinting speed in many mammalian species (Kohn *et al.*, 2011a). Notable limitations of the previous studies include the small sample size as well as the status of the cheetahs which may have affected the accuracy of the results. The present study has a sample size of 10 cheetahs, the highest number ever sampled and analysed for fibre type.

4.2.1.2. Fibre cross-sectional area (CSA)

The CSA of type I and type IIX fibres found to occur in cheetah is also similar to that observed in the lion, caracal, domestic cat and conforms with the findings by Williams *et al.* (1997) (Williams *et al.*, 1997; Toniolo *et al.*, 2008 Kohn, 2011 #90). Type IIX fibres were found to possess the largest CSA in the VL muscle of lions and caracals (3202 ± 657 and $4235 \pm 1119 \mu\text{m}^2$, respectively) followed by type I fibres (2014 ± 432 and $2053 \pm 698 \mu\text{m}^2$, respectively) and type IIA (2005 ± 475 and $1859 \pm 587 \mu\text{m}^2$, respectively). In comparison, cheetah VL muscle displayed large CSAs for type IIX ($5127 \pm 1131 \mu\text{m}^2$) and type I ($3009 \pm 769 \mu\text{m}^2$) fibres, but not significantly different to that of lions and caracals. However, the CSA of type IIA fibres ($4498 \pm 872 \mu\text{m}^2$) in the cheetah was found to be greater than the CSA of type IIA fibres in both the caracal and the lion (Kohn *et al.*, 2011a). Generally, the CSA of type IIX fibres in humans and animals are larger than type IIA and type I fibres; and variable due to interspecies and individual differences (Frontera & Ochala, 2015; Mukund & Subramaniam, 2020). In wild animals, fibre CSA may be highly variable even within the same fibre type as observed in lions, caracals and various antelope species (Kohn *et al.*, 2011a; Kohn, 2014). The large CSA variability observed here is thus not exclusive to the cheetah species. CSA may additionally be affected (but not dictated) by various factors such as age, weight, and sex (Jones *et al.*, 2008). Statistical analysis, however, produced no significant correlations for these factors, thus the large variation in CSA remains unknown.

The CSA of muscle fibres is associated with the force output produced by the muscle such that larger fibres are able to produce more force than muscle fibres having smaller CSAs of the same fibre type (Bottinelli, 2001). Furthermore, different modes of exercise training have also been shown to affect the size and fibre composition of skeletal muscle (Saltin, 1983; Schoenfeld, 2010). This observation is supported by the fact that strength/ resistance and endurance training in humans have been shown to augment fibre composition as well as fibre CSA with a concurrent increase in force production (Shoepe *et al.*, 2003). The CSA of type IIX and type IIA fibres in powerlifters, for instance, is reportedly larger than the CSA of type IIX and type IIA fibres in endurance athletes. Body builders has also been shown to produce more muscular force than recreationally active individuals (Prince *et al.*, 1976;

D'Antona *et al.*, 2006; Kohn *et al.*, 2011a). Despite the large CSA and proportion of type IIX fibres, the power output of skinned single muscle fibres of 1 captive cheetah was reported to be significantly less than the rabbit. However, this is the only study to report an estimate of the power output of cheetah skeletal muscle *in vitro*, and does not reflect the power output *in vivo* (West *et al.*, 2013). Many other factors may additionally contribute to the amount of power muscle can generate including the number of fibres recruited during contraction, fibre diameter, adequate supply of ATP, and MHC content of the fibre type, and therefore is not constrained to muscle fibre proportion and CSA alone (Kohn *et al.*, 2011a; Krivickas *et al.*, 2011; Kohn & Noakes, 2013). Thus, many components may collectively contribute to the force production and sprinting ability of the cheetah.

The skeletal muscle of the cheetah reflects an animal with the potential to produce large amounts of force as mirrored by the large proportion and large CSA of type IIX fibres, thus facilitating the incredible sprinting ability of this animal. The cheetah is a natural sprinter and does not possess enhanced endurance capabilities as observed by its hunting behaviour. This is supported by the high proportion of type IIX fibres compared to type I and IIA fibres. Similar findings were observed in the skeletal muscle profile of other sprinting animals such as cats, horses, rabbits and human sprinters (Talmadge *et al.*, 1996; Serrano *et al.*, 2000; Bianospino *et al.*, 2008; Cristea *et al.*, 2008).

4.2.2 Glycine and skeletal muscle structure

This is the first study to investigate the effects of glycine supplementation on the skeletal muscle morphology of captive cheetah. The main finding presented here is that administration of a 4-week meat-based diet supplemented with glycine had no effect on the skeletal muscle fibre type composition or the CSA of the fibres in the VL of captive cheetah. Thus, glycine supplementation did not result in muscle fibre swelling or shrinking, or initiating fibre type switching due to the potential neurological interaction this supplement may have. Since the baseline and control diets were compositionally identical, no morphological changes were expected between the skeletal muscle of these 2 groups.

Glycine supplementation studies are generally confined to a small number of animal species such as rodents, and meat-producing domesticated animals such as pigs and poultry. Many commercially-attainable livestock feeds are low in CP levels. Lowering the CP levels of feed may pose less of a risk to the environment by reducing faecal and urinary nitrogen excretion and ammonia emissions (Hilliar *et al.*, 2019). Typically, low CP diets are deficient in glycine and serine and may result in impaired growth performance and BW (Siegert & Rodehutschord, 2019). Therefore, supplementing with glycine and/ or other AAs may

potentially subdue this deficiency. Thus, the objective of the majority of the research pertaining to dietary supplementation of glycine specifically in domestic animal species is to ensure a balanced ratio of CP content to essential AA, in order to mitigate the potential effects of an AA deficiency while simultaneously favouring animal growth, development and metabolic maintenance. Glycine has numerous crucial implications in skeletal muscle maintenance and homeostasis in various models of muscle wasting (Koopman *et al.*, 2017).

Regarding the morphological structure of skeletal muscle, glycine has previously been demonstrated to increase the expression of *MyHC7* and decrease the expression of *MyHC1* genes in pigs which encodes for MHC proteins present in oxidative and glycolytic muscle fibres, respectively. Thus, pigs fed a glycine-supplemented diet for 43 days possessed more type I fibres and less type II fibres compared to pigs on a control diet (Zhou *et al.*, 2021). The current study administered 30 g/kg meat glycine supplementation for a period of 4 weeks (31 days) with no differences observed in the composition of fibre type – thus the intervention had no detectable effects. However, it is important to note that the current study determined fibre type on a protein level *via* immunohistochemical analyses, while Zhou *et al.* (2021) measured relative mRNA and protein expression *via* Western blotting. These results should therefore be taken with caution as mRNA transcripts are regulated and can be degraded or repressed before ribosomal translation in the nucleus (Shyu *et al.*, 2008). Thus, mRNA expression is not an accurate representation of fibre type composition (Andersen & Schiaffino, 1997).

Cachectic cancer is characterised by a progressive and continuous loss of skeletal muscle mass with a decreased rate of muscle protein synthesis due to elevated circulating inflammatory cytokines and intracellular Ca^{2+} concentrations which potentiates muscle degradation (Ham *et al.*, 2014). Muscle atrophy is generally characterised by loss of muscle fibres and a reduced fibre size. In a mouse model of cancer cachexia, 21 days of 1 g/kg BW glycine supplementation not only prevented approximately 50% of cancer-induced muscle mass loss in the *Quadriceps femoris*, *Tibialis anterior*, *Plantaris* and *Gastrocnemius* muscles, but also preserved the fibre CSA of the *Tibialis anterior* muscle compared to tumour-bearing mice such that glycine-treated mice displayed ~10% larger CSAs than cancerous mice and ~6% smaller (but not significant) CSAs than the control (Ham *et al.*, 2014). Expectedly, the reduction of fibre CSA was only found to occur in type IIX fibres as they are most responsive to cellular hypertrophy (Schoenfeld, 2010). Furthermore, the addition of exogenous glycine to an *in vitro* culture of C2C12 muscle cells significantly increased the size and diameter of atrophying myotubes, suggesting that glycine is beneficial as a therapeutic agent for muscular atrophy and may have modulating functions in

skeletal muscle protein regulation responsible for muscular growth and tentatively, fibre size (Caldow *et al.*, 2019). In contrast, the supplementation of glycine to the diet of captive cheetah in the present study had no effects on muscle fibre CSA.

Muscular oedema (muscle fibre swelling) has also been suggested to contribute to modifications in muscle fibre size and volume (McMahon *et al.*, 2010). Fibre swelling is thought to be caused by a multitude of factors including autoimmune diseases, mild injuries, rhabdomyolysis and exercise, which may induce changes in the intra- and extracellular water content of muscle fibres (Schoenfeld, 2010). Glycine infusion of skeletal muscle subjected to ischemia and reperfusion injury in canines significantly decreased oedema in the *Gracilis* muscle, decreased muscle necrosis and maintained muscle contractile force, compared to muscle perfused with normal saline (Ascher *et al.*, 2001). Indeed, the supplementation of glycine has been shown to induce structural alterations in skeletal muscle of certain domesticated species, although no studies to date have been performed on captive cheetah. Here it is shown that the fibre type composition and CSA remained unchanged in response to glycine. An important factor to consider is the period of time and type of stimuli required to induce morphological changes in skeletal muscle, as the turnover rate of MHC protein isoforms are generally slow (Schiaffino *et al.*, 2021). Mechanical stimuli such as exercise is usually employed in research reporting a shift in fibre type or change in CSA – and these changes are highly dependent on the species, exercise type, duration and intensity, and individual health status (Saltin, 1983; Serrano *et al.*, 2000; Shoepe *et al.*, 2003). The current study investigated the effect of a dietary intervention on the skeletal muscle of cheetahs, as this information is still unknown. It is therefore comprehensible that no apparent changes were detected, thus glycine had no detrimental effects on their muscle structure.

4.2.2.1. Glycine may modify muscle morphology *via* the regulation of protein synthesis

In humans and animals, imbalances in protein turnover may lead to the progression of skeletal muscle hypertrophy or atrophy (Sun *et al.*, 2016). Glycine may induce changes in the morphology of skeletal muscle by regulating protein metabolism and stimulating myogenic pathways that promote muscle growth. Muscle-specific ring finger 1 (MuRF1) and muscle atrophy F-box (MAFbx)/ atrogin-1 are skeletal muscle ligases that are upregulated during conditions that induce muscle atrophy (Sun *et al.*, 2016). Culture medium supplemented with glycine resulted in a decreased expression of MuRF1 and atrogin-1 in mouse myoblasts and stimulated the Akt/ mTOR pathway (Sun *et al.*, 2016; Schiaffino *et al.*, 2021). A repressed expression of MuRF1 and atrogin-1 are also reported in mice and chicks

following glycine supplementation (Nakashima *et al.*, 2008; Ham *et al.*, 2014). Skeletal muscle growth and hypertrophy are regulated by a number of anabolic pathways that favour the synthesis of proteins over degradation such as the Akt/ mTOR pathway, IGF-1/ PI(3)K pathway and various Ca²⁺-dependant pathways (Schoenfeld, 2010). Glycine has been shown to increase the expression of, and activate key enzymes *via* phosphorylation in the Akt/ mTOR pathway in mice which may lead to an increase in muscle mass (Ham *et al.*, 2014; Sun *et al.*, 2016; Caldow *et al.*, 2019). Calcineurin is an important Ca²⁺-regulated protein in skeletal muscle that mediates myocyte differentiation and various hypertrophic signalling molecules such as myocyte enhancing factor 2 (MEF2) and nuclear factor of activated T cells (NFAT), whereas Ca²⁺-dependant calpains facilitate myofibrillar proteolysis in skeletal muscle (Schoenfeld, 2010). In response to glycine-supplementation, an increased expression of calcineurin A and B as well as its downstream targets MEF2D and NFAT1 were observed in the *Longissimus* muscle of pigs (Zhou *et al.*, 2021). Interestingly, calcineurin has also been shown to induce the expression of slow-twitch fibres and stimulate the conversion of fast-twitch fibres to slow-twitch fibres *via* the upregulation of the *MyHC2A* gene and the concomitant downregulation of the *MyHC2X* and *MyHC2B* genes in mice (da Costa *et al.*, 2007). This may justify the observed increased number of oxidative fibres compared to glycolytic fibres in pigs fed a glycine diet (Zhou *et al.*, 2021). In contrast, the expression of calpains were significantly reduced by glycine in a dose-dependent manner in starved chicks, indicating a suppression in muscle breakdown (Nakashima *et al.*, 2008).

Thus, it appears that structural changes in skeletal muscle elicited in response to glycine may be limited to the amelioration of abnormal muscle conditions. Evidently, glycine supplementation has the ability to alter the skeletal muscle morphology of organisms *via* mechanisms that appear to rely primarily on the modification of myogenic pathways and intramuscular Ca²⁺ regulation in atrophying or diseased skeletal muscle. However, no significant morphological changes are reported here – the captive cheetahs sampled in this study were all apparently healthy with no prior signs of severe disease or illness that may have had detrimental effects on their skeletal muscle structure and function. However, the present study only investigated the fibre type on a protein level and measured CSA as a numerical value whereas glycine has been shown to have modulating effects on the gene level of skeletal muscle fibre regulation. Glycine also affects various components of the anabolic and catabolic pathways that has been shown to lead to the observed morphological changes (such as a shift in fibre type and increased fibre size) reported by other studies (Nakashima *et al.*, 2008; Ham *et al.*, 2014; Sun *et al.*, 2016; Zhou *et al.*, 2021). Collectively, glycine appears to protect skeletal muscle from extreme perturbations as a result of

degenerative conditions or during periods of injury by preserving muscle function, rather than induce changes in already apparently healthy muscle.



Chapter 5: Skeletal muscle metabolism

5.1. Results

5.1.1. Enzyme activities

Maximum enzyme activity was determined by using enzyme assays to evaluate the aerobic (Figure 9A and B) and anaerobic (Figure 10A-D) metabolic capacity in the VL muscle of captive cheetahs on different dietary interventions. Maximum enzyme activities are presented as means \pm S.D. and significance were determined with a repeated measures one-way ANOVA. Tukey's multiple comparison test was utilised to detect significance between treatment groups ($P < 0.05$).

5.1.1.1. Aerobic enzymes

3HAD activity is a marker of β -oxidation which is an indication of fat utilisation, whereas CS is in the TCA cycle and utilises acetyl-CoA from glucose and/ or fat oxidation. Thus, the maximum aerobic enzyme activity of these enzymes is a useful indicator of the oxidative capacity of skeletal muscle.

Figure 9A displays the maximum oxidative enzyme capacity for 3HAD in VL muscle of captive cheetahs. The average 3HAD activity at baseline was $22 \pm 4 \mu\text{mol}\cdot\text{min}^{-1}\cdot\text{g}^{-1}$ protein. Compared to baseline, cheetahs on the control and glycine-supplemented diet displayed significantly higher 3HAD activities – $27 \pm 4 \mu\text{mol}\cdot\text{min}^{-1}\cdot\text{g}^{-1}$ protein and $27 \pm 5 \mu\text{mol}\cdot\text{min}^{-1}\cdot\text{g}^{-1}$ protein, respectively, denoting an increase by a factor of 1.2x. However, no significant differences were observed between the control and glycine-supplemented groups. The range of 3HAD activity for cheetahs at baseline were $16 - 28 \mu\text{mol}\cdot\text{min}^{-1}\cdot\text{g}^{-1}$ protein while the range for the control and glycine groups were $19 - 32 \mu\text{mol}\cdot\text{min}^{-1}\cdot\text{g}^{-1}$ protein and $17 - 37 \mu\text{mol}\cdot\text{min}^{-1}\cdot\text{g}^{-1}$ protein, respectively.

CS activities are shown in Figure 9B. The mean CS activity at baseline ($17 \pm 6 \mu\text{mol}\cdot\text{min}^{-1}\cdot\text{g}^{-1}$ protein) was similar to CS activities in the control and glycine-supplemented group ($18 \pm 4 \mu\text{mol}\cdot\text{min}^{-1}\cdot\text{g}^{-1}$ protein and $19 \pm 6 \mu\text{mol}\cdot\text{min}^{-1}\cdot\text{g}^{-1}$ protein, respectively) with no significant difference between groups, most likely due to the large S.D. as observed by the spread of the data. In accordance, the range of CS activities at baseline was similar to the control group; $10 - 22 \mu\text{mol}\cdot\text{min}^{-1}\cdot\text{g}^{-1}$ protein and $10 - 24 \mu\text{mol}\cdot\text{min}^{-1}\cdot\text{g}^{-1}$ protein, respectively, while the glycine-supplemented group ranged from $6 - 28 \mu\text{mol}\cdot\text{min}^{-1}\cdot\text{g}^{-1}$ protein, containing both the lowest and highest CS activities. Overall, the average 3HAD and CS activities were 25 ± 5 and $18 \pm 5 \mu\text{mol}\cdot\text{min}^{-1}\cdot\text{g}^{-1}$ protein, respectively.

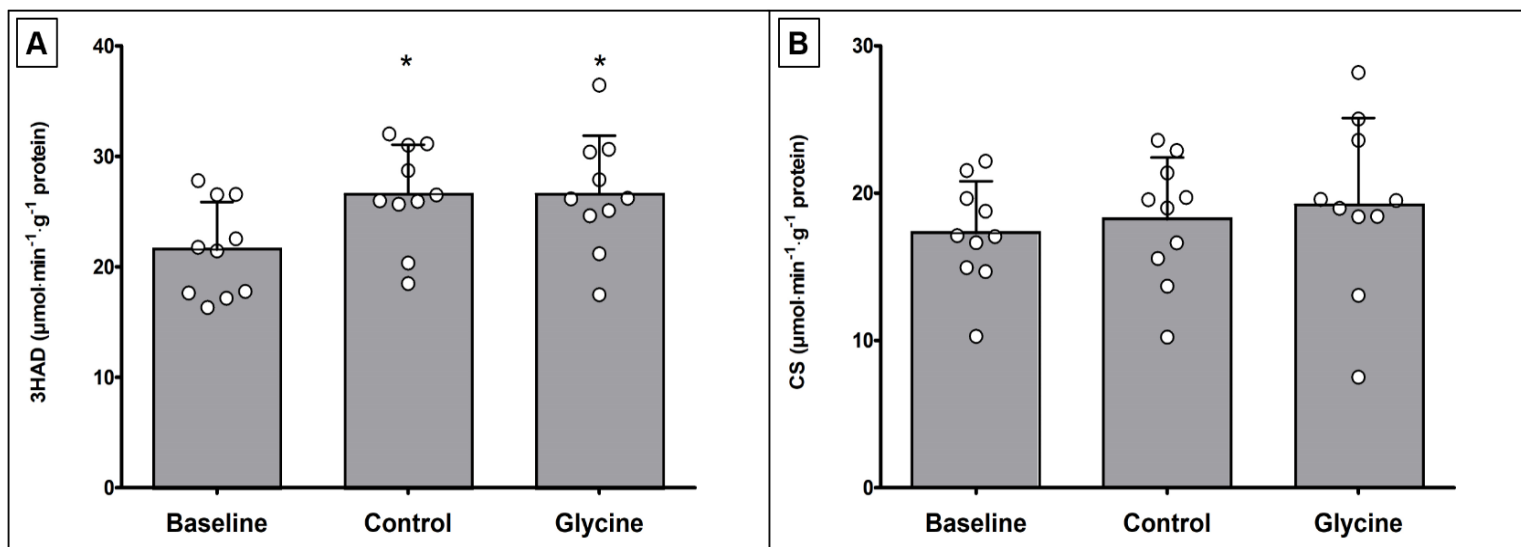


Figure 9: Maximum activity of aerobic enzymes in the VL muscle of 10 captive cheetahs (*Acinonyx jubatus*). Data from different intervention periods were pooled for each group. A, average 3HAD enzyme activity; B, average CS enzyme activity. All enzyme activities are presented as the amount of substrate turnover per minute per gram of protein ($\mu\text{mol}\cdot\text{min}^{-1}\cdot\text{g}^{-1}$ prot.). Light grey bars represent the maximum enzyme activity in each group and displayed as means \pm S.D. for each group. White circles indicate the individual values for each cheetah in the study. *Significantly different from the baseline group ($P < 0.05$).

5.1.1.2. Anaerobic enzymes

Anaerobic enzymes are capable of generating ATP in the absence of oxygen or when oxygen is limited. Figure 10A, C and D shows the maximum activities for enzymes participating in the glycolytic pathway found in cheetah skeletal muscle. Maximum LDH activities were similar for all groups: $2195 \pm 416 \mu\text{mol}\cdot\text{min}^{-1}\cdot\text{g}^{-1}$ protein at baseline, $2164 \pm 253 \mu\text{mol}\cdot\text{min}^{-1}\cdot\text{g}^{-1}$ protein for the control group, and $2074 \pm 379 \mu\text{mol}\cdot\text{min}^{-1}\cdot\text{g}^{-1}$ protein for the glycine-supplemented group. Similarly, the range of LDH activity for all treatments falls within $1544 - 2735 \mu\text{mol}\cdot\text{min}^{-1}\cdot\text{g}^{-1}$ protein (Figure 10A) with a mean of $2144 \pm 345 \mu\text{mol}\cdot\text{min}^{-1}\cdot\text{g}^{-1}$ protein.

Figure 10B displays the average CK activity in the VL muscle of captive cheetahs. Average CK activity was similar at baseline ($10451 \pm 1747 \mu\text{mol}\cdot\text{min}^{-1}\cdot\text{g}^{-1}$ protein), and in the glycine group ($10463 \pm 1298 \mu\text{mol}\cdot\text{min}^{-1}\cdot\text{g}^{-1}$ protein) with the highest CK activity measured in the control group ($11702 \pm 2199 \mu\text{mol}\cdot\text{min}^{-1}\cdot\text{g}^{-1}$ protein). Combined, the mean CK activity was $10872 \pm 1824 \mu\text{mol}\cdot\text{min}^{-1}\cdot\text{g}^{-1}$ protein). Of all the enzyme activities measured, CK activity was the highest in captive cheetahs – approximately 435x and 604x greater than 3HAD and CS, respectively and approximately 5, 76 and 63x greater than LDH, PFK, and PHOS activities, respectively. No significant differences were detected between groups for any of the abovementioned anaerobic enzymes.

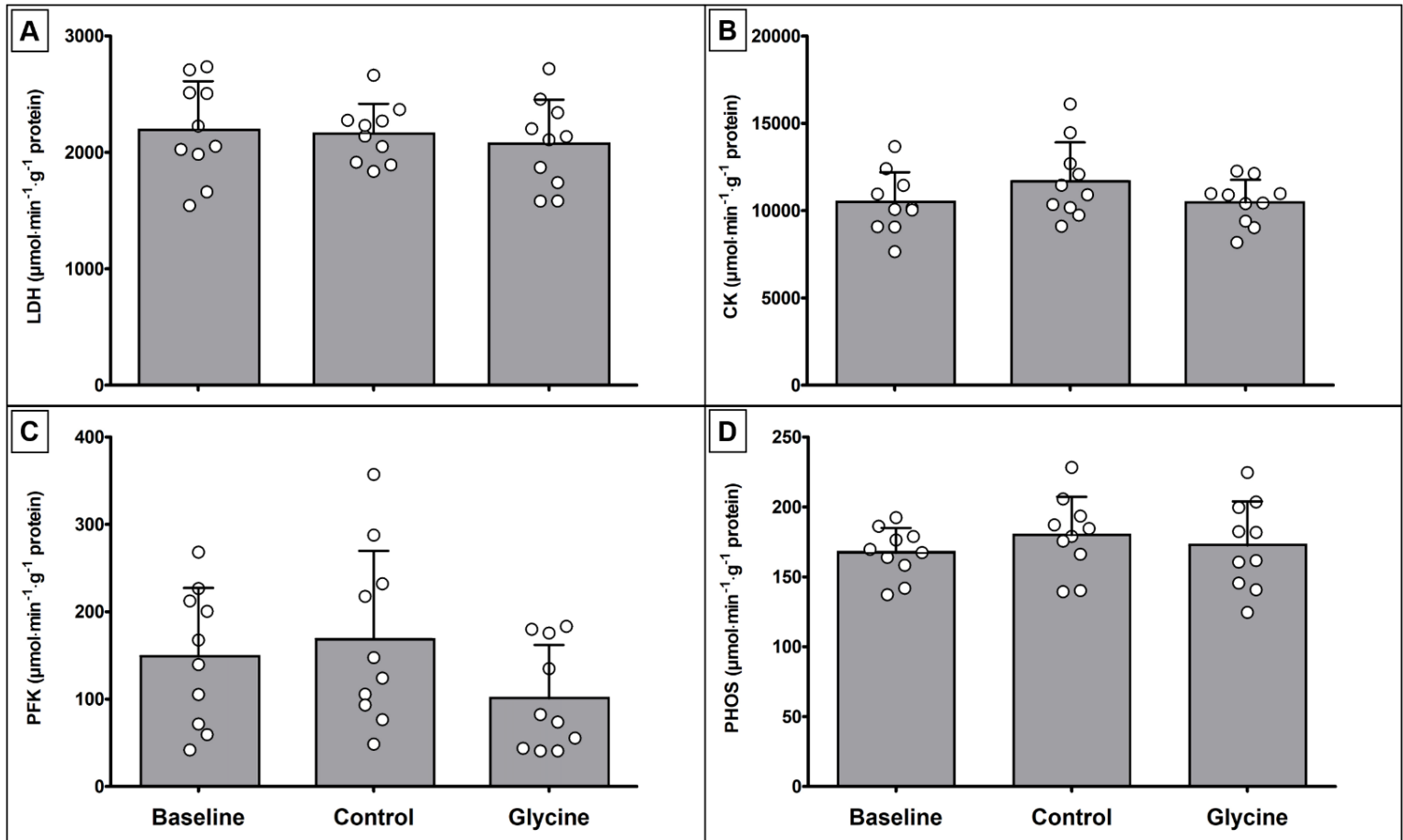


Figure 10: Maximum activities of anaerobic enzymes in VL muscle of 10 captive cheetahs (*Acinonyx jubatus*) on different diets. The light grey bars represent pooled data from different intervention periods of each treatment group. A, average maximum LDH; B, creatine kinase (CK); C, phosphofructokinase (PFK) and D, phosphorylase (PHOS) enzyme activity ($\mu\text{mol}\cdot\text{min}^{-1}\cdot\text{g}^{-1}$ prot.). Data are displayed as means \pm S.D. White circles represent individual values for each cheetah in the study.

Results for PFK activity were found to be highly scattered as seen by the wide distribution of data points in each of the 3 groups. Across all treatments, the mean PFK activity was $140 \pm 84 \mu\text{mol}\cdot\text{min}^{-1}\cdot\text{g}^{-1}$ protein. The average PFK activity at baseline was $149 \pm 78 \mu\text{mol}\cdot\text{min}^{-1}\cdot\text{g}^{-1}$ protein ($42 - 268 \mu\text{mol}\cdot\text{min}^{-1}\cdot\text{g}^{-1}$ protein), $169 \pm 101 \mu\text{mol}\cdot\text{min}^{-1}\cdot\text{g}^{-1}$ protein ($49 - 357 \mu\text{mol}\cdot\text{min}^{-1}\cdot\text{g}^{-1}$ protein) for the control group and $101 \pm 61 \mu\text{mol}\cdot\text{min}^{-1}\cdot\text{g}^{-1}$ protein ($41 - 183 \mu\text{mol}\cdot\text{min}^{-1}\cdot\text{g}^{-1}$ protein) for the glycine-supplemented group (Figure 10C).

PHOS activity for the baseline, control and glycine groups were $167 \pm 18 \mu\text{mol}\cdot\text{min}^{-1}\cdot\text{g}^{-1}$ protein, $180 \pm 27 \mu\text{mol}\cdot\text{min}^{-1}\cdot\text{g}^{-1}$ protein, and $173 \pm 31 \mu\text{mol}\cdot\text{min}^{-1}\cdot\text{g}^{-1}$ protein, respectively. The control group contained the highest average PHOS activity and the lowest PHOS activity was observed at baseline (Figure 10D). The range of PHOS activities were $137 - 192 \mu\text{mol}\cdot\text{min}^{-1}\cdot\text{g}^{-1}$ protein, $139 - 228 \mu\text{mol}\cdot\text{min}^{-1}\cdot\text{g}^{-1}$ protein and $125 - 224 \mu\text{mol}\cdot\text{min}^{-1}\cdot\text{g}^{-1}$ protein for baseline, control and glycine groups, respectively. The average PHOS activity for all treatments was $173 \pm 26 \mu\text{mol}\cdot\text{min}^{-1}\cdot\text{g}^{-1}$ protein).

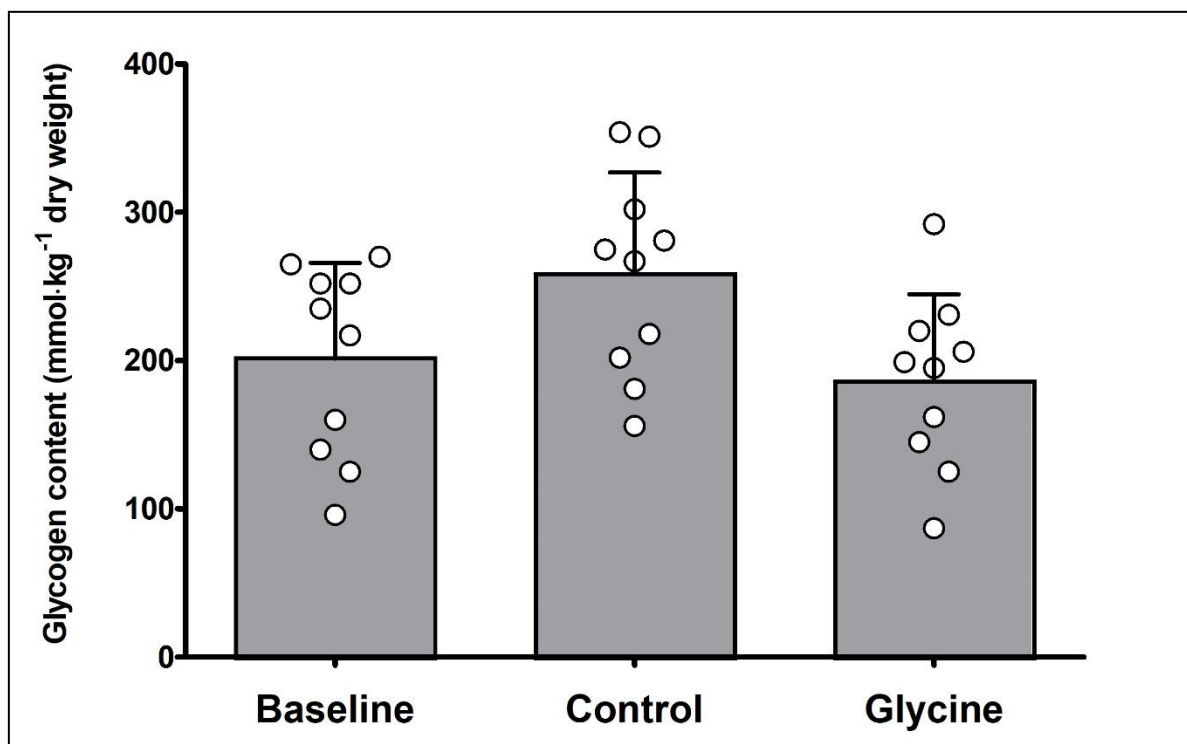


Figure 11: Total glycogen concentration ($\text{mmol}\cdot\text{kg}^{-1}$ d.w.) present in the VL muscle of 10 captive cheetahs (*Acinonyx jubatus*). Light grey bars represent pooled data from different intervention periods and are displayed as means \pm S.D. for each group. White circles depict the values from individual cheetahs.

5.1.2. Glycogen concentration

The glycogen concentration of VL muscle in captive cheetahs are shown in Figure 11. Average baseline glycogen concentration ranged from 96 – 270 $\text{mmol}\cdot\text{kg}^{-1}$ d.w. with an average of 201 ± 65 $\text{mmol}\cdot\text{kg}^{-1}$ d.w. The highest glycogen content was measured in the control group (259 ± 68 $\text{mmol}\cdot\text{kg}^{-1}$ d.w.) with a range of 156 – 354 $\text{mmol}\cdot\text{kg}^{-1}$ d.w., while the group supplemented with glycine displayed the lowest overall glycogen concentration (186 ± 59 $\text{mmol}\cdot\text{kg}^{-1}$ d.w., range; 87 – 292 $\text{mmol}\cdot\text{kg}^{-1}$ d.w.). Overall, the average glycogen content across all groups was 215 ± 38 $\text{mmol}\cdot\text{kg}^{-1}$ d.w. One-way repeated measures ANOVA revealed no significant changes in response to the diet intervention.

5.2. Discussion

5.2.1. Skeletal muscle metabolism of captive cheetah

5.2.1.1. Aerobic metabolism

CS and 3HAD are aerobic mitochondrial enzymes in the TCA cycle and β -oxidation, respectively. The maximum activity of these enzymes gives an indication of the flux through their respective pathways, which reflect the oxidative capacity of the muscle. Here it is

shown that the skeletal muscle of the cheetah does not have a high capacity for aerobic metabolism as indicated by very low CS and 3HAD activities. The skeletal muscle of endurance athletes and animals (including horses and antelope species) are generally associated with high CS and 3HAD activities and are therefore highly oxidative (Essen *et al.*, 1975; Serrano *et al.*, 2000; Kohn *et al.*, 2007; Curry *et al.*, 2012; Kohn, 2014). Endurance exercise additionally elicits metabolic and structural adaptations on skeletal muscle that results in enhanced oxidative capacity including increases in CS and 3HAD activities, larger and more abundant mitochondria, and a dense capillary supply - all of which improves the utilisation of oxygen for the oxidative metabolism of substrates (Hargreaves & Spriet, 2020). During prolonged exercise, carbohydrates and fats (*via* aerobic metabolism) serve as the main fuel for ATP production (Hargreaves & Spriet, 2020). CS is an important indicator of mitochondrial biogenesis and 3HAD reflects the muscle's efficiency at utilising fat as a source of ATP to sustain muscle contraction over extended periods of time (Yang *et al.*, 2005; Akram, 2014). The CS and 3HAD activities of cheetah skeletal muscle was considerably lower compared to endurance athletes and animals, indicating a decreased flux through these metabolic pathways (Serrano *et al.*, 2000; Kohn *et al.*, 2007; Curry *et al.*, 2012; Kohn, 2014). Comparable results are reported for lions and caracals (Kohn *et al.*, 2011a). Aerobic metabolic pathways generate more total ATP compared to glycolytic pathways, but the rate of ATP production is slower, thus the low capacity for oxidative metabolism lies in agreement with the performance of the cheetah, as quick, high-intensity activities such as sprinting rely primarily on rapid ATP production *via* glycolytic pathways (Hargreaves & Spriet, 2020).

Activities for both 3HAD and CS were found to be similar albeit slightly lower than activities of the cheetahs reported by Williams *et al.* (1997). This slight variation may be due to many reasons such as different methods of measuring enzyme activity, status of the animal and potential drug-effects. However, although the study contained both captive and free-ranging cheetah, the enzyme activities reported by Williams *et al.* (1997) only represents the free-ranging population while the current study only represents the captive population, thereby warranting caution when comparing data (Williams *et al.*, 1997). Nonetheless, the results indicate that the cheetah possess low aerobic metabolism which lies in agreement with their low proportion of type I fibres, similar to that seen in caracals and lions (Kohn *et al.*, 2011a).

5.2.1.2. Anaerobic metabolism

Glycolytic enzymes (LDH, PFK and PHOS) and CK are capable of rapid, anaerobic ATP generation. Overall, the results indicate that the cheetah possess a high capacity for anaerobic-based metabolism, supporting the study by Williams *et al.* (1997) and as was found in other felids (Kohn *et al.*, 2011a). The skeletal muscle of cheetahs possesses high

LDH activities, consistent with observations in the lion, caracal, and domestic cat indicating a high turnover rate of pyruvate from anaerobic glycolysis (Nilkumang & Thornton, 1979; Kohn *et al.*, 2011a). As expected, the LDH activity of endurance athletes is almost 50% slower compared to cheetahs as their muscles are more adapted to running far distances which do not require large quantities of immediate ATP replenishment (Kohn *et al.*, 2007). A surprising, yet expected finding was the high CK activity. The main roles of CK in skeletal muscle is the regeneration of ATP *via* the transfer of high-energy phosphates to Cr as well as the shuttling of high-energy phosphates to areas where ATP is needed (Negro *et al.*, 2019). CK activity of cheetahs exceeded that reported for endurance athletes and animals, as well as lions and caracals (Kohn *et al.*, 2011a; Kohn *et al.*, 2011b; Curry *et al.*, 2012; Kohn, 2014). Comparisons should, however, be taken with caution as the methods employed in the determination of enzyme activity may vary between studies. It is therefore tempting to assume that cheetah may possess the highest CK activity compared to all the wild and domestic species that are reported in the literature. A high PFK activity was anticipated due to the anaerobic nature of their metabolism and its regulatory function in glycolysis. However, it was found that captive cheetahs have a relatively low PFK activity – similar to trained and untrained human beings (Gollnick *et al.*, 1972; Kohn *et al.*, 2007). Interestingly, the PFK activity in cheetah is similar to caracal and cat, while being slightly higher than lion. Thus a low PFK activity may be characteristic of this species (Howland, 1981; Kohn *et al.*, 2011a). Reported PFK activity of skeletal muscle is hard to compare due to the large variations reported in the literature, which may be due to the strict regulation of PFK (Mansour, 1972). Although, previous studies have reported increased PFK activities following sprint interval training (Roberts *et al.*, 1982; MacDougall *et al.*, 1998). PHOS activity reflects the ability of skeletal muscle to mobilise stored glycogen as glucose for ATP production which serves as one of the main fuels for skeletal muscle during the fight-or-flight response and high-intensity exercise (Krebs & Fischer, 1964; Ren *et al.*, 1994). This reaction yields glucose units in the form of glucose-1-phosphate which is then metabolised *via* glycolysis. The PHOS activities of captive cheetahs were comparatively lower than both lions and caracal, as well as trained endurance athletes (Kohn *et al.*, 2011a).

This is one of 2 studies that determined the enzyme activities associated with glycolytic capacity in captive cheetahs. The results suggest that metabolism of the cheetah displays a great potential for anaerobic metabolism *via* pyruvate and PCr metabolism, reflected by high LDH and CK activity. Both PFK and PHOS enzymes (directly or indirectly) metabolise substrates that enter glycolysis. The end-product of glycolysis, pyruvate, is either oxidised to acetyl-CoA (*via* PDH) under aerobic conditions or reduced to lactate (*via* LDH) under anaerobic conditions (Akram, 2013; McCommis & Finck, 2015). Therefore, it appears that

the main pathways for ATP generation is *via* anaerobic metabolism of pyruvate and Cr/ PCr rather than the oxidation of glucose from glycolysis and fats from β -oxidation. This assumption is supported by the high LDH activity and reduced rate of PFK and PHOS activities. It would therefore be interesting to measure the PDH relative to LDH activity in the muscle of cheetah.

5.2.1.3. Glycogen content

Glucose is primarily stored as glycogen in the liver and skeletal muscle of vertebrates. In the liver, the main role of glycogen is to maintain blood glucose homeostasis during periods of stress such as exercise or fasting, *via* gluconeogenesis. In skeletal muscle, glycogen serves as a reservoir for ATP production dependant on the metabolic demand (Possik & Pause, 2018). Glycogen has been shown to be depleted after an acute bout of exercise but not in response to fasting, suggesting that the main role glycogenolysis in skeletal muscle is contributing to rapid ATP production following acute stimulation rather than glucose homeostasis (Jensen *et al.*, 2011). Studies regarding glycogen content in response to a glycine diet is very limited. In studies performed on rats, a glycine-supplemented diet caused an immediate replenishment of liver and muscle glycogen following exercise (Todd & Allen, 1958; Hunter *et al.*, 1967).

Supplementation of GAA, which is also synthesised from glycine has been shown to increase total muscle Cr, PCr, and glycogen concentrations in chicks (DeGroot *et al.*, 2019). This AA derivative is a direct precursor to Cr and supplementation has been shown to stimulate the muscle growth of animals and increase Cr stores in humans (Ostojic, 2015; Ostojic *et al.*, 2016; Yan *et al.*, 2021). Glycogen content is also influenced by training status, health, diet, and muscle fibre composition (Knuiman *et al.*, 2015). The low glycogen content of captive cheetahs observed in this study complements the findings by Williams *et al.* (1997) who measured glycogen at rest and after electrical stimulation. Comparatively, the glycogen content in the skeletal muscle of animals well-suited for endurance-type activities such as horses and endurance athletes are almost 2-fold higher than in the cheetah (Serrano *et al.*, 2000; Webster *et al.*, 2016). It has previously been suggested that cheetahs do not stop pursuing their prey due to overheating (Hetem *et al.*, 2013). High-intensity sprinting relies on PCr breakdown for ATP. However, this can only be supported for a few seconds, after which intramuscular glycogen is the main fuel source to maintain muscle contraction (Hargreaves & Spriet, 2020). Thus, the low glycogen content and reduced flux through this pathway may explain why they have to stop after a high-intensity short bout of exercise. It may also imply a lesser reliance on muscle glycogen for ATP production in cheetah, which lies in agreement with the low PHOS activity. This is further supported by the

observation by Williams *et al.* (1997), who showed that glycogen utilisation in the VL of a free-ranging cheetah was delayed following electrical stimulation, and only contributed to ATP production after the depletion of PCr stores. The authors then conclude that PCr may be the primary fuel source for ATP generation in cheetahs during early phases of stimulation, which coincides with the increased flux through the CK pathway. Low glycogen content may also be an indicator of stress experienced by the animal, or a potential side-effect of the analgesic drugs used for sedation during sampling. Anecdotal evidence suggest that these drugs do not appear to manifest metabolic disruptions as vital signs showed no significant fluctuations during anaesthesia. This, however, is still an avenue of interest and uncertainty, and further investigation is warranted.

5.2.2. Glycine and skeletal muscle metabolism

Glycine has many vital roles in the metabolism of humans and mammals including the synthesis of essential metabolites, growth and development, and immunity (Razak *et al.*, 2017). Furthermore, glycine metabolism is affected by chronic conditions such as obesity, type II diabetes, insulin resistance and non-alcoholic fatty liver disease, as these conditions are associated with reduced blood glycine concentrations in humans (Hafidi *et al.*, 2004; Adeva-Andany *et al.*, 2018; Alves *et al.*, 2019; Rom *et al.*, 2020). In skeletal muscle, glycine has crucial roles in maintaining muscle mass and preserving muscle function by regulating protein synthesis and modulating anabolic pathways in skeletal muscle as discussed in the previous chapter. Nonetheless, there is a paucity of research regarding the effects of glycine supplementation on the metabolism of skeletal muscle, and more so in wild animals such as the cheetah. To date, there are no studies that has investigated the effect of glycine supplementation on the maximum enzyme activities in skeletal muscle of any species. Many studies performed on skeletal muscle have either administered BCAAs (leucine, isoleucine and valine) as supplementation or diets varying in macronutrient composition (High-fat diet vs. high-carbohydrate diet). The primary objective for many of these studies is skeletal muscle performance during and after exercise, or during muscle wasting conditions. Supplementary BCAAs display similar mechanisms of action to glycine supplementation with regards to the regulation of myogenic pathways, whereas the general trend in response to a high-fat diet is an enhanced capacity for oxidative metabolism, reflected by increased 3HAD and CS activities (Li *et al.*, 2016; Bowser *et al.*, 2020; Kamei *et al.*, 2020; Mann *et al.*, 2021). The current study is therefore the first to evaluate the effects of glycine supplementation on the oxidative and glycolytic capacity as well as glycogen content of captive cheetahs. The results obtained here may serve as a foundation for future supplementation studies as well as the characterisation of the muscle metabolism of captive cheetahs.

The skeletal muscle metabolism of VL muscle in captive cheetahs following 4 weeks of glycine supplementation remained fairly constant. No significant difference in maximum enzyme activities were observed between the baseline, control and glycine groups for all anaerobic enzymes (LDH, CK, PFK and PHOS) and CS. Interestingly, only the maximum activity of 3HAD was found to increase in the control and glycine groups indicating a potential effect on fat oxidation in the skeletal muscle. Although the exact mechanism for the observed increase in activity is not yet fully established, potential mechanisms by which glycine may have an effect on the metabolism of skeletal muscle is discussed.

In a rat model of myocardial damage, glycine supplementation was shown to increase ATP content and reduce serum lactate levels, thereby potentially improving aerobic metabolism and down-regulating anaerobic metabolism during periods of cellular stress. Addition of glycine also reduced muscle and serum levels of LDH and CK – common markers of muscle damage (Zhang *et al.*, 2013; Han *et al.*, 2018). Glycine can be utilised in the synthesis of many metabolites that may serve as substrates for the enzymes in their respective pathways. Glycine is a precursor to Cr – an important metabolite synthesised in the liver and kidney and stored in the skeletal muscle. It serves as the primary substrate for CK, which facilitates the interconversion of Cr to PCr for rapid regeneration of ATP (Razak *et al.*, 2017). Glycine also acts as cofactor in the formation of glucose and is readily converted to pyruvate *via* the enzymes SHMT and SD which are expressed in the liver and skeletal muscle of rats (White *et al.*, 2020). Glucose can be utilised for aerobic and anaerobic glycolysis where PFK acts as a crucial regulatory and rate-limiting enzyme, whereas pyruvate – an essential metabolite and the end product of glycolysis has two fates dependant on the demand for ATP as well as oxygen availability. Under anaerobic conditions of ATP requirement, pyruvate is reduced into lactate *via* LDH in skeletal muscle, yielding a net of 2 ATP and NADH. Alternatively, in the mitochondrial matrix, pyruvate can be oxidised (*via* the pyruvate dehydrogenase complex) to form acetyl-CoA, a pivotal molecule in skeletal muscle metabolism (Akram, 2013; McCommis & Finck, 2015). In the TCA cycle, acetyl-CoA is utilised as a substrate in the formation of NADH and FADH₂ - reducing equivalents used to generate the proton gradient necessary for aerobic ATP production. It is also required in the formation of citrate *via* the condensation of oxaloacetate and acetyl-CoA – the first committed step in the TCA cycle catalysed by the enzyme CS (Wiegand & Remington, 1986; Yang *et al.*, 2005). Furthermore, acetyl-CoA is produced by the β -oxidation of fatty acids facilitated by 3HAD, and is utilised in the synthesis of fatty acids (McCommis & Finck, 2015). The synthesis and oxidation of fatty acids and the oxidation of pyruvate to acetyl-CoA requires the presence of CoA. This molecule is primarily replenished by the glycine conjugation pathway, which is an important detoxifying metabolic process in mammals that

has recently been specifically implicated in the metabolism of cheetahs (Tordiffe *et al.*, 2017).

5.2.2.1 Glycine may affect fat metabolism

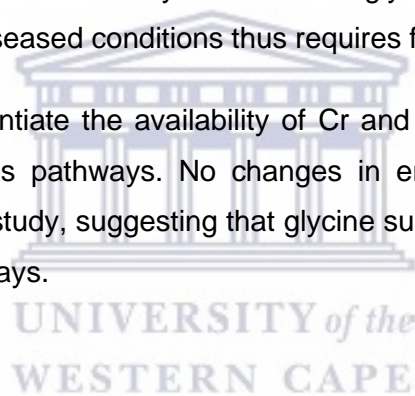
Phenolic and xenobiotic compounds are conjugated to glycine as a means to suppress the toxic effects of the parent metabolite on the host organism while also increasing the hydrophilicity of these compounds to be excreted *via* the urine (Badenhorst *et al.*, 2013). Hippurate is the most abundant organic acid found in urine and it is the glycine conjugate of benzoate. The final step in the formation of hippurate from benzoate involves the binding of benzoate and subsequent acylation of glycine, by GLYAT, yielding hippurate and CoA. Additionally, aromatic compounds such as phenylpropionate, produced from dietary phenols following microbial fermentation in the gut is also catabolised *via* glycine conjugation. These compounds are initially converted to acyl-CoA thioesters before its conjugation with glycine. Metabolic equivalents that may be utilised for muscular ATP generation such as acetyl-CoA, NADH and FADH₂ are produced *via* the glycine conjugation pathway (Badenhorst *et al.*, 2013; Badenhorst *et al.*, 2014). Interestingly, the conversion of phenolic compounds to acyl-CoA thioesters also represents the first step of β -oxidation, which could potentially affect fat metabolism.

Cheetahs have been shown to excrete large quantities of phenolic compounds along with their respective glycine conjugates, as well as metabolites from glycolysis, β -oxidation and the TCA cycle in their urine. In fact, the majority of the metabolites quantified in cheetah urine were found to be from glycine metabolism which may indicate a strong dependence on this pathway to neutralise metabolite toxicity for urinary excretion (Tordiffe *et al.*, 2017). The high CK activity observed in the skeletal muscle of cheetah also suggests a high flux through this metabolic pathway and a potential demand for glycine. Additionally, captive cheetahs were reported to excrete approximately 3x more unconjugated benzoate and 20% less hippurate than free-ranging cheetahs which may suggest insufficient glycine availability for efficient glycine conjugation of benzoate (Tordiffe *et al.*, 2017). Excess ingested benzoate and its conversion to hippurate may lead to glycine deficiency in humans and glycine administration significantly increases the rate of hippurate formation and benzoate clearance, thereby enhancing the efficiency of glycine conjugation (Badenhorst *et al.*, 2013). A depletion of glycine leads to the accumulation of acyl-CoA thioesters and CoA sequestration, which may result in damage to the liver and kidneys (Badenhorst *et al.*, 2014). Sequestration of CoA also impairs important metabolic processes such as gluconeogenesis, β -oxidation and AA metabolism in the TCA cycle, but is alleviated by the addition of glycine. Whether or not the supplementation of glycine has an effect on the proportion of excreted

urinary phenolic compounds and glycine conjugates in captive and wild cheetah is yet to be determined.

In obese, insulin resistant and/ or diabetic individuals, the reduced level of plasma and serum glycine is associated with an elevation of fatty acyl-CoA esters as a result of incomplete lipolysis, leading to increased levels of circulating FFAs. These FFAs are then conjugated to glycine for excretion, thereby limiting the amount of glycine for other metabolic processes (Adeva-Andany *et al.*, 2018; Wittemans *et al.*, 2019). In rats, glycine supplementation reverted the elevation in sucrose-induced triglyceride levels and reduced fat accumulation. In the same study, glycine improved mitochondrial respiration and concomitantly enhanced fat oxidation (Hafidi *et al.*, 2004). Superfluous glycine may therefore have an indirect effect on skeletal muscle metabolism and fatty acid oxidation by acting as a donor of substrates and/ or cofactors that can be used to regenerate ATP. However, no direct interactions were observed between glycine supplementation and enzyme activity or metabolite concentration in the current study. The effect of glycine on the metabolism of fatty acids in healthy muscle and diseased conditions thus requires further investigation.

In hindsight, glycine may potentiate the availability of Cr and other metabolites for muscle energy metabolism *via* various pathways. No changes in enzyme activities or glycogen content were observed in this study, suggesting that glycine supplementation does not affect these specific metabolic pathways.



Chapter 6: Conclusion and future directions

Captive cheetah experience high mortality and morbidity rates due to poor fecundity, compromised immune health and an increased incidence of chronic diseases rarely seen in their free-ranging counterparts. Lack of heterozygosity, increased captivity related stress and divergent gut microbiota were previously thought to be potential causal factors of their poor performance in captivity (Gillis-Germitsch *et al.*, 2017). However, previous studies found that the occurrence and strain of pathogenic bacteria were found to be similar in the captive and free-ranging population regardless of health status and disease severity, and the high occurrence of disease in captive cheetah may not be due to stress from captivity alone (Terio *et al.*, 2005; Wachter *et al.*, 2011; Menke *et al.*, 2017). Recent studies indicated that the macronutrient composition of captive diets may be linked to the aetiology and severity of chronic disorders suffered by captive cheetahs, but no study to date has confirmed any direct dietary interactions (Lane *et al.*, 2012; Whitehouse-Tedd *et al.*, 2015).

Connective tissue components such as bone, cartilage, skin and hair are natural sources of glycine which constitutes the general diet of free-ranging cheetahs. In contrast, commercial preparations and lean muscle-based diets are the primary diets for captive cheetahs (Lane *et al.*, 2012; Depauw *et al.*, 2013). These diets usually lack an apparent source of glycine and may not contain the optimum nutrient composition for captive cheetahs, as most feed preparations are based on the metabolic requirements of domestic cats (Dierenfeld *et al.*, 2015). Other than the numerous important physiological functions of glycine as well as the benefits of glycine administration, one of the primary arguments for supplementing the diet of captive cheetah with glycine is due to increased risk of a deficiency arising from a reduced dietary intake and a high metabolic demand (Tordiffe, 2017). Glycine may also be used in the treatment of gastrointestinal disorders, such as gastritis (Razak *et al.*, 2017). The role of glycine in skeletal muscle repair, function and maintenance is well-documented in humans and domestic models, but no studies thus far has investigated glycine supplementation in wild animals. Consequently, the central aims of the current study were to determine the effects of glycine supplementation on the skeletal muscle morphology and metabolism of captive cheetahs. This is therefore the first study to investigate the effects of glycine dietary supplementation on the skeletal muscle properties in a wild species. In addition, and more indirectly, this is the first study that had a large sample size of cheetahs (n=10) which will serve as a more accurate reference for cheetah skeletal muscle properties.

The administration of a meat-based diet supplemented with additional glycine appears to have had no apparent effects on the structure and metabolism in the skeletal muscle of

captive cheetah. Type IIX fibres were the most predominant fibre type in the captive cheetah followed by type IIA and type I. Additionally, the CSA of type IIX fibres were the largest, followed by type IIA and type I fibres. These results agree with previous studies on cheetah skeletal muscle (Williams *et al.*, 1997; Goto *et al.*, 2013). MHC isoform analysis could potentially be performed in future studies to compare MHC size and weight between fibre types. Past studies suggest that glycine may influence muscle morphology by enhancing protein synthesis and decreasing protein degradation, thereby increasing the size and CSA of muscle cells (Ham *et al.*, 2014; Sun *et al.*, 2016). Glycine may also facilitate the shifting of glycolytic to oxidative muscle fibres *via* various Ca²⁺-dependant signalling cascades (Zhou *et al.*, 2021). No fibre type switching was found for the cheetah.

Metabolically, captive cheetahs share characteristics with the lion and caracal such that they possess similar muscle oxidative and glycolytic capacities (Kohn *et al.*, 2011a). The most notable findings were the high LDH and CK activities and the low 3HAD and CS activities. This indicates that the cheetah is highly adapted at utilising anaerobic metabolism for ATP generation rather than aerobic metabolism, which links to their high proportion of type IIX fibres and low proportion of type I fibres. Interestingly, the glycolytic enzymes PFK and PHOS were found to be lower compared to humans as well as other felids, suggesting that oxidation of glucose *via* glycolysis may not be the predominant pathway for ATP generation (Kohn *et al.*, 2011a). The flux through these pathways may also provide an indication of the preferred substrate utilised for ATP production. Thus, high energy phosphates such as PCr and the conversion of pyruvate to lactate may be the preferred substrate metabolised during muscle contraction, rather than glucose from blood, glycogenolysis or fatty acid oxidation *via* β -oxidation. This may also justify the relatively low PHOS activity as well as the low glycogen content found in cheetah skeletal muscle. In accordance with this observation, Williams *et al.* (1997) demonstrated that even though glycogen utilisation was delayed following electrical stimulation of skeletal muscle in cheetah, ATP was still being generated which was most likely due to PCr hydrolysis. Future research can potentially confirm these hypotheses by measuring total Cr and PCr content in cheetah skeletal muscle at rest and after a high-speed sprint.

There is a limited number of studies pertaining to cheetah skeletal muscle, as opposed to human skeletal muscle. Current available data can only confirm that cheetahs possess a higher proportion of type IIX fibres compared to humans, and their capacity for glycolytic metabolism and Cr/ PCr turnover far exceeds human muscle fibres (Williams *et al.*, 1997; Kohn *et al.*, 2011a). Single fibre analyses may be utilised in future research to investigate

fibre-specific metabolism and substrate turnover, sarcomere length contraction speed, force generation and power output which would add new insight to the existing literature.

The significant increase observed in 3HAD activity in the control and glycine groups compared to the baseline values was unexpected and requires further investigation. At present, it is largely unknown as to why this difference occurred in 3HAD as the control and baseline groups consisted of the same diet. The diet intervention of all treatment groups (baseline, control and glycine) consisted of a meat-based diet with Panthera Supplement that was not included in the diets of the cheetahs prior to the study. Thus, the addition of this supplement, or a potential side-effect of any one of the administered drugs may have chronically affected fat metabolism. The present study is a part of a larger study investigating the entire metabolome of captive cheetahs in response to glycine supplementation. Metabolomics analyses will be performed on the current samples and may be utilised to investigate potential links to fatty acid oxidation pathways. Nonetheless, there are existing studies that suggest glycine may influence fat metabolism (Wittebans *et al.*, 2019; White *et al.*, 2020; Zhou *et al.*, 2021). The glycine conjugation pathway may therefore be linked to alterations in fat metabolism as CoA sequestration (as a result of glycine depletion) may impair fatty acid oxidation as well as limit availability of vital metabolites for muscle metabolism (Badenhorst *et al.*, 2013; Badenhorst *et al.*, 2014). Additional glycine has also been shown to enhance the glycine conjugation pathway, resulting in reduced CoA sequestration while stimulating the synthesis of metabolites that can be utilised by skeletal muscle for ATP generation. Therefore, supplementary glycine may potentially increase the flux through certain pathways by increasing the availability of their preferred metabolites. However, such changes were overall not detected here and the effects on 3HAD warrants further investigation.

The morphology and metabolism of cheetah muscle suggest a potential requirement for glycine, and although glycine had no effects on the muscle of captive cheetah, it may still be highly beneficial as a supplement especially in captivity. Captive cheetahs may experience a higher risk of developing degenerative muscle disorders as aging has been shown to be associated with muscle atrophy (due to inactivity or disuse) (Ham *et al.*, 2014). The concentration of serum glycine, serine, proline and hydroxyproline, as well as CoA were also significantly reduced by age (Tordiffe & Mienie, 2019). Thus, captive cheetahs may experience a continuous loss of glycine and CoA the longer they live in captivity, which may have progressive detrimental metabolic effects. Creatine also serves as an important fuel for energy production in spermatozoa, facilitating sperm and flagellar motility (Tombs & Shapiro, 1985; Lee *et al.*, 1988). Future studies could determine semen quality in this

population, as cheetahs are reported to reproduce poorly in captivity (Terrell *et al.*, 2010; Gillis-Germitsch *et al.*, 2017).

In conclusion, 4 weeks of glycine supplementation did not have any effects on the skeletal muscle morphology and metabolism of captive cheetah, but may serve as a cheaper alternative to carcass feeding. The skeletal muscle of cheetah is represented by a high proportion of type II fibres (predominantly type IIX) and a low proportion of type I fibres. The metabolism indicates poor oxidative capacity and a strong affinity for anaerobic-based metabolism, mainly from high-energy phosphates and lactate production. Overall, the skeletal muscle profile of the cheetah supports its lifestyle and facilitates its incredible sprinting ability.

This study is the first to investigate the effects of glycine on skeletal muscle in the cheetah. Additionally, this is the first study to measure the maximum enzyme activities of a number of glycolytic and oxidative enzymes in a large cohort of cheetahs (>3). Therefore, the results obtained here may serve as a foundation for the progression of future research pertaining to cheetah muscle as well as the effects of a glycine supplement.

Limitations of the study

This is the first study to evaluate the effects of exogenous glycine on skeletal muscle, and also the first to do so in captive cheetahs. Due to the novelty, acquiring literature for accurate data analysis and comparison within and between species was challenging. Factors including different instrumentation used for analyses, various methods of determination (mRNA levels, protein expression), status of the animal, sampling method, site and sampling depth also affect the reproducibility of results. This is highlighted by discrete variations in the reported data for muscle fibre composition of the cheetah. There are no data in cheetahs on some of the enzyme activities reported here, therefore no means of comparison was available. Owing to this, the results of the current study may serve as baseline values for future research.

As outlined in Chapter 3, the supplements of the cheetahs prior to the study were different compared to during the diet intervention, and initial sampling was only performed after completion of the habituation period. If there were indeed any residual effects of any supplement, it could not be concluded by the present study, as no baseline data before administration of the intervention diet was acquired.

As the current cohort of cheetahs were born in captivity, and already acclimated to their enclosure/ environment as well as their respective caregivers, the data presented here are

limited to the captive population only and may not provide an accurate representation of the muscle profile of the free-ranging population. Given the effects that varying diets and (potentially) supplements have on the health of captive cheetah, inclusion of more captive populations (from different sanctuaries, as diets vary) may reveal further insight into the metabolism of this species.

Finally, no changes were observed in response to glycine supplementation in the current study. Potentially, the intervention period, feeding frequency and/ or amount of glycine powder was insufficient to elicit any detectable effects and could be increased for future studies. As for the current study, the management and execution of the project was completed in consideration of the financial and time constraints.



Bibliography

- Acevedo LM & Rivero J-LL. (2006). New insights into skeletal muscle fibre types in the dog with particular focus towards hybrid myosin phenotypes. *Cell and tissue research* **323**, 283-303.
- Adeva-Andany M, Souto-Adeva G, Ameneiros-Rodríguez E, Fernández-Fernández C, Donapetry-García C & Domínguez-Montero A. (2018). Insulin resistance and glycine metabolism in humans. *Amino Acids* **50**, 11-27.
- Akinde D. (2014). Amino acid efficiency with dietary glycine supplementation: Part 1. *World's Poultry Science Journal* **70**, 461-474.
- Akram M. (2013). Mini-review on glycolysis and cancer. *Journal of Cancer Education* **28**, 454-457.
- Akram M. (2014). Citric acid cycle and role of its intermediates in metabolism. *Cell biochemistry and biophysics* **68**, 475-478.
- Alexander RM. (2003). *Principles of animal locomotion*. Princeton University Press.
- Altringham JD & Johnston IA. (1990). Modelling muscle power output in a swimming fish. *Journal of Experimental Biology* **148**, 395-402.
- Alves A, Bassot A, Bulteau A-L, Pirola L & Morio B. (2019). Glycine metabolism and its alterations in obesity and metabolic diseases. *Nutrients* **11**, 1356.
- Andersen J, Weiss A, Sandri C, Schjerling P, Thonell L, Pedrosa-Domellof F, Leinwand L & Schiaffino S. (2002). The 2B myosin heavy chain gene is expressed in human skeletal muscle. In *Journal of Physiology-London*, pp. 29P-30P. Cambridge Univ Press 40 West 20th St, New York, NY 10011-4221 USA.
- Andersen JL & Schiaffino S. (1997). Mismatch between myosin heavy chain mRNA and protein distribution in human skeletal muscle fibers. *American Journal of Physiology-Cell Physiology* **272**, C1881-C1889.
- Ascher E, Hanson JN, Cheng W, Hingorani A & Scheinman M. (2001). Glycine preserves function and decreases necrosis in skeletal muscle undergoing ischemia and reperfusion injury. *Surgery* **129**, 231-235.
- Badenhorst CPS, Erasmus E, Van der Sluis R, Nortje C & Van Dijk AA. (2014). A new perspective on the importance of glycine conjugation in the metabolism of aromatic acids. *Drug metabolism reviews* **46**, 343-361.
- Badenhorst CPS, van der Sluis R, Erasmus E & Van Dijk AA. (2013). Glycine conjugation: importance in metabolism, the role of glycine N-acyltransferase, and factors that influence interindividual variation. *Expert opinion on drug metabolism & toxicology* **9**, 1139-1153.
- Baldwin JE & Krebs H. (1981). The evolution of metabolic cycles. *Nature* **291**, 381-382.
- Barnard RJ, Edgerton VR & Peter J. (1970). Effect of exercise on skeletal muscle. I. Biochemical and histochemical properties. *Journal of applied physiology* **28**, 762-766.

- Bauer H & De longh H. (2005). Lion (*Panthera leo*) home ranges and livestock conflicts in Waza National Park, Cameroon. *African journal of ecology* **43**, 208-214.
- Bechert U, Mortenson J, Dierenfeld ES, Cheeke P, Keller M, Holick M, Chen TC & Rogers Q. (2002). Diet composition and blood values of captive cheetahs (*Acinonyx jubatus*) fed either supplemented meat or commercial food preparations. *Journal of Zoo and Wildlife Medicine* **33**, 16-28.
- Bellof G, Most E & Pallauf J. (2007). Concentration of copper, iron, manganese and zinc in muscle, fat and bone tissue of lambs of the breed German Merino Landsheep in the course of the growing period and different feeding intensities. *Journal of animal physiology and animal nutrition* **91**, 100-108.
- Berg JM, Tymoczko JL & Stryer L. (2002). *Biochemistry*, vol. 5th Ed. New York: WH Freeman.
- Bessman SP & Carpenter CL. (1985). The creatine-creatine phosphate energy shuttle. *Annual review of biochemistry* **54**, 831-862.
- Bianospino E, Moura ASAMT, Wechsler FS, Fernandes S & Dal-Pai-Silva M. (2008). Age-related changes in muscle fiber type frequencies and cross-sectional areas in straightbred and crossbred rabbits. *animal* **2**, 1627-1632.
- Bond JC & Lindburg DG. (1990). Carcass feeding of captive cheetahs (*Acinonyx jubatus*): the effects of a naturalistic feeding program on oral health and psychological well-being. *Applied Animal Behaviour Science* **26**, 373-382.
- Bottinelli R. (2001). Functional heterogeneity of mammalian single muscle fibres: do myosin isoforms tell the whole story? *Pflügers Archiv* **443**, 6-17.
- Bottinelli R, Canepari M, Pellegrino M & Reggiani C. (1996). Force-velocity properties of human skeletal muscle fibres: myosin heavy chain isoform and temperature dependence. *The Journal of physiology* **495**, 573-586.
- Bottinelli R, Schiaffino S & Reggiani C. (1991). Force-velocity relations and myosin heavy chain isoform compositions of skinned fibres from rat skeletal muscle. *The Journal of physiology* **437**, 655-672.
- Bowser SM, McMillan RP, Boutagy NE, Tarpey MD, Smithson AT, Osterberg KL, Neilson AP, Davy BM, Davy KP & Hulver MW. (2020). Serum endotoxin, gut permeability and skeletal muscle metabolic adaptations following a short term high fat diet in humans. *Metabolism* **103**, 154041.
- Bradford MM. (1976). A rapid and sensitive method for the quantitation of microgram quantities of protein utilizing the principle of protein-dye binding. *Analytical biochemistry* **72**, 248-254.
- Caldow MK, Ham DJ, Trieu J, Chung JD, Lynch GS & Koopman R. (2019). Glycine protects muscle cells from wasting in vitro via mTORC1 signaling. *Frontiers in Nutrition* **6**, 172.
- Caro T. (1994). *Cheetahs of the Serengeti Plains: group living in an asocial species*. University of Chicago Press.

- Charruau P, Fernandes C, OROZCO-terWENGEL P, Peters J, Hunter L, Ziaie H, Jourabchian A, Jowkar H, Schaller G & Ostrowski S. (2011). Phylogeography, genetic structure and population divergence time of cheetahs in Africa and Asia: evidence for long-term geographic isolates. *Molecular Ecology* **20**, 706-724.
- Cieslik KA, Sekhar RV, Granillo A, Reddy A, Medrano G, Heredia CP, Entman ML, Hamilton DJ, Li S & Reineke E. (2018). Improved cardiovascular function in old mice after N-Acetyl cysteine and glycine supplemented diet: inflammation and mitochondrial factors. *The Journals of Gerontology: Series A* **73**, 1167-1177.
- Corzo A, Fritts C, Kidd M & Kerr B. (2005). Response of broiler chicks to essential and non-essential amino acid supplementation of low crude protein diets. *Animal feed science and technology* **118**, 319-327.
- Corzo A, Kidd M, Burnham D & Kerr B. (2004). Dietary glycine needs of broiler chicks. *Poultry science* **83**, 1382-1384.
- Cristea A, Korhonen M, Häkkinen K, Mero A, Alén M, Sipilä S, Viitasalo J, Koljonen M, Suominen H & Larsson L. (2008). Effects of combined strength and sprint training on regulation of muscle contraction at the whole-muscle and single-fibre levels in elite master sprinters. *Acta Physiologica* **193**, 275-289.
- Curry JW, Hohl R, Noakes TD & Kohn TA. (2012). High oxidative capacity and type IIx fibre content in springbok and fallow deer skeletal muscle suggest fast sprinters with a resistance to fatigue. *Journal of Experimental Biology* **215**, 3997-4005.
- Curt MJ-C, Voicu P-M, Fontaine M, Dessein A-F, Porchet N, Mention-Mulliez K, Dobbelaere D, Soto-Ares G, Cheillan D & Vamecq J. (2015). Creatine biosynthesis and transport in health and disease. *Biochimie* **119**, 146-165.
- D'Antona G, Lanfranconi F, Pellegrino MA, Brocca L, Adami R, Rossi R, Moro G, Miotti D, Canepari M & Bottinelli R. (2006). Skeletal muscle hypertrophy and structure and function of skeletal muscle fibres in male body builders. *The Journal of physiology* **570**, 611-627.
- da Costa N, Edgar J, Ooi P-T, Su Y, Meissner JD & Chang K-C. (2007). Calcineurin differentially regulates fast myosin heavy chain genes in oxidative muscle fibre type conversion. *Cell and tissue research* **329**, 515-527.
- Dada S, Henning F, Feldmann DC & Kohn TA. (2018). Baboon (*Papio ursinus*) single fibre contractile properties are similar to that of trained humans. *Journal of muscle research and cell motility* **39**, 189-199.
- Dean D, Bidner T & Southern L. (2006). Glycine supplementation to low protein, amino acid-supplemented diets supports optimal performance of broiler chicks. *Poultry Science* **85**, 288-296.
- DeGroot A, Braun U & Dilger R. (2019). Guanidinoacetic acid is efficacious in improving growth performance and muscle energy homeostasis in broiler chicks fed arginine-deficient or arginine-adequate diets. *Poultry science* **98**, 2896-2905.
- Depauw S, Heilmann RM, Whitehouse-Tedd K, Hesta M, Steiner JM, Suchodolski JS & Janssens GP. (2014). Effect of diet type on serum and faecal concentration of S100/calgranulins in the captive cheetah. *Journal of Zoo and Aquarium Research* **2**, 33-38.

- Depauw S, Hesta M, Whitehouse-Tedd K, Vanhaecke L, Verbrugghe A & Janssens G. (2013). Animal fibre: The forgotten nutrient in strict carnivores? First insights in the cheetah. *Journal of animal physiology and animal nutrition* **97**, 146-154.
- Dierenfeld E, Kerr K & Whitehouse-Tedd K. (2015). Cheetah nutrition: recent advances and revised spp recommendations. In *Proceedings of the Eleventh Conference on Zoo and Wildlife Nutrition*. Portland, OR.
- Donnier-Maréchal M & Vidal S. (2016). Glycogen phosphorylase inhibitors: a patent review (2013-2015). *Expert opinion on therapeutic patents* **26**, 199-212.
- Durant S, Mitchell N, Ipavec A & Groom R. (2015). *Acinonyx jubatus*. The IUCN Red List of Threatened Species 2015: e. T219A50649567. *Mammal Species*, 1545-1410.
- Durant SM, Mitchell N, Groom R, Pettorelli N, Ipavec A, Jacobson AP, Woodroffe R, Böhm M, Hunter LT & Becker MS. (2017). The global decline of cheetah *Acinonyx jubatus* and what it means for conservation. *Proceedings of the National Academy of Sciences* **114**, 528-533.
- Eaton RL. (1970). Hunting behavior of the cheetah. *The Journal of Wildlife Management*, 56-67.
- Essén-Gustavsson B & Henriksson J. (1984). Enzyme levels in pools of microdissected human muscle fibres of identified type: adaptive response to exercise. *Acta physiologica Scandinavica* **120**, 505-515.
- Essen B, Jansson E, Henriksson J, Taylor A & Saltin B. (1975). Metabolic characteristics of fibre types in human skeletal muscle. *Acta physiologica Scandinavica* **95**, 153-165.
- Farhadinia MS, Hunter LT, Jourabchian A, Hosseini-Zavarei F, Akbari H, Ziaie H, Schaller GB & Jowkar H. (2017). The critically endangered Asiatic cheetah *Acinonyx jubatus venaticus* in Iran: a review of recent distribution, and conservation status. *Biodiversity and Conservation* **26**, 1027-1046.
- Farhana A & Lappin SL. (2020). *Biochemistry, lactate dehydrogenase*. StatPearls.
- Feher J. (2017). 7.4 - Tubular Reabsorption and Secretion. In *Quantitative Human Physiology (Second Edition)*, ed. Feher J, pp. 719-729. Academic Press, Boston.
- Frontera WR & Ochala J. (2015). Skeletal muscle: a brief review of structure and function. *Calcified tissue international* **96**, 183-195.
- Gibson NR, Jahoor F, Ware L & Jackson AA. (2002). Endogenous glycine and tyrosine production is maintained in adults consuming a marginal-protein diet. *The American journal of clinical nutrition* **75**, 511-518.
- Gillies AR & Lieber RL. (2011). Structure and function of the skeletal muscle extracellular matrix. *Muscle & nerve* **44**, 318-331.
- Gillis-Germitsch N, Vybiral PR, Codron D, Clauss M, Kotze A & Mitchell EP. (2017). Intrinsic factors, adrenal gland morphology, and disease burden in captive cheetahs (*Acinonyx jubatus*) in South Africa. *Zoo biology* **36**, 40-49.

- Gollnick P, Armstrong R, Saubert 4th C, Piehl K & Saltin B. (1972). Enzyme activity and fiber composition in skeletal muscle of untrained and trained men. *Journal of applied physiology* **33**, 312-319.
- Goto M, Kawai M, Nakata M, Itamoto K, Miyata H, Ikebe Y, Tajima T & Wada N. (2013). Distribution of muscle fibers in skeletal muscles of the cheetah (*Acinonyx jubatus*). *Mammalian biology* **78**, 127-133.
- Gray SR, Söderlund K & Ferguson RA. (2008). ATP and phosphocreatine utilization in single human muscle fibres during the development of maximal power output at elevated muscle temperatures. *Journal of sports sciences* **26**, 701-707.
- Hafidi ME, Pérez I, Zamora J, Soto V, Carvajal-Sandoval G & Banos G. (2004). Glycine intake decreases plasma free fatty acids, adipose cell size, and blood pressure in sucrose-fed rats. *American Journal of Physiology-Regulatory, Integrative and Comparative Physiology* **287**, R1387-R1393.
- Hafkenschied J & Hectors M. (1975). An enzymic method for the determination of the glycine/taurine ratio of conjugated bile acids in bile. *Clinica Chimica Acta* **65**, 67-74.
- Hall JC. (1998). Glycine. *Journal of Parenteral and Enteral Nutrition* **22**, 393-398.
- Ham DJ, Murphy KT, Chee A, Lynch GS & Koopman R. (2014). Glycine administration attenuates skeletal muscle wasting in a mouse model of cancer cachexia. *Clinical nutrition* **33**, 448-458.
- Han NR, Kim HY, Kim NR, Lee WK, Jeong H, Kim HM & Jeong HJ. (2018). Leucine and glycine dipeptides of porcine placenta ameliorate physical fatigue through enhancing dopaminergic systems. *Molecular Medicine Reports* **17**, 4120-4130.
- Hänninen O & Atalay M. (1998). Oxidative metabolism in skeletal muscle. In *Oxidative stress in skeletal muscle*, pp. 29-42. Springer.
- Hargreaves M & Spriet LL. (2020). Skeletal muscle energy metabolism during exercise. *Nature Metabolism* **2**, 817-828.
- Hayward M, Hofmeyr M, O'brien J & Kerley GI. (2006). Prey preferences of the cheetah (*Acinonyx jubatus*)(Felidae: Carnivora): morphological limitations or the need to capture rapidly consumable prey before kleptoparasites arrive? *Journal of Zoology* **270**, 615-627.
- Hetem RS, Mitchell D, de Witt BA, Fick LG, Meyer LC, Maloney SK & Fuller A. (2013). Cheetah do not abandon hunts because they overheat. *Biology Letters* **9**, 20130472.
- Hilliar M, Huyen N, Girish C, Barekatin R, Wu S & Swick R. (2019). Supplementing glycine, serine, and threonine in low protein diets for meat type chickens. *Poultry Science* **98**, 6857-6865.
- Holbrook JJ, Liljas A, Steindel SJ & Rossmann MG. (1975). 4 lactate dehydrogenase. In *The enzymes*, pp. 191-292. Elsevier.
- Holloszy JO & Booth FW. (1976). Biochemical adaptations to endurance exercise in muscle. *Annual review of physiology* **38**, 273-291.

- Hou Y, Yao K, Yin Y & Wu G. (2016). Endogenous synthesis of amino acids limits growth, lactation, and reproduction in animals. *Advances in Nutrition* **7**, 331-342.
- Howland RD. (1981). The etiology of acrylamide neuropathy: enolase, phosphofructokinase, and glyceraldehyde-3-phosphate dehydrogenase activities in peripheral nerve, spinal cord, brain, and skeletal muscle of acrylamide-intoxicated cats. *Toxicology and applied pharmacology* **60**, 324-333.
- Hu S, Nawaratna G, Long B, Bazer F, Johnson G, Brosnan J & Wu G. (2017). The hydroxyproline–glycine pathway for glycine synthesis in neonatal pigs. *Journal of Animal Science* **95**, 45.
- Hudson PE, Corr SA, Payne-Davis RC, Clancy SN, Lane E & Wilson AM. (2011a). Functional anatomy of the cheetah (*Acinonyx jubatus*) forelimb. *Journal of Anatomy* **218**, 375-385.
- Hudson PE, Corr SA, Payne-Davis RC, Clancy SN, Lane E & Wilson AM. (2011b). Functional anatomy of the cheetah (*Acinonyx jubatus*) hindlimb. *Journal of anatomy* **218**, 363-374.
- Hudson PE, Corr SA & Wilson AM. (2012). High speed galloping in the cheetah (*Acinonyx jubatus*) and the racing greyhound (*Canis familiaris*): spatio-temporal and kinetic characteristics. *Journal of Experimental Biology* **215**, 2425-2434.
- Hunter S, Laastuen L & Todd W. (1967). Amino acid imbalance and liver glycogen changes in rats fed glycine. *The Journal of Nutrition* **92**, 133-137.
- Hyatt JPK, Roy RR, Rugg S & Talmadge RJ. (2010). Myosin heavy chain composition of tiger (*Panthera tigris*) and cheetah (*Acinonyx jubatus*) hindlimb muscles. *Journal of Experimental Zoology Part A: Ecological Genetics and Physiology* **313**, 45-57.
- IUCN/SSC. (2007). Regional conservation strategy for the cheetah and African wild dog in Southern Africa. *IUCN Species Survival Commission Gland*.
- IUCN/SSC. (2015). Review of the Regional Conservation Strategy for the Cheetah and African Wild Dogs in Southern Africa. IUCN Species Survival Commission Gland, Switzerland.
- Jacobson AP, Gerngross P, Lemeris Jr JR, Schoonover RF, Anco C, Breitenmoser-Würsten C, Durant SM, Farhadinia MS, Henschel P & Kamler JF. (2016). Leopard (*Panthera pardus*) status, distribution, and the research efforts across its range. *PeerJ* **4**, e1974.
- Jansson E & Kaijser L. (1977). Muscle adaptation to extreme endurance training in man. *Acta Physiologica Scandinavica* **100**, 315-324.
- Jansson E & Sylvén C. (1983). Myoglobin concentration in single type I and type II muscle fibres in man. *Histochemistry* **78**, 121-124.
- Jensen J, Rustad PI, Kolnes AJ & Lai Y-C. (2011). The role of skeletal muscle glycogen breakdown for regulation of insulin sensitivity by exercise. *Frontiers in physiology* **2**, 112.
- Jones EJ, Bishop PA, Woods AK & Green JM. (2008). Cross-sectional area and muscular strength: a brief review. *Sports Medicine* **38**, 987-994.

- Kamei Y, Hatazawa Y, Uchitomi R, Yoshimura R & Miura S. (2020). Regulation of skeletal muscle function by amino acids. *Nutrients* **12**, 261.
- Karatzafiri C, De Haan A, Ferguson R, Van Mechelen W & Sargeant A. (2001). Phosphocreatine and ATP content in human single muscle fibres before and after maximum dynamic exercise. *Pflügers Archiv* **442**, 467-474.
- Knuiman P, Hopman MT & Mensink M. (2015). Glycogen availability and skeletal muscle adaptations with endurance and resistance exercise. *Nutrition & metabolism* **12**, 1-11.
- Kohlmeier M. (2015). Amino Acids and Nitrogen Compounds. pp. 265-477.
- Kohn TA. (2014). Insights into the skeletal muscle characteristics of three southern African antelope species. *Biology open* **3**, 1037-1044.
- Kohn TA, Burroughs R, Hartman MJ & Noakes TD. (2011a). Fiber type and metabolic characteristics of lion (*Panthera leo*), caracal (*Caracal caracal*) and human skeletal muscle. *Comparative Biochemistry and Physiology Part A: Molecular & Integrative Physiology* **159**, 125-133.
- Kohn TA, Curry JW & Noakes TD. (2011b). Black wildebeest skeletal muscle exhibits high oxidative capacity and a high proportion of type IIx fibres. *Journal of Experimental Biology* **214**, 4041-4047.
- Kohn TA, Essén-Gustavsson B & Myburgh KH. (2007). Do skeletal muscle phenotypic characteristics of Xhosa and Caucasian endurance runners differ when matched for training and racing distances? *Journal of Applied Physiology* **103**, 932-940.
- Kohn TA, Kritzing B, Hoffman LC & Myburgh KH. (2005). Characteristics of impala (*Aepyceros melampus*) skeletal muscles. *Meat science* **69**, 277-282.
- Kohn TA & Myburgh KH. (2007). Regional specialization of rat quadriceps myosin heavy chain isoforms occurring in distal to proximal parts of middle and deep regions is not mirrored by citrate synthase activity. *Journal of Anatomy* **210**, 8-18.
- Kohn TA & Noakes TD. (2013). Lion (*Panthera leo*) and caracal (*Caracal caracal*) type IIx single muscle fibre force and power exceed that of trained humans. *Journal of experimental Biology* **216**, 960-969.
- Koopman R, Caldow MK, Ham DJ & Lynch GS. (2017). Glycine metabolism in skeletal muscle: implications for metabolic homeostasis. *Current Opinion in Clinical Nutrition & Metabolic Care* **20**, 237-242.
- Krausman PR & Morales SM. (2005). *Acinonyx jubatus*. *Mammalian Species* **2005**, 1-6.
- Krebs EG & Fischer EH. (1964). Phosphorylase and related enzymes of glycogen metabolism. *Vitamins & Hormones* **22**, 399-410.
- Krivickas LS, Dorer DJ, Ochala J & Frontera WR. (2011). Relationship between force and size in human single muscle fibres. *Experimental physiology* **96**, 539-547.
- Lane E, Miller S, Lobetti R, Caldwell P, Bertschinger H, Burroughs R, Kotze A & Van Dyk A. (2012). Effect of diet on the incidence of and mortality owing to gastritis and renal

- disease in captive cheetahs (*Acinonyx jubatus*) in South Africa. *Zoo Biology* **31**, 669-682.
- Lee H, Fillers W & Iyengar M. (1988). Phosphocreatine, an intracellular high-energy compound, is found in the extracellular fluid of the seminal vesicles in mice and rats. *Proceedings of the National Academy of Sciences* **85**, 7265-7269.
- Li P & Wu G. (2018). Roles of dietary glycine, proline, and hydroxyproline in collagen synthesis and animal growth. *Amino acids* **50**, 29-38.
- Li X, Higashida K, Kawamura T & Higuchi M. (2016). Alternate-day high-fat diet induces an increase in mitochondrial enzyme activities and protein content in rat skeletal muscle. *Nutrients* **8**, 203.
- Li X, Rezaei R, Li P & Wu G. (2011). Composition of amino acids in feed ingredients for animal diets. *Amino acids* **40**, 1159-1168.
- Liu Y, Wang X, Hou Y, Yin Y, Qiu Y, Wu G & Hu C-AA. (2017). Roles of amino acids in preventing and treating intestinal diseases: recent studies with pig models. *Amino Acids* **49**, 1277-1291.
- Loveridge AJ, Valeix M, Davidson Z, Murindagomo F, Fritz H & Macdonald DW. (2009). Changes in home range size of African lions in relation to pride size and prey biomass in a semi-arid savanna. *Ecography* **32**, 953-962.
- MacDougall JD, Hicks AL, MacDonald JR, McKelvie RS, Green HJ & Smith KM. (1998). Muscle performance and enzymatic adaptations to sprint interval training. *Journal of applied physiology* **84**, 2138-2142.
- MacIntosh BR, Gardiner PF & McComas AJ. (2006). *Skeletal muscle: form and function*. Human kinetics.
- Mann G, Mora S, Madu G & Adegoke OA. (2021). Branched-chain amino acids: catabolism in skeletal muscle and implications for muscle and whole-body metabolism. *Frontiers in Physiology* **12**.
- Mansour TE. (1972). Phosphofructokinase. *Current topics in cellular regulation* **5**, 1-46.
- Marieb EN & Hoehn K. (2007). *Human anatomy & physiology*. Pearson education.
- Marker L, Dickman A, Mills MG, Joo R & Macdonald DW. (2008). Spatial ecology of cheetahs on north-central Namibian farmlands. *Journal of Zoology* **274**, 226-238.
- Markert CL. (1984). Lactate dehydrogenase. Biochemistry and function of lactate dehydrogenase. *Cell Biochemistry and Function: Cellular biochemistry and its modulation by active agents or disease* **2**, 131-134.
- Marnewick K, Beckhelling A, Cilliers D, Lane E, Mills G, Herring K, Caldwell P, Hall R & Meintjes S. (2007). The status of the cheetah in South Africa. *Cat News* **3**, 27-31.
- Martin LJ, Blossey B & Ellis E. (2012). Mapping where ecologists work: biases in the global distribution of terrestrial ecological observations. *Frontiers in Ecology and the Environment* **10**, 195-201.

- Mason GJ. (2010). Species differences in responses to captivity: stress, welfare and the comparative method. *Trends in Ecology & Evolution* **25**, 713-721.
- McCommis KS & Finck BN. (2015). Mitochondrial pyruvate transport: a historical perspective and future research directions. *Biochemical journal* **466**, 443-454.
- McMahon CJ, Wu JS & Eisenberg RL. (2010). Muscle edema. *American Journal of Roentgenology* **194**, W284-W292.
- Meléndez-Hevia E, de Paz-Lugo P, Cornish-Bowden A & Cárdenas ML. (2009). A weak link in metabolism: the metabolic capacity for glycine biosynthesis does not satisfy the need for collagen synthesis. *Journal of biosciences* **34**, 853-872.
- Menke S, Melzheimer J, Thalwitzer S, Heinrich S, Wachter B & Sommer S. (2017). Gut microbiomes of free-ranging and captive Namibian cheetahs: Diversity, putative functions and occurrence of potential pathogens. *Molecular ecology* **26**, 5515-5527.
- Mukund K & Subramaniam S. (2020). Skeletal muscle: A review of molecular structure and function, in health and disease. *Wiley Interdisciplinary Reviews: Systems Biology and Medicine* **12**, e1462.
- Munson L, Terio KA, Worley M, Jago M, Bagot-Smith A & Marker L. (2005). Extrinsic factors significantly affect patterns of disease in free-ranging and captive cheetah (*Acinonyx jubatus*) populations. *Journal of wildlife diseases* **41**, 542-548.
- Nakashima K, Yakabe Y, Ishida A & Katsumata M. (2008). Effects of orally administered glycine on myofibrillar proteolysis and expression of proteolytic-related genes of skeletal muscle in chicks. *Amino acids* **35**, 451-456.
- Negro M, Avanzato I & D'Antona G. (2019). Creatine in Skeletal Muscle Physiology. In *Nonvitamin and Nonmineral Nutritional Supplements*, pp. 59-68. Elsevier.
- Ngo A, Coon C & Beecher G. (1977). Dietary glycine requirements for growth and cellular development in chicks. *The Journal of nutrition* **107**, 1800-1808.
- Nickols M. (2016). Effects of feeding method and exercise on the physiological status of captive cheetah (*Acinonyx jubatus*). In *Animal and Wildlife Sciences*, pp. 111. University of Pretoria, University of Pretoria.
- Nilkumang P & Thornton J. (1979). Plasma and tissue enzyme activities in the cat. *Journal of Small Animal Practice* **20**, 169-174.
- Norton A. (1985). Radio tracking of leopards and caracals in the Stellenbosch area, Cape Province. *South African Journal of Wildlife Research-24-month delayed open access* **15**, 17-24.
- Nowak L & Reyes PF. (2008). Muscle biopsy: a diagnostic tool in muscle diseases. *Journal of Histotechnology* **31**, 101-108.
- Olson BJ & Markwell J. (2007). Assays for determination of protein concentration. *Current Protocols in Pharmacology* **38**, A. 3A. 1-A. 3A. 29.
- Ostojic SM. (2015). Advanced physiological roles of guanidinoacetic acid. *European journal of nutrition* **54**, 1211-1215.

- Ostojic SM, Drid P & Ostojic J. (2016). Guanidinoacetic acid increases skeletal muscle creatine stores in healthy men. *Nutrition* **32**, 723.
- Pandy MG, Lai AK, Schache AG & Lin YC. (2021). How muscles maximize performance in accelerated sprinting. *Scandinavian Journal of Medicine & Science in Sports* **31**, 1882-1896.
- Parimi PS, Gruca LL & Kalhan SC. (2005). Metabolism of threonine in newborn infants. *American Journal of Physiology-Endocrinology and Metabolism* **289**, E981-E985.
- Passonneau JV & Lowry OH. (1993). *Enzymatic analysis: a practical guide*. Springer Science & Business Media.
- Pette D. (1985). Metabolic heterogeneity of muscle fibres. *Journal of Experimental Biology* **115**, 179-189.
- Possik E & Pause A. (2018). Biochemical measurement of glycogen: method to investigate the AMPK-glycogen relationship. In *AMPK*, pp. 57-67. Springer.
- Prince FP, Hikida RS & Hagerman FC. (1976). Human muscle fiber types in power lifters, distance runners and untrained subjects. *Pflügers Archiv* **363**, 19-26.
- Prost S, Machado AP, Zumbroich J, Preier L, Mahtani-Williams S, Guschanski K, Brealey JC, Fernandes C, Vercammen P & Godsall-Bottriell L. (2020). Conservation Genomic Analyses of African and Asiatic Cheetahs (*Acinonyx jubatus*) Across Their Current and Historic Species Range. *BioRxiv*.
- Razak MA, Begum PS, Viswanath B & Rajagopal S. (2017). Multifarious beneficial effect of nonessential amino acid, glycine: a review. *Oxidative medicine and cellular longevity* **2017**.
- Ren J-M, Semenkovich CF, Gulve EA, Gao J & Holloszy JO. (1994). Exercise induces rapid increases in GLUT4 expression, glucose transport capacity, and insulin-stimulated glycogen storage in muscle. *Journal of Biological Chemistry* **269**, 14396-14401.
- Riddle ES, Stipanuk MH & Thalacker-Mercer AE. (2016). Amino acids in healthy aging skeletal muscle. *Front Biosci (Elite Ed)* **8**, 326-350.
- Rivero J-LL & Hill EW. (2016). Skeletal muscle adaptations and muscle genomics of performance horses. *The Veterinary Journal* **209**, 5-13.
- Roberts A, Billeter R & Howald H. (1982). Anaerobic muscle enzyme changes after interval training. *International journal of sports medicine* **3**, 18-21.
- Rocha Leão MHM. (2003). Glycogen. In *Encyclopedia of Food Sciences and Nutrition (Second Edition)*, ed. Caballero B, pp. 2930-2937. Academic Press, Oxford.
- Rom O, Liu Y, Liu Z, Zhao Y, Wu J, Ghrayeb A, Villacorta L, Fan Y, Chang L & Wang L. (2020). Glycine-based treatment ameliorates NAFLD by modulating fatty acid oxidation, glutathione synthesis, and the gut microbiome. *Science translational medicine* **12**, eaaz2841.
- Saltin B. (1983). Skeletal muscle adaptability: significance for metabolism and performance. *Skeletal muscle*.

- Sadow A. (1970). Skeletal muscle. *Annual review of physiology* **32**, 87-138.
- Schiaffino S & Reggiani C. (2011). Fiber types in mammalian skeletal muscles. *Physiological reviews* **91**, 1447-1531.
- Schiaffino S, Reggiani C, Akimoto T & Blaauw B. (2021). Molecular mechanisms of skeletal muscle hypertrophy. *Journal of Neuromuscular Diseases* **8**, 169-183.
- Schoenfeld BJ. (2010). The mechanisms of muscle hypertrophy and their application to resistance training. *The Journal of Strength & Conditioning Research* **24**, 2857-2872.
- Schulz H. (1991). Beta oxidation of fatty acids. *Biochimica et Biophysica Acta (BBA)-Lipids and Lipid Metabolism* **1081**, 109-120.
- Scott W, Stevens J & Binder-Macleod SA. (2001). Human skeletal muscle fiber type classifications. *Physical therapy* **81**, 1810-1816.
- Seevaratnam R, Patel BP & Hamadeh MJ. (2009). Comparison of total protein concentration in skeletal muscle as measured by the Bradford and Lowry assays. *Journal of biochemistry* **145**, 791-797.
- Serrano A, Quiroz-Rothe E & Rivero J-L. (2000). Early and long-term changes of equine skeletal muscle in response to endurance training and detraining. *Pflügers Archiv* **441**, 263-274.
- Shaffer F & Neblett R. (2010). Practical anatomy and physiology: The skeletal muscle system. *Biofeedback* **38**, 47-51.
- Sharp N. (1997). Timed running speed of a cheetah (*Acinonyx jubatus*). *Journal of Zoology* **241**, 493-494.
- Shoepe TC, Stelzer JE, Garner DP & Widrick JJ. (2003). Functional adaptability of muscle fibers to long-term resistance exercise. *Medicine & Science in Sports & Exercise* **35**, 944-951.
- Shoulders MD & Raines RT. (2009). Collagen structure and stability. *Annual review of biochemistry* **78**, 929-958.
- Shyu AB, Wilkinson MF & Van Hoof A. (2008). Messenger RNA regulation: to translate or to degrade. *The EMBO journal* **27**, 471-481.
- Siegert W & Rodehutsord M. (2019). The relevance of glycine and serine in poultry nutrition: A review. *British poultry science* **60**, 579-588.
- Sillero-Zubiri C, Rostro-García S, Burruss D, Matchano A, Harouna A & Rabeil T. (2015). Saharan cheetah *Acinonyx jubatus hecki*, a ghostly dweller on Niger's Termit massif. *Oryx* **49**, 591-594.
- Simoneau J-A & Bouchard C. (1989). Human variation in skeletal muscle fiber-type proportion and enzyme activities. *American Journal of Physiology-Endocrinology And Metabolism* **257**, E567-E572.
- Spamer C & Pette D. (2019). Metabolic subpopulations of rabbit skeletal muscle fibres. In *Plasticity of muscle*, pp. 19-30. De Gruyter.

- Stein AB, Fuller TK, DeStefano S & Marker LL. (2011). Leopard population and home range estimates in north-central Namibia. *African Journal of Ecology* **49**, 383-387.
- Sun K, Wu Z, Ji Y & Wu G. (2016). Glycine regulates protein turnover by activating protein kinase B/mammalian target of rapamycin and by inhibiting MuRF1 and atrogen-1 gene expression in C2C12 myoblasts. *The Journal of nutrition* **146**, 2461-2467.
- Talmadge RJ, Grossman EJ & Roy RR. (1996). Myosin heavy chain composition of adult feline (*Felis catus*) limb and diaphragm muscles. *Journal of Experimental Zoology* **275**, 413-420.
- Talmadge RJ & Roy RR. (1993). Electrophoretic separation of rat skeletal muscle myosin heavy-chain isoforms. *Journal of Applied Physiology* **75**, 2337-2340.
- Terio K, Munson L, Marker L, Aldridge B & Solnick JV. (2005). Comparison of *Helicobacter* spp. in cheetahs (*Acinonyx jubatus*) with and without gastritis. *Journal of clinical microbiology* **43**, 229-234.
- Terio KA, Marker L & Munson L. (2004). Evidence for chronic stress in captive but not free-ranging cheetahs (*Acinonyx jubatus*) based on adrenal morphology and function. *Journal of Wildlife Diseases* **40**, 259-266.
- Terrell KA, Wildt DE, Anthony NM, Bavister BD, Leibo SP, Penfold LM, Marker LL & Crosier AE. (2010). Evidence for compromised metabolic function and limited glucose uptake in spermatozoa from the teratospermic domestic cat (*Felis catus*) and cheetah (*Acinonyx jubatus*). *Biology of reproduction* **83**, 833-841.
- Tesch PA & Karlsson J. (1985). Muscle fiber types and size in trained and untrained muscles of elite athletes. *Journal of Applied Physiology* **59**, 1716-1720.
- Todd W & Allen M. (1958). Synthesis of tissue glycogen in rats prefed diets with added glycine. *American Journal of Physiology-Legacy Content* **194**, 338-340.
- Tombes RM & Shapiro BM. (1985). Metabolite channeling: a phosphorylcreatine shuttle to mediate high energy phosphate transport between sperm mitochondrion and tail. *Cell* **41**, 325-334.
- Toniolo L, Cancellara P, Maccatrozzo L, Patruno M, Mascarello F & Reggiani C. (2008). Masticatory myosin unveiled: first determination of contractile parameters of muscle fibers from carnivore jaw muscles. *American Journal of Physiology-Cell Physiology* **295**, C1535-C1542.
- Toniolo L, Maccatrozzo L, Patruno M, Pavan E, Caliaro F, Rossi R, Rinaldi C, Canepari M, Reggiani C & Mascarello F. (2007). Fiber types in canine muscles: myosin isoform expression and functional characterization. *American Journal of Physiology-Cell Physiology* **292**, C1915-C1926.
- Tordiffe A. (2017). The metabolic profiling of cheetahs (*Acinonyx jubatus*): A systems biology approach to understanding the chronic diseases they suffer in captivity. North-West University.
- Tordiffe AS, Wachter B, Heinrich SK, Reyers F & Mienie LJ. (2016). Comparative serum fatty acid profiles of captive and free-ranging cheetahs (*Acinonyx jubatus*) in Namibia. *PLoS one* **11**, e0167608.

- Tordiffe ASW & Mienie LJ. (2019). Serum and urine amino acid profiles of captive cheetahs (*Acinonyx jubatus*). *Comparative Clinical Pathology* **28**, 287-296.
- Tordiffe ASW, Van Reenen M, Reyers F & Mienie LJ. (2017). Gas chromatography-mass spectrometry profiles of urinary organic acids in healthy captive cheetahs (*Acinonyx jubatus*). *Journal of Chromatography B* **1049**, 8-15.
- van der Meer E. (2016). *The cheetahs of Zimbabwe: distribution and population status 2015*. Esther van der Meer.
- Vuori E, Huunan-Seppälä A, Kilpiö JO & Salmela SS. (1979). Biologically active metals in human tissues: II. The effect of age on the concentration of cadmium in aorta, heart, kidney, liver, lung, pancreas and skeletal muscle. *Scandinavian journal of work, environment & health*, 16-22.
- Wachter B, Thalwitzer S, Hofer H, Lonzer J, Hildebrandt TB & Hermes R. (2011). Reproductive history and absence of predators are important determinants of reproductive fitness: the cheetah controversy revisited. *Conservation Letters* **4**, 47-54.
- Waldroup P, Jiang Q & Fritts C. (2005). Effects of glycine and threonine supplementation on performance of broiler chicks fed diets low in crude protein. *Int J Poult Sci* **4**, 250-257.
- Wallimann T & Hemmer W. (1994). Creatine kinase in non-muscle tissues and cells. *Molecular and cellular biochemistry* **133**, 193-220.
- Wang W, Dai Z, Wu Z, Lin G, Jia S, Hu S, Dahanayaka S & Wu G. (2014). Glycine is a nutritionally essential amino acid for maximal growth of milk-fed young pigs. *Amino acids* **46**, 2037-2045.
- Wang W, Wu Z, Dai Z, Yang Y, Wang J & Wu G. (2013). Glycine metabolism in animals and humans: implications for nutrition and health. *Amino acids* **45**, 463-477.
- Webster CC, Noakes TD, Chacko SK, Swart J, Kohn TA & Smith JA. (2016). Gluconeogenesis during endurance exercise in cyclists habituated to a long-term low carbohydrate high-fat diet. *The Journal of Physiology* **594**, 4389-4405.
- Weise FJ, Lemeris Jr JR, Munro SJ, Bowden A, Venter C, van Vuuren M & van Vuuren RJ. (2015). Cheetahs (*Acinonyx jubatus*) running the gauntlet: an evaluation of translocations into free-range environments in Namibia. *PeerJ* **3**, e1346.
- Weise FJ, Vijay V, Jacobson AP, Schoonover RF, Groom RJ, Horgan J, Keeping D, Klein R, Marnewick K & Maude G. (2017). The distribution and numbers of cheetah (*Acinonyx jubatus*) in southern Africa. *PeerJ* **5**, e4096.
- West TG, Toepfer CN, Woledge RC, Curtin NA, Rowleson A, Kalakoutis M, Hudson P & Wilson AM. (2013). Power output of skinned skeletal muscle fibres from the cheetah (*Acinonyx jubatus*). *Journal of Experimental Biology* **216**, 2974-2982.
- White PJ, Lapworth AL, McGarrah RW, Kwee LC, Crown SB, Ilkayeva O, An J, Carson MW, Christopher BA & Ball JR. (2020). Muscle-liver trafficking of BCAA-derived nitrogen underlies obesity-related glycine depletion. *Cell reports* **33**, 108375.

- Whitehouse-Tedd KM, Lefebvre SL & Janssens GP. (2015). Dietary factors associated with faecal consistency and other indicators of gastrointestinal health in the captive cheetah (*Acinonyx jubatus*). *PLoS One* **10**, e0120903.
- Wiegand G & Remington SJ. (1986). Citrate synthase: structure, control, and mechanism. *Annual review of biophysics and biophysical chemistry* **15**, 97-117.
- Williams T, Dobson G, Mathieu-Costello O, Morsbach D, Worley M & Phillips J. (1997). Skeletal muscle histology and biochemistry of an elite sprinter, the African cheetah. *Journal of Comparative Physiology B* **167**, 527-535.
- Wilson JW, Mills MG, Wilson RP, Peters G, Mills ME, Speakman JR, Durant SM, Bennett NC, Marks NJ & Scantlebury M. (2013). Cheetahs, *Acinonyx jubatus*, balance turn capacity with pace when chasing prey. *Biology letters* **9**, 20130620.
- Wittemans LB, Lotta LA, Oliver-Williams C, Stewart ID, Surendran P, Karthikeyan S, Day FR, Koulman A, Imamura F & Zeng L. (2019). Assessing the causal association of glycine with risk of cardio-metabolic diseases. *Nature communications* **10**, 1-13.
- Wolf C & Ripple WJ. (2017). Range contractions of the world's large carnivores. *Royal Society open science* **4**, 170052.
- Wolfe RR. (2006). The underappreciated role of muscle in health and disease. *The American journal of clinical nutrition* **84**, 475-482.
- Wu G. (2009). Amino acids: metabolism, functions, and nutrition. *Amino acids* **37**, 1-17.
- Wu G. (2010). Recent advances in swine amino acid nutrition. *Journal of Animal Science and Biotechnology* **1**, 118-130.
- Wu G, Bazer FW, Burghardt RC, Johnson GA, Kim SW, Knabe DA, Li P, Li X, McKnight JR & Satterfield MC. (2011). Proline and hydroxyproline metabolism: implications for animal and human nutrition. *Amino acids* **40**, 1053-1063.
- Wu G, Wu Z, Dai Z, Yang Y, Wang W, Liu C, Wang B, Wang J & Yin Y. (2013). Dietary requirements of "nutritionally non-essential amino acids" by animals and humans. *Amino acids* **44**, 1107-1113.
- Wyss M & Kaddurah-Daouk R. (2000). Creatine and creatinine metabolism. *Physiological reviews* **80**, 1107-1213.
- Xie S-w, Tian L-x, Jin Y, Yang H-j, Liang G-y & Liu Y-j. (2014). Effect of glycine supplementation on growth performance, body composition and salinity stress of juvenile Pacific white shrimp, *Litopenaeus vannamei* fed low fishmeal diet. *Aquaculture* **418**, 159-164.
- Xie S, Zhou W, Tian L, Niu J & Liu Y. (2016). Effect of N-acetyl cysteine and glycine supplementation on growth performance, glutathione synthesis, anti-oxidative and immune ability of Nile tilapia, *Oreochromis niloticus*. *Fish & shellfish immunology* **55**, 233-241.
- Yan BX & Sun YQ. (1997). Glycine residues provide flexibility for enzyme active sites. *Journal of Biological Chemistry* **272**, 3190-3194.

- Yan Z, Yan Z, Liu S, Yin Y, Yang T & Chen Q. (2021). Regulative Mechanism of Guanidinoacetic Acid on Skeletal Muscle Development and Its Application Prospects in Animal Husbandry: A Review. *Frontiers in Nutrition* **8**, 714567.
- Yang SY, He XY & Schulz H. (2005). 3-Hydroxyacyl-CoA dehydrogenase and short chain 3-hydroxyacyl-CoA dehydrogenase in human health and disease. *The FEBS journal* **272**, 4874-4883.
- Zhang J, Blustzjn JK & Zeisel SH. (1992). Measurement of the formation of betaine aldehyde and betaine in rat liver mitochondria by a high pressure liquid chromatography-radioenzymatic assay. *Biochimica et Biophysica Acta (BBA)-General Subjects* **1117**, 333-339.
- Zhang Y, Lv S-j, Yan H, Wang L, Liang G-p, Wan Q-x & Peng X. (2013). Effects of glycine supplementation on myocardial damage and cardiac function after severe burn. *Burns* **39**, 729-735.
- Zhou X, Liu Y, Zhang L, Kong X & Li F. (2021). Serine-to-glycine ratios in low-protein diets regulate intramuscular fat by affecting lipid metabolism and myofiber type transition in the skeletal muscle of growing-finishing pigs. *Animal Nutrition* **7**, 384-392.
- Ziegler-Meeks K. (2009). Husbandry manual for the cheetah (*Acinonyx jubatus*). *Jacksonville, FL: White Oaks Conservation Centre.*



Appendices

Appendix A: Immunohistochemistry protocol

Reagents and buffers

- Acetone.
- Phosphate buffered saline (PBS) 0.15M pH 7.4: NaCl (0.14M), Na₂HPO₄ anhydrous (8.8mM), KCl (2.7mM), KH₂PO₄ (1.5mM), stored at 4°C.
- Donkey serum blocking solution (5%) prepared in PBS.
- Mowiol with anti-fade for mounting.

Antibodies

- Primary antibodies: Monoclonal mouse BA-D5 IgG2b (anti-MHCI), monoclonal mouse SC-71 IgG1 (anti-MHCIIA), monoclonal mouse 6H1 IgM (anti-MHCIIIX), monoclonal mouse C4 IgG1 (anti-laminin), purchased from Developmental Studies Hybridoma Bank (DSHB, University of Iowa, USA).
- Secondary antibodies: Polyclonal AMCA AffiniPure goat anti-mouse IgG2b, polyclonal Alexa Fluor® 488 AffiniPure goat anti-mouse IgG1, polyclonal CyTM3 AffiniPure donkey anti-mouse IgM, purchased from Jackson ImmunoResearch Laboratories Inc. (Pennsylvania, USA).

Sample preparation

1. Keep fresh muscle tissue on gauze wet with saline
2. Determine the direction of the muscle fibres, cut the tissue to an appropriate size (≈3x3mm)
3. Mount the tissue on a small piece of cork with mounting media (TissueTek), ensuring the correct orientation of the muscle fibres.
4. Rapidly freeze the sample in liquid nitrogen, store in cryovials at -80°C.

Sectioning

1. Label pre-coated glass microscope slide.
2. Remove sample from -80°C ensuring the tissue does not thaw.
3. Section samples 10µm thick using a cryostat set to -25°C. Capture 4 cross-sections on a glass microslide as illustrated by the figure below.
4. All to air dry and store at 4°C.

1	2
3	4

Staining

1. Remove slides from storage and allow to equilibrate to room temperature.
2. Fix sections by immersing in pre-chilled acetone at -20°C for 2 minutes. Tap off excess acetone and air-dry.
3. Outline all sections with a wax pen to prevent spill-over of blocking solution and antibodies.
4. Dunk sections in PBS 10x followed by a 2-minute immersion. Tap off the excess PBS.
5. Dilute blocking solution with PBS; pipette $200\mu\text{l}$ 5% donkey blocking solution ($50\mu\text{l}$ /section) onto each slide and incubate for 1 hour at room temperature in a humidifying chamber. Tap off excess blocking solution.
6. Dilute primary antibodies using PBS: BA-D5, SC-71, 6H1 (1:50), C4 (1:100). Pipette $200\mu\text{l}$ of primary antibody ($50\mu\text{l}$ /section) onto each slide. Place in a humidifying chamber and allow to incubate overnight at 4°C .
7. The following day, remove slides from storage and tap off excess primary antibody.
8. Hydrate samples by dunking 10x in PBS followed by a 2-minute immersion at room temperature. Tap off excess PBS. Repeat hydration step.
9. All proceeding steps are carried out in the dark; dilute secondary antibodies using PBS: AMCA IgG2b (1:500), Alexa Fluor® IgG1 (1:500), CyTM3 IgM (1:500). Pipette $200\mu\text{l}$ secondary antibody ($50\mu\text{l}$ /section) onto each slide. Place in a humidifying chamber and allow to incubate for 2 hours at room temperature.
10. Prepare mounting media (Mowiol): add a pinch of anti-fade to a volume ($\approx 40\mu\text{l}$ /section) of Mowiol. Centrifuge and place in heating block.
11. Following the 2-hour incubation, tap off excess antibody. Hydrate samples by dunking 10x in PBS followed by a 2-minute immersion. Tap off excess PBS and repeat.
12. Pipette $40\mu\text{l}$ Mowiol in the centre of the section. Place the cover slip over the section, ensuring the Mowiol spreads and covers all sections. Gently tap the cover slip to eliminate air bubbles.
13. Store slide in the dark overnight and store at 4°C .

14. Using a fluorescent microscope, visualize sections and capture images of a selected section at the specific excitation/ emission wavelength for each fluorophore representing each fibre type.

Image and processing

The following steps are carried out in the image processing software ImageJ (v1.8.0).

1. To merge images, open ImageJ and drag images into the software.
2. Select "Image" > "Colour" > "Merge channels".
3. Assign the image to the appropriate colour (i.e. BA-D5 corresponds to the blue channel) and create a composite image displaying all fibres types on one image.
4. To insert a scale bar, open the 10x calibration image in ImageJ.
5. Click the straight-line tab. Drag a straight line measuring 0.1mm from the 1mm line.
6. Calibrate the scale by clicking "Analyze" > "set scale". The known distance is 100µm. Change the units to µm in the "Unit of length" tab.
7. Set the scale to Global and close the calibration image.
8. Open immunostained image in ImageJ.
9. Click "Analyze" > "Tools" > "Scale bar". Select appropriate width, size and font. Scale bars are generally 100-200µm at the bottom right of the image.
10. Save the image.
11. To calculate cross-sectional area of fibres, click the freehand line tab.
12. Trace the outline of a single muscle fibre and click "Analyze" > "Measure". Alternatively, press Ctrl + M to measure. Measurements are recorded in a table.
13. Measure the CSA of minimum 20 fibres per fibre type.
14. Copy the table into a separate spreadsheet.

Appendix B: Fluorometric enzyme analysis

Muscle preparation for fluorometric analysis

Chemicals

KH ₂ PO ₄	Merck 1.04873
K ₂ HPO ₄	Merck 5099

Stock solutions:

A. KH₂PO₄ 0.1 M Mw 136.1
0.6804 g / 50 ml dH₂O

B. K₂HPO₄ 0.1 M Mw 174.2
0.871 g / 50 ml d H₂O

Add 30 ml of buffer B to a small beaker and place pH probe into that solution. Use buffer A and adjust buffer to pH 7.30. This buffer can be stored at -20°C.

Homogenizing the muscle sample:

- Muscle samples are first diluted with homogenizing buffer to a ratio specific to each animal species (i.e., 1:100 dilution = 100 µl homogenizing buffer for every 1 mg muscle). Further dilution might be required for very rapid reactions.
- Samples are then sonicated on ice and stored at -80°C.

Assay	Dilution (ww)	Read time (min)	Interval (s)	Sample volume (µl)	Reagent volume (µl)
CS	1:19	5	30	5	250
LDH	1:100	1	10	2	250
3-HAD	1:19	4	30	5	250
PFK	1:100	4	30	3	250
CK	1:800	4	30	2	250
PHOS	1:100	8	30	5	250

Specifications for enzyme assays (cheetah)

NADH and NADPH standard curve

Chemicals

NADH	Roche 107 735
NADPH	Sigma N7505
Na ₂ CO ₃	Merck6392
NaHCO ₃	Merck6329

Buffer:

Na₂CO₃ 0.08 M Mw 105.99 0.848 g

NaHCO₃ 0.02 M Mw 84.01 0.168 g

Make up to 100 ml dH₂O

NADH ±5 mM Mw 709.3 ~36 mg

Dissolve in 10 ml buffer

Heat NADH solution for 10 min in a water bath at 60°C to destroy NAD⁺

NADPH ± 5 mM Mw 833.4 25 mg

Dissolve in 6 ml buffer

Heat NADPH solution for 10 min in a water bath at 60°C to destroy

NADP⁺

Generating NADH/ NADPH standard curve:

1. Use black or white plates, depending on the sensitivity of the assay (determined by the concentration of the muscle sample used). Make sure the fluorometer is switched on for at least 20 minutes. Set the excitation wavelength to 340/11 nm and the emission wavelength to 460/40 nm.
2. Read the background fluorescence of each well.
3. Dilute the original NADH standard 11 times (1:10) with dH₂O. Dilute the original NADPH standard 3 times (1:2) with dH₂O.
4. Pipette 0, 2, 4, 6, 8, 10 µl in duplicate in each well
5. Add 250 µl 0.05 M (Tris or Imidazole) buffer to each well and read.
6. Subtract the blank value from each NADH/ NADPH read.
7. Subtract the blank value from the rest of the measurements.

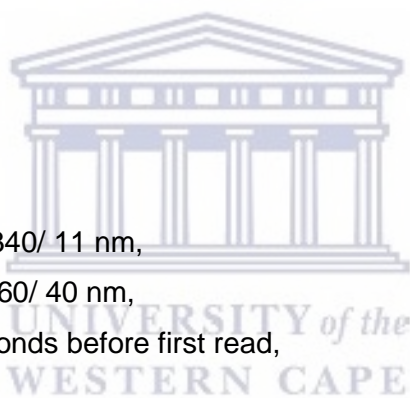
8. Draw a graph with the fluorescence values on the Y-axis and NADH/ NADPH concentration (μM) on the X-axis.
9. Determine the slope, expressed as fluorescent units / μM .

Enzyme assays

Principle: Fluorometry relies on the measured fluorescence which comes from reduced forms of NAD^+ and NADP^+ . The reaction can either in itself cause the increase or decrease in e.g. $\text{NADH} + \text{H}^+$, or be coupled to such a reaction, as in this case. During analysis, the fluorescence is measured at known time intervals and difference per minute is calculated. Knowing the protein concentration of the sample and its dilution, the enzyme activity, expressed as $\text{mmol}\cdot\text{min}^{-1}\cdot\text{g}^{-1}$ protein substrate turnover, is calculated. All enzyme assays were performed using fluorometric analyses.

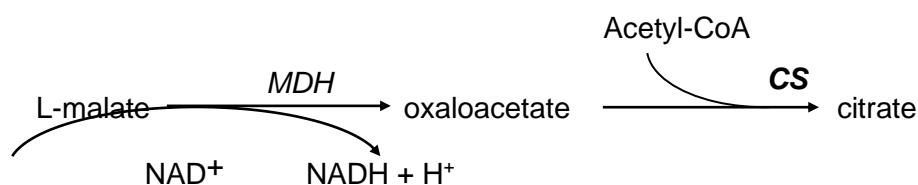
Microplate reader settings

- A. Gain: Manual, 500 V,
- B. Integration time: 10 ms,
- C. Read height: 1.23 mm,
- D. Excitation wavelength: 340/ 11 nm,
- E. Emission wavelength: 460/ 40 nm,
- F. Shaking duration: 3 seconds before first read,
- G. Temperature: 25°C.



Citrate synthase

Reaction:



Chemicals:

Tris base	Sigma T-1503
-----------	--------------

Ethylenediaminetetra acetic acid (EDTA)	Sigma E-5134
NAD ⁺	Roche 127 965
L-Malate	Sigma M-1125
Malate dehydrogenase (MDH)	Roche 127 256
Acetyl-CoA	Sigma A-2056
NADH	Roche 107 735

Stock solutions:

Tris-buffer 0.2 M, pH 8.0 Mw 121.1
2.4 g / 100 ml dH₂O; adjust pH

EDTA 0.1 M Mw 372.2
3.7 g / 100 ml dH₂O

NAD⁺ 0.1 M Mw 663.4
69 mg / 1 ml dH₂O
Freeze at -80°C in aliquots

L-malate 0.1 M Mw 156.1
78 mg / 5 ml dH₂O
Freeze at -80°C in aliquots

Acetyl-CoA 3 mM Mw 809.6
Freeze at -80°C in aliquots

Dissolve 5 mg in 2 ml dH₂O, exact amount depending on analysis of each batch as indicated on vial. This will result in the [final] in 260 µl to be 60 µM.

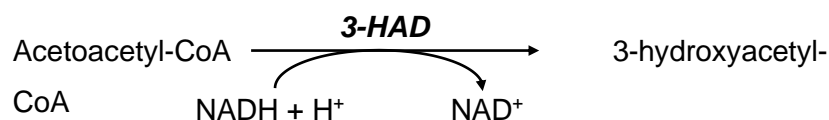
Working reagent:

Chemical	[Stock]	25 ml:	50 ml:	120ml:	[Final]
Tris buffer	0.2M, pH 8.0	12.5 ml	25 ml	60 ml	0.1 M
EDTA	0.1 M	625 µl	1.25 ml	3.0 ml	2.5 mM
NAD ⁺	0.1 M	125 µl	250 µl	600 µl	0.5 mM
L-malate	0.1 M	250 µl	500 µl	1.2 ml	1.0 mM
MDH	5 mg/ml	40 µl	80 µl	192 ml	8 µg/ml

Fill up with dH₂O to desired volume. Check pH 8.0. NADH standard curve and procedure as described, with 50mM Tris buffer, pH 8.0.

3-Hydroxyacetyl Co-A Dehydrogenase

Reaction:



Chemicals

Imidazole	Sigma I-0125
Ethylenediaminetetra acetic acid (EDTA)	Sigma E-5134
Acetoacetyl-CoA	Sigma A-1625
NADH	Roche 107 735

Stock solutions:

Imidazole buffer	1 M, pH 7.0 6.8g / 100 ml dH ₂ O; adjust pH	Mw 68.1
EDTA	0.1 M 3.722 g / 100 ml dH ₂ O; pH to 7.00	Mw 372.2
NADH	0.1 M 17.7 mg / 250 µl dH ₂ O Freeze at -80°C wrapped in tin foil for not longer than 2 months.	Mw 709.4
Acetoacetyl-CoA	1 mM	Mw 971.6

Dissolve 5 mg in approximately 1 ml dH₂O (4.9 mM). Dilute this to 1 mM aliquots and freeze at -80°C for later use. This will result in the [final] in 260 µl to be 20 µM.

Working reagent:

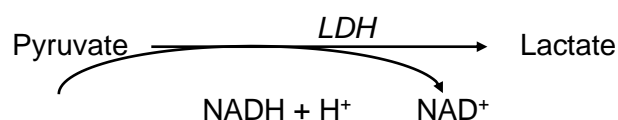
Chemical	[Stock]	25 ml:	50 ml:	120ml:	[Final]
Imidazole buffer	1 M	1.25 ml	2.5 ml	6 ml	50 mM

EDTA	0.1 M	1 ml	2 ml	4.8 ml	4 mM
NADH	0.1 M	7.5 μ l	15 μ l	36 μ l	30 μ M

Fill up with dH₂O to desired volume. Check pH 7.0. Keep reagent in the dark. NADH standard curve and procedure as described, with 50mM Imidazole buffer, pH 8.0

Lactate dehydrogenase

Reaction:



Chemicals:

Tris base	Sigma T-1503
Ethylenediaminetetra acetic acid (EDTA)	Sigma E-5134
NADH	Roche 107 735
Pyruvate	Roche 128 147

Stock solutions: (Store at -40° C):

Tris-buffer	0.2 M, pH 8.0 2.4g / 100 ml dH ₂ O; adjust pH	Mw 121.1
EDTA	0.1 M 3.722 g / 100 ml dH ₂ O	Mw 372.2
NADH	0.1 M 17.7 mg / 250 μ l dH ₂ O Freeze at -80°C in aliquots wrapped in tin foil for no longer than 2 months.	Mw 709.4
Pyruvate	1.0 M 220 mg / 2 ml dH ₂ O Freeze at -80°C in aliquots. [Final] will be 2 mM in 260 μ l.	Mw 110.0

Working reagent:

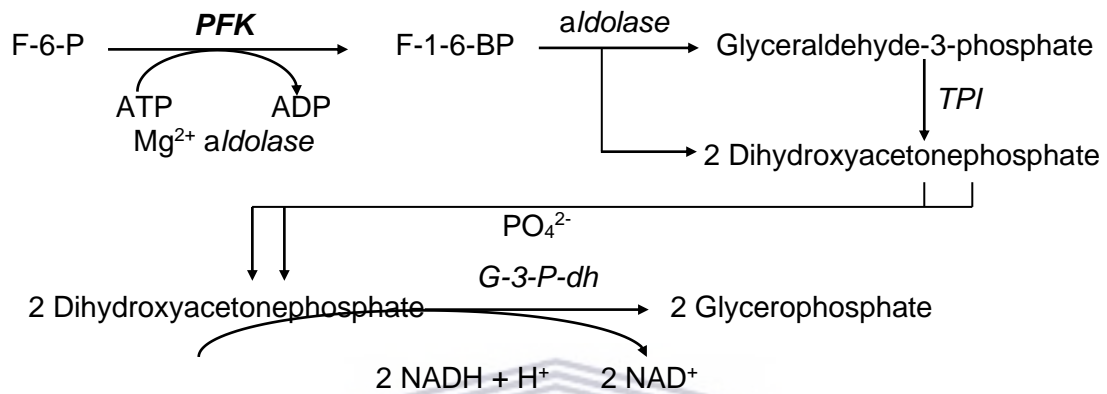
Chemical	[Stock]	25 ml:	50 ml:	120ml:	[Final]
Tris buffer	0.2 M	6.25 ml	12.5 ml	30 ml	50 mM

EDTA	0.1 M	1 ml	2 ml	4.8 ml	4 mM
Pyruvate	1.0 M	50 μ l	100 μ l	240 μ l	2mM

Fill up with dH₂O to desired volume. Check pH 7.60. NADH standard curve and procedure as described, with 50mM Tris buffer pH 8.0.

Phosphofructokinase

Reaction:



Chemicals

Tris base	Sigma T-1503
ATP	Sigma A-2383
MgCl ₂	Merck 5833
Na ₂ HPO ₄	Merck 6580
Fructose-6-phosphate – Na ₂	Sigma F-3627
NADH	Roche 107 735
β -Mercaptoethanol	Sigma M-6250
Aldolase	Roche 102 644
Glyceraldehyde-3-phosphate-dehydrogenase	Sigma G1881
/ Triosphosphate-isomeras (TPI)	
Bovine serum albumin (BSA)	Sigma A-2153

Stock solutions (Store at -20°C):

Tris-buffer	0.2 M, pH 8.0 2.4g / 100 ml dH ₂ O; adjust pH	Mw 121.1
ATP	0.1 M 110 mg / 2 ml dH ₂ O Freeze at -80°C in aliquots	Mw 551.1
MgCl ₂	1 M 2.0331 g / 10 ml dist. H ₂ O	Mw 203.31
Na ₂ HPO ₄	0.25 M 2.225 g / 50 ml dist. H ₂ O	Mw 177.99
F-6-P	0.1 M 68 mg / 2 ml dH ₂ O Freeze at -80°C in aliquots	Mw 340.1
NADH	0.1 M 17.7 mg / 250 µl dH ₂ O Freeze at -80°C in aliquots wrapped in tinfoil	Mw 709.4
BSA	10% 1g / 10 ml dH ₂ O Freeze at -80°C in aliquots.	

Working reagent:

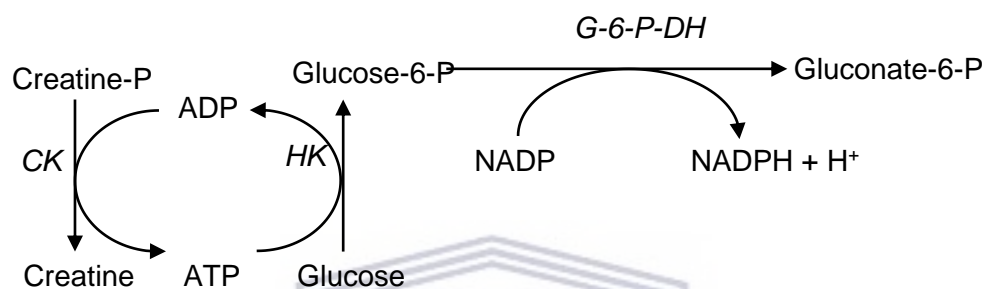
Chemical	[Stock]	25 ml:	50 ml:	120ml:	[Final]
Tris buffer	0.2 M, pH 8.0	6.25ml	12.5 ml	30 ml	0.05 M
ATP	0.1 M	250 µl	500 µl	1200 µl	1 mM
MgCl ₂	1 M	50 µl	100 µl	240 µl	2 mM
Na ₂ HPO ₄	0.25 M	125 µl	250 µl	600 µl	1.25 mM
F-6-P	0.1 M	250 µl	500 µl	1200 µl	1 mM
NADH	0.1 M	2.5 µl	5 µl	12 µl	10 µM
BSA	10%	125 µl	250µl	600 µl	0.05 %
β-Mercaptoethanol	14.2 M	2 µl	4 µl	9.6 µl	1 mM

Aldolase	20 mg/2ml	30 μ l	60 μ l	144 μ l	12 μ g/ml
TPI	50 000 U/ml	8 μ l	16 μ l	38 μ l	15 U/ml
G-3-P-dh	2 mg/ml	20 μ l	40 μ l	96 μ l	2.2 U/ml
GDH/TPI combo	1440 U/ml	38 μ l	75 μ l	180 μ l	2.2 U/ml

Fill up with dH₂O to desired volume. Check pH 7.60. NADH standard curve and procedure as described, with 50mM Tris buffer pH 8.0

Creatine kinase

Reaction:



Chemicals

Imidazole	Sigma I-0250
EDTA	Sigma E-5134
Magnesium acetate	Sigma M-5661
Glucose	Sigma G-7528
ADP	Sigma A-2754
AMP	Sigma A-1752
Creatine phosphate	Roche 621722
Diadenosine Pentaphosphate (DAPP)	Sigma D-4022
NADP+	Roche 128058
N-Acetylcysteine (NAC)	Sigma A-7250
Hexokinase	Roche 142 6362
Glucose-6-phosphate DH	Roche 127 655
NADPH-4Na+	Sigma N-7505

Stock solutions:

Imidazole-EDTA-Mg-acetate stock

EDTA 0.149 g Mw 372.2

Imidazole	1.361 g	Mw 68.1
Magnesium acetate	0.429 g	Mw 214.5
• Dissolve the above in 150 ml dH ₂ O and pH to 6.7 with HCl.		
Glucose	0.5 M 915 mg / 2 ml dH ₂ O	Mw 180.16
ADP	0.5 M 213 mg / 1 ml dH ₂ O	Mw 427.2
AMP	0.5 M 175 mg / 1 ml dH ₂ O	Mw 347.2
Creatine phosphate	0.5 M 327 mg / 2 ml dH ₂ O	Mw 327.2
Diadenosine Pentaphosphate (DAPP)	10 mg/ml	Mw 916.4
NADP ⁺	0.1 M 79 mg / 1 ml dH ₂ O	Mw 787.4
N-Acetylcysteine (NAc)	0.5 M 82 mg / 1 ml dH ₂ O	Mw 163.2

Working reagent:

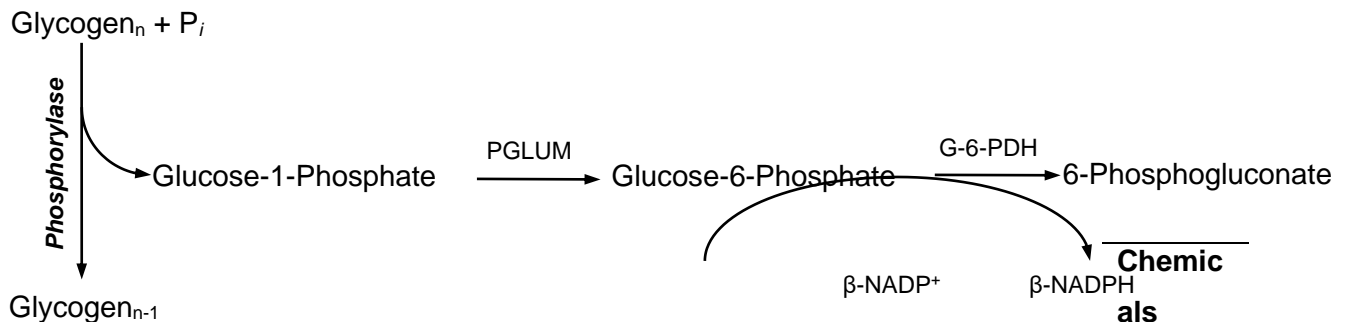
Chemical	[Stock]	10 ml:	20 ml:	120ml:	[Final]
Imidazole-EDTA-Mg stock, pH 6.7		7.5 ml	15 ml	90 ml	
Glucose	0.5 M	80 µl	160 µl	960 µl	4 mM
ADP	0.5 M	40 µl	80 µl	480 µl	2 mM
AMP	0.5 M	100 µl	200µl	1.2 ml	5 mM
Creatine phosphate	0.5 M	600 µl	1.2 ml	7.2 ml	30 mM
Diadenosine Pentaphosphate (DAPP)	11 mM	9.15 µl	18.3 µl	110 µl	10 µM
NADP ⁺	0.1 M	80 µl	160 µl	960 µl	800 µM
N-Acetylcysteine (NAc)	0.5 M	400 µl	800 µl	4.8 ml	20 mM
*Hexokinase	1500 U/ml	16.7 µl	33.3 µl	200 µl	2.5 U/ml

*Glucose-6-phosphate DH 1750 U/ml 8.6 µl 17.1 µl 103 µl 1.5 U/ml

Fill up with dH₂O to desired volume. Check pH 6.70. NADPH standard curve and procedure as described, with 50mM Imidazole buffer pH 8.0. *Added immediately prior to use.

Phosphorylase

Reaction:



- Chemicals**
-
- Imidazole
 - Glycogen (Glucose units)
 - K₂HPO₄
 - Dithiothreitol
 - MgCl₂
 - EDTA
 - pH 7.00
 - β-NADP⁺
 - D-Glucose-1,6-BP
 - BSA
 - Phosphoglucose mutase
 - Glucose-
-

Stock solutions:

Imidazole-acetate buffer	0.5 M, pH 7.0 6.8 g / 100 ml dH ₂ O	Mw 68.1
Glycogen (Glucose units)	40 mg/ml 40 mg / 1 ml dH ₂ O	Mw 180.2
K ₂ HPO ₄	1.0 M 8.71 g / 50 ml dH ₂ O	Mw 174.2
Dithiothreitol	0.5 M 31 mg / 200 µl dH ₂ O	Mw 154.25
MgCl ₂	1.0 M 0.203 g / 1 ml dH ₂ O	Mw 203.3
EDTA	0.1 M, pH 7.0 3.7 g / 100 ml dH ₂ O	Mw 372.2
β-NADP ⁺	0.1 M 40 mg / 500 µl dH ₂ O	Mw 787.4
D-Glucose-1,6-BP	10 mM 1.6 mg / 200 µl dH ₂ O	Mw 808.9
BSA	10% 1g / 10 ml dH ₂ O Freeze at -80°C in aliquots	

Working reagent:

Chemical	[Stock]	10 ml:	50 ml:	120ml:	[Final]
Imidazole-acetate buffer, pH 7.0	0.5 M	1 ml	5 ml	12 ml	50 mM

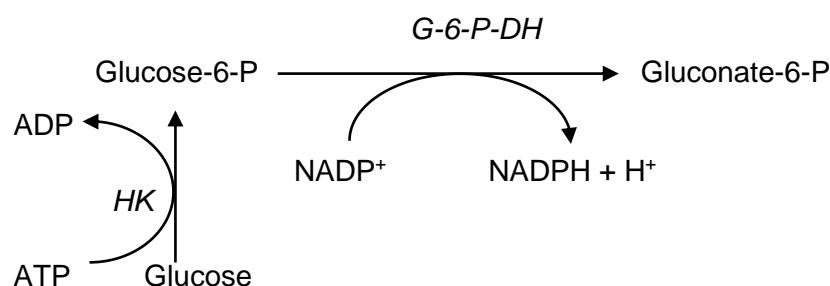
Glycogen	40 mg/ml (222mM)	400 µl	2 ml	4.8 ml	1.6 mg/ml (8.9 mM)
K ₂ HPO ₄	1 M	200 µl	1.0 ml	2.4 ml	20 mM
MgCl ₂	1 M	5 µl	25 µl	60 µl	0.5 mM
EDTA	100 mM	100 µl	500 µl	1.2 ml	1 mM
β-NADP ⁺	100 mM	40 µl	200 µl	480 µl	0.4 mM
D-Glucose-1,6-BP	10 mM	2 µl	10 µl	24 µl	2 µM
AMP	100 mM	100 µl	500 µl	1.2 ml	1 mM
DTT	500 mM	10 µl	50 µl	120 µl	0.5 mM
BSA	10%	25 µl	125 µl	300 µl	0.025%
Phosphoclucomutase	885 U/ml	7 µl	35 µl	84 µl	0.6 U/ml
Glucose-6-P dehydrogenase	1750 U/ml	6 µl	30 µl	72 µl	1.0 U/ml

Fill up with dH₂O to desired volume. Check pH 7.0. NADPH standard curve and procedure as described, with 50 mM Imidazole buffer pH 8.0.

Appendix C: Glycogen assay

Principle: Muscle glycogen is measured as glucose equivalents. Following alkaline digestion and subsequent precipitation, the glycogen is hydrolysed to glucose with a strong acid. The glucose is then measured after neutralization of the hydrolysate. Muscle glycogen content is then calculated using the glucose concentration. Glucose concentration was determined spectrophotometrically.

Reaction:



Chemicals

Tris base	Sigma T-1503
KOH	

Abs. EtoH (molecular analysis grade)	
HCl (37%)	
NaOH	
MgCl ₂	Merck 5833
ATP	Sigma A-2383
NADP ⁺	Roche 128058
Hexokinase	Sigma/Roche 11426362001
Glucose-6-phosphate DH	Roche 127 655
Glucose	Sigma G-7528
Bromothymol blue	

Stock solution

Tris buffer	0.2 M, pH 7.5 & pH 8.1 2.4 g / 100 ml dH ₂ O	Mw 121.1
KOH	40% 40g / 100 ml dH ₂ O	Mw 56.1
HCl	2 M 1.64 ml / 10 ml dH ₂ O	Mw 36. 46
MgCl ₂	1.0 M 0.203 g / 1 ml dH ₂ O	Mw 203.3
NADP ⁺	0.1 M 40 mg / 500 µl dH ₂ O	Mw 787.4
ATP	0.1 M 110 mg / 2 ml dH ₂ O Freeze at -80°C in aliquots	Mw 551.1
Bromothymol blue		Mw
	Add 1 drop / 500 µl dH ₂ O or 0.2 M Tris buffer pH 7.5	

Glucose reagent:

Chemical	[Stock]	10 ml:	20 ml:	60ml:	[Final]
----------	---------	--------	--------	-------	---------

Tris buffer	0.2 M, pH 8.1	500 µl	1 ml	3 ml	50 mM
ATP	0.1 M	50 µl	100 µl	300 µl	500 µM
NADP ⁺	0.1 M	50 µl	100 µl	300 µl	500 µM
MgCl ₂	1 M	10 µl	20 µl	60 µl	1 mM
*Hexokinase	1500 U/ml	3.5 µl	7 µl	20 µl	0.5 U/ml
*G-6-P-DH	1750 U/ ml	0.46 µl	1 µl	3 µl	0.08 U/ml

Fill up with dH₂O to desired volume. Reaction time: 15 minutes. *Added last to the reagent.

Procedure

Day 1:

1. Label and weigh empty microtubes. Record the weight. *NB: ink has weight, hence the tubes should be labelled before weighing.*
2. Switch on heating block to 95°C. Collect muscle samples from the freezer and insert into tubes. Allow muscles to thaw, but keep on ice for the remaining steps.
3. Weigh the tubes to determine muscle weight, record weight. Muscle weight ranges between approximately 6mg and 20 mg.
4. Add 200 µl cold 40% KOH to all tubes. Invert tubes to mix.
5. Place in heating block (95°C) for 30 minutes. Apply a weight to the tubes to prevent them from opening. Regularly check and mix every 10 minutes.
6. Allow samples to cool to room temperature.
7. Add 800 µl absolute ethanol to the tubes.
8. Mix tubes by inversion and centrifuge at 2000 RPM for 3 minutes.
9. Store the samples overnight in the refrigerator (4°C).

Day 2:

1. Remove samples from the refrigerator. Centrifuge tubes for 15 minutes at 14000 RPM and aspirate the supernatant. Avoid disturbing the pellet.
2. Add 200 µl absolute ethanol to wash the pellets. Centrifuge the tubes for one minute at 14000 RPM.
3. Aspirate the supernatant, then invert tube onto tissue paper to remove excess liquid.
4. Add 200 µl 2M HCl to each tube. Invert/mix and centrifuge the samples for one minute at 14000 RPM.
5. Place samples in the heating block (95°C) for 3 hours. Place a weight on the tubes to prevent them from opening. Check and mix every hour.
6. Allow samples to cool to room temperature. Centrifuge tubes for 3 minutes at 14000 RPM.
7. Add 100 µl 0.2M Tris buffer (pH 7.5) to each tube.
8. Add 150 µl 2M NaOH to each tube.
9. Add 4 µl of bromothymol blue indicator (pH 6.5 to 7.5) to each tube. Mix contents and allow 30 seconds for the colour to change.

*The ideal colour is greenish-blue/turquoise which will indicate a pH around 7 to 7.5.

10. Adjust the pH as necessary. If the sample is yellow, add NaOH. If the sample is blue, add HCl. Very small volumes of HCl or NaOH should be added each time as the colour can change rapidly (0.5 to 2 μ l).
11. Weigh the tubes for the final weight and record. Steps 9 to 11 can be done prior to glucose analysis.
12. Store at -20°C until glucose analysis.

Measuring Glucose

1. Make up a glucose standard curve, tend towards lower concentrations but may need to validate depending on linearity. For 30 μ L sample volume – glucose concentrations of 0mM, 0.25mM, 0.5mM, 1mM, 1.5mM and 2mM. *NB: At high concentrations the reaction will be saturated.*
2. Make up the glucose reagent and cover with foil. Make up to necessary volume with dH₂O.
3. In a clear-bottom 96-well elisa plate, pipette in duplicate 30 μ l of each glucose standard curve sample and 30 μ l of unknown sample.
4. Add 250 μ L glucose reagent to each well. Incubate for 15 minutes, cover plate with foil. The reaction should plateau between 10 to 15 minutes.
5. Set the spectrophotometer to an absorbance endpoint reading at 340nm. Read the samples. Export data to spreadsheet.
6. Calculate the glucose concentration of the unknown samples using the standard curve equation (ensure that it is linear).
7. Calculate the glycogen concentration using the equation below.

$$[\text{Glycogen}] (\text{mmol} \cdot \text{kg}^{-1} \text{ wet weight}) = [\text{glucose}] (\text{mmol} \cdot \text{l}^{-1}) \left(\frac{Wf(g) - Wt(g)}{Ws(g)} \right) \times 4$$

Wf, final weight; Wt microtube weight; Ws, muscle sample weight

****For wet weight samples the glycogen concentration should be multiplied by 4 in order to account for water content.**

Appendix D: Cheetah pre-study diets

Name	Sex	Age (years)	Recent body weight (kg)	Meat type, organs etc	Supplements	Diet comments about animal
Qaiser	Male	5	54,20 kg	1,3 kg horse/ donkey muscle mince, 100g organ mince, 100g skin mince	Carnivore calcium mixture (1 tsp/alternate day), Predator supplement (1 tbs/alternate day), 1 tsp iodated salt (1 tsp/day)	Receive bones with meat weekly.
Qiana	Female	5	41,25 kg	1,6 kg horse/ donkey muscle mince, 100g organ mince, 100g skin mince	Carnivore calcium mixture (1 tsp/alternate day), Predator supplement (1 tbs/alternate day), 1 tsp iodated salt (1 tsp/day)	Receive bones with meat weekly.
Quest	Male	5	48,75 kg	1,4 kg horse/donkey muscle mince	Carnivore calcium mixture (1 tsp/alternate day), Predator supplement (1 tbs/alternate day), 1 tsp iodated salt (1 tsp/day)	Vomits up organ and skin mince when offered, so diet consists of muscle mince or bones with meat on. Receive bones with meat weekly.
Quinn	Male	5	50,25 kg	1,3 kg horse/ donkey muscle mince, 100g organ mince, 100g skin mince	Carnivore calcium mixture (1 tsp/alternate day), Predator supplement (1 tbs/alternate day), 1 tsp iodated salt (1 tsp/day)	Receive bones with meat weekly.
Rafiki	Male	4	47,65 kg	2,0 kg horse/donkey muscle mince	Carnivore calcium mixture (1 tsp/alternate day), Predator supplement (1 tbs/alternate day), 1 tsp iodated salt (1 tsp/day)	Refuses to eat the organ and skin mince when placed in diet. Receive bones with meat weekly.
Sansa	Female	2	44kg	1,8kg horse/ donkey muscle mince, 100g organ mince, 100g skin mince	Carnivore calcium mixture (1 tsp/alternate day), Predator supplement (1 tbs/alternate day), 1 tsp iodated salt (1 tsp/day)	Receive bones with meat weekly.
Shae	Female	2	43,55 kg	1,6 kg horse/ donkey muscle mince, 100g organ mince, 100g skin mince	Carnivore calcium mixture (1 tsp/alternate day), Predator supplement (1 tbs/alternate day), 1 tsp iodated salt (1 tsp/day)	Receive bones with meat weekly.
Stark	Female	2	42,70 kg	1,3kg horse/ donkey muscle mince, 100g organ mince, 100g skin mince	Carnivore calcium mixture (1 tsp/alternate day), Predator supplement (1 tbs/alternate day), 1 tsp iodated salt (1 tsp/day)	Receive bones with meat weekly.

Appendix E: Permit certificates

Animal Research Committee (AREC) (University of the Western Cape)



UNIVERSITY of the
WESTERN CAPE



03 July 2020

Prof TA Kohn
Medical Biosciences
Faculty of Natural Science

Ethics Reference Number: AR20/3/4

Project Title: The effects of glycine supplementation on skeletal muscle and sperm quality in captive cheetahs (*Acinonyx jubatus*)

Approval Period: 01 July 2020 – 01 July 2023

I hereby certify that the Animal Research Ethics Committee of the University of the Western Cape approved the methodology and ethics of the above mentioned research project.

This approval is subject to submitting an annual progress report by 30 November for the duration of your project and subsequent approval of the report. If the project do not require a renewal, a final project report must be submitted no later than two months after completing the study.

Any amendments, extension or other modifications to the protocol must be submitted to the Ethics Committee for approval.

The Committee must be informed of any serious adverse event and/or termination of the study.

Prof TK Monsees, PhD
Chairperson: Animal Research Ethics Committee (AREC)
University of the Western Cape

Director: Research Development
University of the Western Cape
Private Bag X 17
Bellville 7535
Republic of South Africa
Tel: +27 21 959 4111
Email: research-ethics@uwc.ac.za

NHREC Registration Number: BMREC-130416-050

FROM HOPE TO ACTION THROUGH KNOWLEDGE.

Department of Agriculture, Forestry and Fisheries (DAFF)



agriculture, forestry & fisheries

Department:
Agriculture, Forestry and Fisheries
REPUBLIC OF SOUTH AFRICA

Directorate Animal Health, Department of Agriculture, Forestry and Fisheries
Private Bag X138, Pretoria 0001

Enquiries: Mr Herry Gololo • Tel: +27 12 319 7532 • Fax: +27 12 319 7470 • E-mail: HerryG@daff.gov.za
Reference: 12/11/1/7 (387)

Prof Tertius Kohn
Department of Medical Biosciences
University of the Western Cape
Tel: 021 959 2189
E-mail: kathrynvanboom@gmail.com tkohn@uwc.ac.za

Dear Prof Khon

RE: PERMISSION TO DO RESEARCH IN TERMS OF SECTION 20 OF THE ANIMAL DISEASES ACT, 1984 (ACT NO 35 OF 1984)

Your application dated 22 November 2019 requesting permission under Section 20 of the Animal Disease Act, 1984 (Act No. 35 of 1984) to perform a research project or study, refers.

I am pleased to inform you that permission is hereby granted to perform the following study, with the following conditions:

Conditions:

1. This permission does not relieve the researcher of any responsibility which may be placed on him by any other act of the Republic of South Africa;
2. This permission is given upon finding the biosecurity of the research project as described to be acceptable to DAFF. This permission does not serve as any approval or endorsement by DAFF for the use or registration of any supplement for any purpose in South Africa;
3. The research project is approved as per the application form dated 22 November 2019 and the correspondence thereafter. Written permission from the Director:

Animal Health must be obtained prior to any deviation from the conditions approved for this research project under this Section 20 permit. Please apply in writing to HerryG@daff.gov.za;

4. If required, an application for an extension must be made by the responsible researcher at least one month prior to the expiry of this Section 20 permit. Please apply in writing to HerryG@daff.gov.za;
5. No part of this research project may begin until the valid ethical approval has been obtained in writing from the relevant South African authority and all relevant permissions in terms of all applicable nature conservation legislation have been obtained;
6. It is the responsibility of the researcher to obtain written consent from the owners of the cheetah to be sampled in this research project, prior to such sampling occurring;
7. This Section 20 approval does not serve as an instruction for any person or organization to partake in the research project;
8. Only blood, muscle, semen and urine samples from cheetahs may be collected and analysed in this research project. Samples may only be collected from properties for which a state veterinary letter of no restriction has been provided to DAFF, i.e. Cango Wildlife Ranch and Conservation Centre in Oudshoorn, Western Cape Province. It is the responsibility of the researcher to contact the responsible state veterinarian to ensure no restrictions have been placed on the property prior to movement and to facilitate the issuing of veterinary movement permits if required.
9. This research project must be conducted in compliance with the Fertilizers, Farm Feeds, Agricultural Remedies and Stock Remedies Act 1947 (Act no 36 of 47) and/or the Medicines and Related Substances Control Act 1965 (Act no 101 of 65);
10. It is the responsibility of the researcher and relevant laboratory or facility managers to ensure that the human safety aspects of this research project are adequately addressed;
11. Any incidence or suspected incidence of a controlled or notifiable animal disease in terms of the Animal Diseases Act 1984 (Act no 35 of 84), must be reported immediately to the state veterinarian of the area;
12. Samples must be packaged and transported in accordance with International Air Transport Association (IATA) requirements and/or the National Road Traffic Act, 1996 (Act No. 93 of 1996);
13. All potentially infectious material utilised or generated during or by the research project is to be destroyed at completion of the research project. Only a registered

waste disposal company may be used for the removal of all potentially infectious waste from the research project;

14. Records must be kept for five years for auditing purposes;

Title of research/study: The metabolic effects of glycine supplementation in captive cheetahs (*Acinonyx jubatus*)

Researcher: Prof Tertius Kohn


Institution: Cango Wildlife Ranch and Conservation Centre, Oudshoorn; Myology Laboratory, University of the Western Cape; Centre for Human Metabolomics, North West University

Permit Expiry date: 31 December 2023

Our ref Number: 12/11/1/7 (387)

Your ref: None provided

Kind regards,



DR. MPHOMAJA
DIRECTOR OF ANIMAL HEALTH
Date: 2019-12-19

- 3 -

SUBJECT: PERMISSION TO DO RESEARCH IN TERMS OF SECTION 20 OF THE ANIMAL DISEASES ACT, 1984 (ACT NO. 35 OF 1984) 12/11/1/7 (387)

Threatened Or Protected Species (TOPS) permit



STANDING PERMIT

(Issued in terms of the provisions of the National Environmental Management: Biodiversity Act 2004, Act 10 of 2004)

PERMIT NUMBER: S 02559

NAME OF ISSUING AUTHORITY	
NAME	DEPT OF ENVIRONMENTAL AFFAIRS
ADDRESS	PRIVATE BAG X 447 PRETORIA 0001
PROVINCE	NATIONAL DEPARTMENT

PROVINCIAL DEPARTMENT	NATIONAL DEPARTMENT
PROTECTED AREA MANAGEMENT AUTHORITY	VETERINARIAN
REGISTERED CAPTIVE BREEDING OPERATION	REGISTERED SCIENTIFIC INSTITUTION <input checked="" type="checkbox"/>
REGISTERED SANCTUARY	REGISTERED REHABILITATION FACILITY
REGISTERED COMMERCIAL EXHIBITION FACILITY	REGISTERED GAME FARM
REGISTERED WILDLIFE TRADER	REGISTERED NURSERY
UNIQUE REGISTRATION NUMBER N78/7707135156084	

DETAILS OF PERMIT HOLDER		
NAME	University of Pretoria	ID NO. 7707135156084
SURNAME	Dr Vinny Naidoo	PASSPORT NO.
	POSTAL ADDRESS	RESIDENTIAL ADDRESS
ADDRESS	Faculty of Veterinary Science	Faculty of Veterinary Science
ADDRESS	University of Pretoria	University of Pretoria
ADDRESS	Private bag x 04	Old Southpan Road
TOWN	Onderstepoort	Onderstepoort
POSTAL CODE	0110	0110
PROVINCE	Gauteng	Gauteng

PROPERTY WHERE RESTRICTED ACTIVITIES WILL BE CARRIED OUT	
NAME AND SURNAME OF APPLICANT	University of Pretoria
NAME AND SURNAME: RESPONSIBLE PERSON	Vinny Naidoo
NAME AND SURNAME OF AGENT	
PHYSICAL ADDRESS OF FACILITY	University of Pretoria
PHYSICAL ADDRESS OF FACILITY	Faculty of Veterinary Science
DISTRICT	Old Southpan Road
PROVINCE	Gauteng
REGISTERED NAME AND NUMBER (in the case of game farm)	

DETAILS OF SPECIES INVOLVED				
SPECIES		SEX	QUANTITY	MARKING
COMMON NAME	SCIENTIFIC NAME	(if known)		(if applicable)
All avian, reptile, mammalian and fish species listed as threatened or protected in terms of Section 56 of the National Environmental Management Biodiversity Act (Act No 10 of 2004)				

DETAILS OF RESTRICTED ACTIVITIES INVOLVED
Collecting / gathering samples, receiving, transporting, removing, receiving as donation, giving, temporary possession, darting and capturing

PERMIT VALIDATION		
PERIOD OF VALIDITY	FROM: 12/02/2019	TO: 11/02/2022
RECEIPT NUMBER		
SIGNATURE OF ISSUING OFFICER	SIGNATURE PERMIT HOLDER	
DATE STAMP:		
2019 -02- 12		
PRETORIA 0001		
DEPT. OF ENVIRONMENTAL AFFAIRS		



STANDARD PERMIT CONDITIONS

1. This permit is not transferable.

2. Any unauthorised alteration to this permit shall render it invalid.

3. This permit is subject to the provisions of any applicable law in force during the period of validity of the permit.

4. This permit is valid only within the province where it was issued.

5. The holder of this permit shall, at the request of a person authorised in terms of applicable legislation so to demand, forthwith produce such permit to such person.

6. This permit shall be invalid until such time that it is signed by the permit holder.

7. This permit shall be deemed invalid when it is lost or destroyed and no copy thereof shall be issued.

8. This permit may be withdrawn by an authorised person if the execution of any activity may be detrimental to the welfare of any wild animal or the safety of any person, provided that the permit holder is given notice of such intention and be granted the opportunity to appeal to such withdrawal.

9. The prescribed fees paid for the issuing of this permit shall not be refunded.

10. If the holder of this permit contravenes or fails to comply with any permit condition or requirement to which this permit is subject, he or she shall be guilty of an offence.

11. This permit shall be subject to any applicable norms and standards in existence at the time of issuance of this permit.

DEPT. VAN OMGEWINGSAKE
 PRIVAATSAK / PRIVATE BAG X 447
 2019-02-12
 PRETORIA 0001

SPECIAL CONDITIONS

1. The issuing authority shall determine the species and restricted activities for which this permit will apply.

2. If this permit applies to a registered game farm, the holder of this permit must:

a. Have a copy of this permit authorising the hunt, on his or her person during the hunt;

b. Within 21 days after the hunt, furnish the issuing authority with a written return on the hunt stating:

(i) the permit number and date of issuance if the permit;

(ii) the species, sex and number of animals hunted; and

(iii) the location where the hunt took place.

c. Return all used copies of the game farm hunting permits within 3 weeks after the end of the calendar year following the issuance of the game farm hunting permit, to the Issuing Authority.

PERMIT VALIDATION

PERIOD OF VALIDITY FROM: 15/02/2019 TO: 11/02/2022

RECEIPT NUMBER: 115010022

SIGNATURE PERMIT HOLDER: [Signature]

DEPT. VAN OMGEWINGSAKE
 PRIVAATSAK / PRIVATE BAG X 447
 2019-02-12
 PRETORIA 0001

ANNEXURE A

**STANDING PERMIT**

(Issued in terms of the provisions of the National Environmental Management: Biodiversity Act 2004, Act 10 of 2004)

Standing permit no: S 02559

Registration certificate no:29471

NAME OF ISSUING AUTHORITY	
NAME	DEPARTMENT OF ENVIRONMENTAL AFFAIRS
ADDRESS	PRIVATE BAG X 447 PRETORIA 0001
PROVINCE	NATIONAL DEPARTMENT

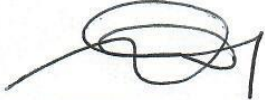

DETAILS OF SPECIES INVOLVED

All avian, reptile mammalian and fish species that are listed as threatened or protected in terms of section 56 of the National Environmental Management: Biodiversity Act (Act No.10 of 2004).

DETAILS OF RESTRICTED ACTIVITIES INVOLVED AND SPECIAL CONDITIONS

- This permit authorizes the Faculty of Veterinary Science in the University of Pretoria to carry out the following restricted activities:
 - Collection/gathering of samples
 - Receiving;
 - Transporting or moving;
 - Receiving as donation;
 - Giving;
 - Temporary possession/ exercise physical control over;
 - Darting and
 - Capturing
- This permit authorizes the Faculty of Veterinary Science of the University of Pretoria to carry out the restricted activities as specified in paragraph 1 of this permit, involving blood and tissue samples of listed threatened or protected avian, reptiles and mammalian species, for diagnostic analysis and research purposes.
- This permit authorizes the Faculty of Veterinary Science of the University of Pretoria to receive and temporary keep live specimens of listed threatened or protected mammalian, avian and reptile species for treatment purposes.
- This permit authorizes the carrying of the restricted activities as specified in paragraph 2 and 3 of this permit, only by employees and registered students carrying out restricted activities on behalf of the Faculty of Veterinary Science of the University of Pretoria.
- This permit authorizes the restricted activities, and for the purpose as specified in paragraph 2 of this permit within the boundaries of the Republic of South Africa.
- The holder of this permit may give/receive blood and tissue samples of listed threatened or protected avian, reptiles, mammalian and fish species, only to or from a person who is in possession of a permit issued in terms of the National Environmental Management: Biodiversity Act (Act No.10 of 2004), that authorizes the possession and

- receiving/giving/donation of such specimens.
7. Blood or tissue samples collected/received in terms of this permit may not be offered for sale.
 8. In the event that the permit holder receives specimens of listed threatened or protected avian, reptiles, mammalian and fish species, the permit holder must report in writing, by the end of each year during the period of validity of this permit, to the Department of Environmental Affairs (DEA) the following information:
 - Name and physical address of person who the specimens have been received from;
 - Permit number of the person who the specimens have been received from (where applicable);
 - Particulars of the species, number and type of specimens received and markings (where applicable).
 9. The permit holder must make the report available to the DEA, upon request from DEA.
 10. All restricted activities involving rhinoceros must be carried out in compliance with the Norms and Standards for the marking of the rhinoceros and rhinoceros horn and for the hunting of the rhinoceros for trophy hunting purposes as published in terms of the National Environmental Management: Biodiversity Act (Act No. 10 of 2004).
 11. The permit holder must comply with the National Norms and Standards for the Management of Elephants in South Africa as published in terms of the National Environmental Management: Biodiversity Act (Act No. 10 of 2004).
 12. The carrying out of the restricted activities referred to in paragraph 1 by the permit holder is subject to the provisions of the Threatened or Protected Species regulations.
 13. This permit does not absolve the permit holder to obtain any permit that may be required in terms of any other applicable legislation.

PERMIT VALIDATION			
PERIOD OF VALIDITY	FROM:	12/02/2019	TO: 11/02/2022
			
SIGNATURE OF ISSUING OFFICER		SIGNATURE PERMIT HOLDER	
<p>DATE STAMP:</p> <div style="border: 1px solid black; padding: 5px; margin: 10px auto; width: fit-content;"> <p style="font-size: small; margin: 0;">DEPT. VAN OMGEWINGSAKE</p> <p style="font-size: small; margin: 0;">PRIVAATSAK / PRIVATE BAG X 447</p> <p style="font-size: large; font-weight: bold; margin: 5px 0;">2019 -02- 12</p> <p style="font-size: small; margin: 0;">PRETORIA 0001</p> <p style="font-size: small; margin: 0;">DEPT. OF ENVIRONMENTAL AFFAIRS</p> </div>			